UNIVERSIDAD DE SANTIAGO DE COMPOSTELA
FACULTAD DE FARMACIA
Departamento de Farmacia y Tecnología Farmacéutica

Beta-Lapachona: Estudios de Preformulación y Aproximaciones Tecnológicas para su Formulación

Marcílio Sérgio Soares da Cunha Filho

Santiago de Compostela, 2007

MARIANA LANDÍN PÉREZ Y RAMÓN MARTÍNEZ PACHECO, PROFESORA TITULAR Y CATEDRÁTICO, RESPECTIVAMENTE, DE FARMACIA Y TECNOLOGÍA FARMACÉUTICA DE LA UNIVERSIDAD DE SANTIAGO DE COMPOSTELA.

CERTIFICAMOS: Que la presente memoria titulada "*Beta-Lapachona: Estudios de Preformulación y Aproximaciones Tecnológicas para su Formulación*" elaborada por el Licenciado en Farmacia Don Marcílio Sérgio Soares da Cunha Filho ha sido realizada bajo nuestra dirección, en el Departamento de Farmacia y Tecnología Farmacéutica y, hallándose concluida, autorizamos su presentación a fin de que pueda ser juzgada por el tribunal correspondiente.

Y, para que conste, expedimos y firmamos la presente certificación en Santiago de Compostela a 01 de octubre de dos mil siete.

M. Landín Pérez R. Martínez Pacheco

Marcílio Sérgio Soares da Cunha Filho

Santiago de Compostela, 08 de octubre de 2007

A minha avó *Alaíde* (*in memoriam*),

Una persona que pese a las profundas marcas de sufrimiento
personal siempre me hizo sentir amado.

AGRADECIMIENTOS

Según dicen, viajar a *Santiago de Compostela* transforma la vida de las personas. Lo que puedo decir tras el largo camino hasta llegar a estas líneas es que sí, es cierto. La atmósfera de la ciudad compostelana me ha convertido en un peregrino más, conduciéndome por las desconocidas rutas de la ciencia. Es, por tanto, la primera a la que rindo homenaje.

Quería expresar mi agradecimiento a la cooperación desinteresada de tantas personas que se han cruzado en mi camino a lo largo de estos años y que han contribuido de alguna manera al resultado final y sin las cuales esta tesis no hubiera sido posible.

Agradezco a *Lívia*, por estar a mi lado en todos los momentos, por animarme a emprender este viaje, por no dejarme caer y por hacerme creer cada día que puedo ir más lejos.

A mi familia, mi madre - *Juliana* y mis hermanos – *Lamartine*, *Luana y Socorro,* por su apoyo en busca de mi sueño. A mis suegros, *Renêuza* y *Wílson*, por abrirme las puertas de su casa y ayudarme en todo lo que les fue posible.

A mis directores de tesis, *Ramón* y *Mariana*, por haberme dado la oportunidad de hacer la tesis con un producto de mi país, por introducirme en el fascinante mundo de la tecnología farmacéutica y por haberme dado suficiente autonomía para conducir este trabajo, haciéndome crecer como investigador.

A mis compañeros del *Departamento de Farmacia y Tecnología Farmacéutica,* de los cuales aprendí mucho más que ciencia. A *Ana Gómez*, por su trato tan humano, a *Felipe Álvarez* por escucharme en los momentos de agobio, a *Adriana Trapani* por su amistad sincera, a *Dayami* por su ayuda y buena voluntad, a *Rafa Romero, Rafa Barreiro, Marcos, Ana Rodríguez, Carmen Tenreiro, Fernando, Marta, Elena, Álvaro, Raquel, Nano, Manolo, Luis, Laura, Vicky, Nela*, *Ana Grenha, Yolanda y María de la Fuente*.

A los profesores *Ángel Concheiro, Fran, Juan Torres, Chelo, José Luis, Pepe, Begoña Seijo* y en especial a *Carmen Álvarez* por su amistad desinteresada y sus valiosos consejos durante la realización de este trabajo.

A Marga, por la generosidad de compartir su familia y su tiempo, por el trato tan cercano, y por la confianza demostrada durante estos años.

Quería también agradecer a todas las personas de otros departamentos de la Universidad de Santiago de Compostela, a las que tuve que recurrir en reiteradas ocasiones y que tuvieron la amabilidad de atenderme. Hago mención a *Ana Teresa Silva* y al profesor *Perfecto Paseiro* del Departamento de Bromatología, a *Chachi* del Departamento de Química Orgánica, a la profesora *Maria González Caamaño*, de la Facultad de Biología y a la profesora *Maria del Carmen Barciela* del Departamento de Química Analítica. Al Servicio General de la Universidad de Santiago de Compostela (CACTUS), en especial a *Bruno da Cunha*, *Inés* y *Antonio Llamas* del Servicio de Rayos-X, a *Manolo* de servicio de RMN y a *Ramiro, Merche* y *Raquel* del servicio de Microscopia Electrónica.

Y como no, mi agradecimiento a los organismos económicos que financiaron esta investigación. Al *Laboratorio Farmacêutico do Estado de Pernambuco* (LAFEPE) que por intermedio del profesor *Pedro Rolim* me suministró la materia prima, objeto principal de estudio de esta tesis. Al *Programa de Becas de Estudio de Alto Nivel de la Unión Europea para Latinoamérica* (*ALBAN*) que me brindó una beca durante estos años.

A mis amigos de Brasil, *Mônica*, *Fábio, Sarah, Brena, Jussara, Daniele, Taciana, Mario, D. Lúcia* y a tantos otros que me han ofrecido su apoyo a pesar de la distancia.

A todos, mi más sincero agradecimiento.

ÍNDICE

Recife, Brasil

Capítulo 1

Introducción

1.1. LA β-LAPACHONA [βLAP]

Hasta la fecha, algunos de los antitumorales más efectivos - antraciclinas, alcaloides de vinca, taxanos y canfotecinas - se han desarrollado a partir de productos naturales, fundamentalmente plantas y microorganismos (García-Fernández y col., 2002). Lejos de perder actualidad, la obtención de fármacos de origen natural sigue teniendo un indudable interés como consecuencia de la enorme diversidad química de los compuestos presentes en estos productos y de que su potencial está poco explorado (Newman y col., 2000; Butle, 2005). En este sentido, la flora brasileña constituye un reducto importantísimo para alcanzar este objetivo (Gottleib y Mors, 1980) como lo demuestra el hecho de que grandes compañías farmacéuticas han visto en ella una auténtica reserva de nuevos fármacos.

El *Instituto de Antibióticos de la Universidade Federal de Pernambuco* (Brasil) fue pionero en el estudio de las naftoquinonas - y, en particular, de la β-lapachona [βLAP] - obtenidas a partir del *Ipê roxo* (*Tabebuia avellanedae* Lor.), árbol tradicionalmente utilizado en la medicina popular brasileña (Gonçalves de Lima y col., 1956). Los estudios *in vitro* e *in vivo* llevados a cabo en las décadas centrales del siglo pasado, pusieron de manifiesto un amplio espectro de actividades biológicas, en especial su potencial antineoplásico (Gonçalves de Lima y col., 1962; Ferreira de Santana y col., 1968; D`Albuquerque y col., 1972).

En lo que se refiere a la actividad antitumoral de βLAP, aunque su mecanismo de acción hasta el momento no haya sido completamente esclarecido, se desveló que actúa sobre los dispositivos de comprobación del ADN, haciendo que la célula cancerígena recupere la

capacidad de detección y de respuesta ante los errores de replicación del ácido nucleico. Este proceso permite la destrucción de las células tumorales de forma selectiva, a través de la activación de los mecanismos naturales de defensa celular, lo que constituye una innovación en el tratamiento del cáncer (Pardee y col., 2002).

Publicaciones y Patentes

Actualmente, la βLAP es objetivo de estudios enmarcados en distintas áreas de conocimiento. En la figura 1.1, se puede apreciar el interés creciente que ha despertado este compuesto con 430 publicaciones científicas y más de 20 revisiones bibliográficas, según datos de SciFinder Scholar (Versión 2006, American Chemical Society). Su investigación resulta particularmente abundante en los 15 últimos años, en los que se han registrado más de 40 patentes y se ha despertado el interés de compañías como la *Hoffman-La Roche.*

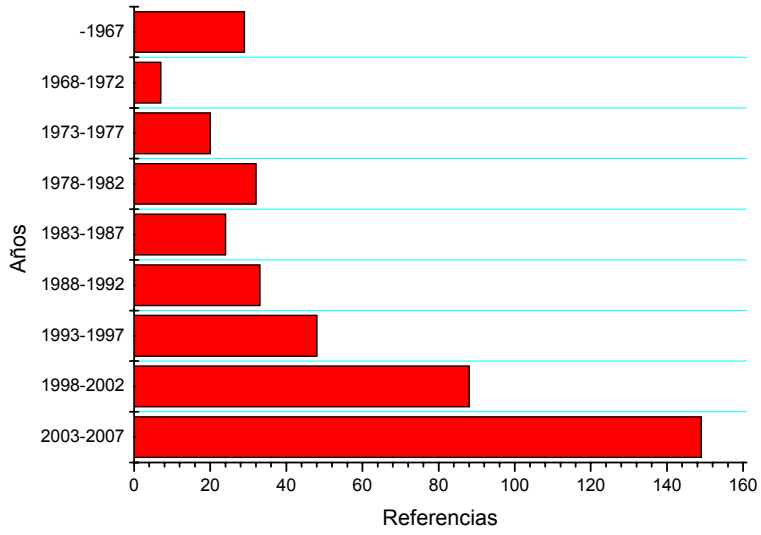

Figura 1.1. Evolución del número de publicaciones sobre βLAP en los últimos años.

Grupos de investigación

De las investigaciones llevadas a cabo con βLAP, es necesario destacar la labor de cuatro equipos, responsables de importantes avances producidos en la delimitación de sus potencialidades terapéuticas.

El grupo de investigación liderado por A.B. Pardee y C.J. Li, vinculados al *Dana-Faber Cancer Institute* (EEUU) y a la *Harvard Medical School* (EEUU) ha registrado 20 patentes relacionadas con βLAP, fruto de un trabajo desarrollado, de forma continuada, desde los años 80. Sus aportaciones se centran en la profundización en el conocimiento del mecanismo de acción de βLAP a nivel celular. Este grupo es responsable de los primeros estudios clínicos con βLAP, con la empresa estadounidense *Arqule* en colaboración con la farmacéutica *Hoffman-La Roche*.

Deben destacarse también las investigaciones realizadas por el profesor D.A. Boothman del *Department of Pharmacology and Oncology of Texas* (EEUU) vinculado al *Simmons Comprehensive Cancer Center* (EEUU) que, en colaboración con el profesor J. Gao, del *Department of Biomedical Engineering of Case Western Reserve University* (EEUU), han llevado a cabo trabajos de indudable importancia acerca de los mecanismos de actuación de βLAP responsables de su actividad antitumoral. En los últimos años sus trabajos se han dirigido al desarrollo de sistemas útiles para la liberación controlada de βLAP.

Los profesores A. Stoppani y M. Dubin de la *Facultad de Medicina de la Universidad de Buenos Aires* (Argentina) han centrado su trabajo sobre los procesos redox desencadenados por βLAP y su uso potencial en el tratamiento de la enfermedad de Chagas.

El profesor A.V. Pinto del *Instituto Oswaldo Cruz de Rio de Janeiro* (Brasil) ha registrado en dos patentes los principales resultados de su investigación sobre quinonas de origen natural y derivados lapachónicos semisintéticos para el tratamiento de tripanosomiasis y de procesos tumorales.

En España, las investigaciones con βLAP y otras naftoquinonas relacionadas se han llevado a cabo en el *Instituto Universitario de Bio-orgánica Antonio González de La Laguna* y en el *Instituto Canario de Investigación del Cáncer* por parte de las investigadoras E. Perez-Sacau y A. Estevez-Braun.

1.2. EL IPÊ ROXO

El Ipê Roxo (Figura 1.2) es un árbol que puede alcanzar hasta 30 metros de altura y unos 90 cm de diámetro en su tronco que cubre una corteza de pequeño espesor y de color oscuro pardo-cenizo (Longhi, 1995).

En Brasil crece naturalmente en el sur y el oeste del estado de Bahia y en los estados de Espírito Santo, Minas Gerais, Mato Grosso do Sul, Rio de Janeiro, Rio Grande do Sul, Santa Catarina y São Paulo. También se encuentra con frecuencia en el nordeste de Argentina, en el sur de Bolivia, Paraguay, Uruguay y en latitudes comprendidas entre 13ºS y 30ºS (Carvalho, 2003).

Figura 1.2. Ipê Roxo (*Tabebuia avellanedae* Lorentz). En detalle su floración.

Ipê roxo es una de las innumerables denominaciones populares de este árbol, del género *Tabebuia sp*, que comprende al menos 26 especies identificadas (Lewis y col., 2005) y del que se presentan, a continuación, algunos datos taxonómicos.

- *Familia*: Bignoniaceae
- *Especie*: *Tabebuia avellanedae* Lorentz
- *Sinonimia popular*: En Brasil: cabroé, graraíba, ipê, ipê-de-flor-roxa, ipê-piranga, ipê-preto, ipê-rosa, ipê-roxo-anão, ipê-uva, pau-d'arco, pau-d'arco-rosa, pau-d'arco-roxo y piuva. En Argentina: lapacho. En Paraguai: lapacho negro.

Aunque se trata de un árbol frecuentemente utilizado en ornamentación de calles y plazas de Brasil, el potencial biológico de las sustancias presentes en esta planta - naftoquinonas, lignanos o triterpenos - le han convertido en objeto de interés tanto científico como, desde hace ya muchos años, de la medicina popular (Carvalho, 2003; Lemos y col., 2007).

La corteza del Ipê Roxo es el componente más importante en lo que a su potencial terapéutico se refiere (Figura 1.3), ya que a partir de la corteza se obtuvieron los extractos a los que la medicina popular atribuye varias propiedades curativas. Así, sus infusiones se han utilizado tradicionalmente para el tratamiento de diabetes, gripes, artritis, anemia y cáncer (Carvalho, 2003; Neto y Morais, 2003).

Figura 1.3. Corteza del tronco de Ipê roxo. En detalle su tronco

1.3. OBTENCIÓN Y PURIFICACIÓN DE βLAP

La βLAP es un constituyente minoritario de los extractos de corteza del Ipê roxo. Por ello, para su producción a gran escala ha sido necesario acudir a la semisíntesis, en concreto a la reacción de ciclización ácida descrita por Hooker en 1892, que utiliza como producto de partida el lapachol, compuesto natural abundante en los extractos de Ipê roxo (Hooker y col., 1936).

El Lapachol (Figura 1.4A) se extrae del tronco del Ipê Roxo con acetato de etilo. El extracto se trata con una disolución acuosa de NaCl al 2 % y, posteriormente, se trata la fracción alcalina con HCl concentrado hasta su precipitación. El lapachol así obtenido se purifica por cromatografía de capa fina de gel de sílice, utilizando una mezcla hexano:benceno (80:20) como fase móvil. La fracción de color amarillo corresponde al lapachol purificado (D´Albuquerque y col., 1972).

La βLAP (Figura 1.4.B) se sintetiza a partir del lapachol por hidrólisis ácida con sulfúrico concentrado. La purificación se lleva a cabo por cromatografía en columna de gel de sílice, con hexano:benceno (50:50) como eluyente. La fracción de color rojo, que corresponde a βLAP, se somete a sucesivas etapas de cristalización (D´Albuquerque y col., 1972).

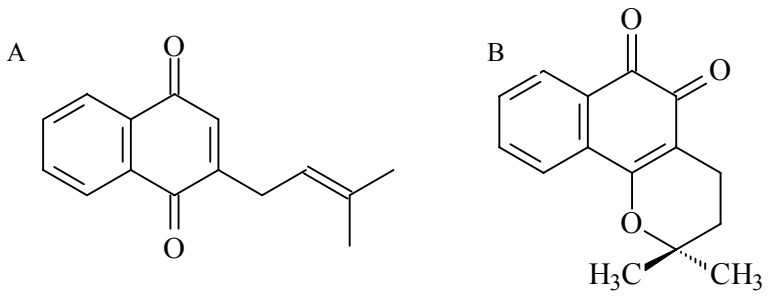

Figura 1.4. Estructura química de Lapachol (A) y de β-lapachona (B).

1.4. PERFIL FARMACOLÓGICO DE βLAP

Ya en los años sesenta del siglo pasado, investigaciones del *Instituto de Antibióticos de la Universidade Federal de Pernambuco*, dieron cuenta de numerosas actividades biológicas de los extractos de *Ipê roxo*. Posteriormente, la βLAP purificada ha confirmado un amplio espectro farmacológico.

El grupo de investigación argentino liderado por Docampo y Stoppani fue pionero en la descripción de la actividad de βLAP frente al *Trypanosoma cruzi*, agente etiológico de la enfermedad de Chagas, una dolencia endémica de Latinoamérica que afecta a más de 18 millones de personas (OMS, 2005). La βLAP demostró una actividad anti-tripanosómica, superior a otras naftoquinonas naturales, relacionada con la generación de radicales libres que provocan daños en el ADN del parásito con la correspondiente inhibición en su síntesis proteica (Docampo y col., 1977; Boveris y col., 1977; Boveris y col., 1978; Lopes y col., 1978; Molina Portela y Stoppani, 1996). Otros estudios llevados a cabo en el *Instituto Oswaldo Cruz del Rio de Janeiro* con distintos derivados imidazólicos, obtenidos a partir de βLAP, han permitido poner de manifiesto notables incrementos de su actividad antiparasitaria (Pinto y col., 2000; Neves-Pinto y col., 2002; De Moura y col., 2004; Menna-Barreto y col., 2005).

Varios autores (Gonçalves de Lima y col., 1962; D`Albuquerque y col., 1972; Cruz y col., 1978; Antunes y col., 2006) han atribuido a βLAP una intensa actividad antibiótica frente a *Bacillus subtillis, Bacillus stearothermophilus, Brucella melitensis, Pseudomonas aeruginosa, Staphylococcus aureus y Streptococcus faecalis*. En un estudio más

reciente, Pereira y colaboradores (2006) pusieron de manifiesto la actividad antibacteriana de βLAP frente a cepas de *Staphylococcus aureus* resistentes a meticilina.

Guiraud y colaboradores (1994) han descrito un efecto anti-fúngico de βLAP superior al ketoconazol, en varias de las especies ensayadas.

Estudios llevados a cabo, tanto *in vitro* como *in vivo,* han puesto de manifiesto la actividad de βLAP frente a las dos variedades del parásito - *Plasmodium falciparum* y *Plasmodium berghei* – causantes de la malaria (Fieser, 1948; Brandão y col., 1993). En la actualidad se están evaluando nuevos derivados de βLAP, con actividad antimalárica más intensa (Andrade-Neto y col., 2004; Perez-Sacau y col., 2005).

Entre los efectos más prometedores de βLAP, cabe señalar su capacidad inhibitoria de los procesos de replicación de algunos retrovirus, aspecto que ha sido objeto de varias patentes recientemente registradas. Ya en 1978, Schuerch y Wehrli dieron cuenta de la potente actividad inhibitoria de este fármaco sobre los procesos de transcripción del virus avícola de la mieloblastosis y del virus de la leucemia de Rauscher. Más recientemente, el *Dana-Farber Cancer Institute* de Boston publicó un estudio en el que se demostraba la efectividad de βLAP en el bloqueo selectivo del mecanismo enzimático implicado en la replicación del virus HIV-1 (Li y col., 1993a).

También ha sido objeto de varias patentes la actividad antipsoriásica de βLAP, de la que Mueller y colaboradores dieron cuenta en 1999, demostrando su capacidad de inhibición del crecimiento de los queratinocitos en modelos celulares.

Finalmente se han señalado otros usos terapéuticos potenciales de βLAP frente a esquistosomosis (Pinto y col.,1977) y como fármaco antiinflamatorio (Moon y col., 2007).

1.5. ACTIVIDAD ANTINEOPLÁSICA DE βLAP

Estudios iniciales

Los primeros datos de la posible actividad antitumoral de los compuestos naftoquinónicos extraídos del Ipê roxo proceden, una vez más, del *Instituto de Antibióticos de la Universidade Federal de Pernambuco* (Ferreira de Santana y col., 1968; D`Albuquerque y col., 1972). Estudios llevados a cabo, de manera simultánea, en EEUU confirmaron estos datos (Perdue y Hartwell, 1969). Aunque el Lapachol no presentó la efectividad antineoplásica esperada, probablemente como consecuencia de las pequeñas dosis orales ensayadas (50 mg/Kg), llegó a ser comercializado por el *Laboratorio Farmacéutico del Estado de Pernambuco* (LAFEPE) en la pasada década (Fonseca y col., 2004).

El interés por las naftoquinonas del Ipê roxo y en particular por la βLAP, se recuperó a partir de la década de los noventa del siglo pasado con una avalancha de patentes y de estudios científicos que reafirman su potencial frente al cáncer a través de mecanismos de acción totalmente novedosos, como se documenta en los siguientes párrafos.

Estudios *in vitro*

Son muy numerosos los estudios llevados a cabo en los últimos años dirigidos a desvelar los mecanismos bioquímicos implicados en la actividad antitumoral de βLAP en diferentes modelos celulares de cáncer, como los de mama, pulmón, colo-rectal o de próstata, así como

melanomas y leucemias (Li y col., 1999; Pardee y col., 2002). A pesar de los esfuerzos dedicados en esta dirección, aún no se han podido esclarecer en su totalidad los mecanismos de acción antineoplásica de βLAP.

Los primeros estudios en este ámbito relacionaron la actividad de βLAP con la inhibición de la topoisomerasa I, enzima involucrada en los procesos de replicación y de trascripción del ADN. Además, esta capacidad inhibitoria, se diferencia de la de otros agentes quimioterápicos como la camptotecina. La βLAP retiene la topoisomerasa I en el ADN bloqueando, de esta forma, la continuidad del proceso replicativo e induciendo la apoptosis (Li y col., 1993b; Planchon y col., 1995; Li y col., 1995).

Posteriormente, se probó la acción de βLAP sobre la topoisomerasa II, que ejerce una inhibición catalítica irreversible (Krishnan y Bastow, 2000; Krishnan y Bastow, 2001).

Algunos trabajos han atribuido la recuperación de la capacidad apoptótica a la generación de radicales libres por parte de βLAP. De hecho, se observó una inhibición de la apoptosis cuando βLAP se administró en presencia de vitamina C (Molina-Portela y col., 1996; Shiah y col., 1999).

Los resultados de los estudios desarrollados por el grupo de Boothman mostraron claras evidencias de la actuación de βLAP sobre la enzima NAD(P)H: quinona oxireductasa (NQO1) que, a través de procesos redox, activa mediadores de la apostosis (calpaina) que pueden ser responsables de su citotoxicidad en células tumorales de mama y de próstata (Pink y col., 2000; Planchon y col., 2001).

Este mismo grupo de investigación puso de manifiesto la existencia de una sinergia entre la quimioterapia con βLAP y la

radioterapia, lo que amplía su utilidad potencial como antineoplásico (Boothman y col., 1989; Park y col., 2005). Este tipo de efectos sinérgicos se han descrito también para las asociaciones de βLAP con taxol, mitomicina, genisteína y gencitabina (Li y col., 1999; Park y col., 2005; Li, 2005).

En 2003, el grupo dirigido por Chiang Li y Arthur Pardee realizaron un importante descubrimiento al probar que la inducción de la apoptosis por βLAP está relacionada con la modulación directa de la expresión de la proteína E2F1, responsable de puntos de comprobación del ADN (*checkpoints*) en la fase S del ciclo celular de replicación (Li y col., 2003).

Estudio *in vivo*

En la tabla 1.1 y 1.2 se han concentrado los resultados de los estudios *in vivo* publicados sobre la actividad antineoplásica y la toxicidad de βLAP. Como puede observarse, los datos disponibles de estudios en animales son escasos y con resultados que adolecen de una considerable variabilidad.

Algunos de estos estudios fueron realizados hace varias décadas momento en el que se empleaban diferentes criterios de experimentación animal. Súmase a esto, la variabilidad debida a la vía de administración, al modelo animal empleado, al régimen posológico y a la pureza y forma de dosificación de βLAP, además de la variabilidad propia de los estudios en animales, que, en conjunto, justifican las amplias diferencias encontradas.

Las dosis terapéuticas administradas varían desde los 7 $mg \cdot Kg^{-1}$ hasta los 250 $mg \cdot Kg^{-1}$ (Tabla 1.1). Las dosis tóxicas se sitúan en valores similares a los encontrados para la actividad terapéutica, en el intervalo

de 9 $mg \cdot Kg^{-1}$ a 125 $mg \cdot Kg^{-1}$ (Tabla 1.2). La mejora en la biodisponibilidad de βLAP cuando se administra con hidroxi-propil-β-ciclodextrina se traduce en una reducción de la DL_{50} hasta los 50 $mg \cdot Kg^{-1}$, claramente menor que la obtenida con el empleo de suspensiones o de disoluciones oleosas (Nasongkla y col., 2003). Por otra parte, la administración tópica de βLAP, incluso a dosis de 800 $mg \cdot Kg^{-1}$, no provoca la aparición de signos de irritabilidad dérmica, lo que abre perspectivas interesantes para la utilización de esta vía.

Con los datos disponibles actualmente, resulta muy complicado estimar una dosis efectiva de βLAP, ya que a los factores asociados al paciente como edad, sexo, condición física y extensión del tumor, es necesario añadir otros relacionados con la vía y la forma de dosificación seleccionada y el régimen de administración seguido. En este sentido, las dosis que aporten los ensayos clínicos en marcha serán fundamentales para la protocolización de los tratamientos con βLAP.

Tabla 1.1. Recopilación de los estudios farmacológicos con βLAP en animales publicados hasta la fecha.

Dosis ($mg \cdot Kg^{-1}$)	Cáncer	Animal	Vía	Régimen de administración	Proveedor de βLAP	Vehículo	Resultados y observaciones	Referencia
7	Sarcoma de Yoshida	Rata	v.o.	9 dosis	UFPE/ Brasil	Suspensión acuosa	Inhibición del tumor en 16,2 %	Ferreira de Santana, 1968
7	Carcino-sarcoma de walker	Rata	v.o.	9 dosis	UFPE/ Brasil	Suspensión acuosa	Inhibición del tumor en 33,5 %	Ferreira de Santana, 1968
10 y 11,5	Sarcoma de Yoshida	-	i.p.	-	UFPE/ Brasil	-	Inhibición de 50 % del tumor para la dosis de 10 y de 62 % para la dosis de 11,5.	D`Albuquerque, 1972
15,6 y 31,3	Sarcoma de Rous	Pollo	v.o.	Entre 6 y 12 dosis	Ciba-Geigy /Suiza	Suspensión acuosa	Aumento alrededor a 100 % en el tiempo de supervivencia medio.	Schaffner-Sabba, 1984
62,5, 125 y 250	Leucemia de Rauscher	Ratón	v.o.	5 dosis/semana durante 4 semanas	Ciba-Geigy/ Suiza	Suspensión acuosa	La dosis de 62,5 no se mostró efectiva, la de 125 prolongó de forma significativa la supervivencia mientras que la dosis de 250 causó una reducción en el tiempo de supervivencia de los animales.	Schaffner-Sabba, 1984
31, 62 y 125	Linfoma de Burkitt	Ratón	v.o.	30 dosis diarias	Ciba-Geigy/ Suiza	Suspensión acuosa	Reducciones significativas del tumor en la dosis de 125 $mg \cdot Kg^{-1}$	Di Gianni, 1997
25 y 50	Ovario	Ratón	i.p.	10 dosis en días alternos en terapia aislada y combinada con Taxol.	Ciba-Geigy/ Suiza	Disolución de lipiodol®	Reducción de 75 % del tumor en terapia aislada. La asociación con taxol hace desaparecer por completo el tumor. No se verificaron anomalías en los órganos internos autopsiados.	Li, 1999

Tabla 1.1. Recopilación de los estudios farmacológicos con βLAP en animales publicados hasta la fecha. **Continuación**.

Dosis ($mg \cdot Kg^{-1}$)	Cáncer	Animal	Vía	Régimen de administración	Proveedor de βLAP	Vehículo	Resultados y observaciones	Referencia
50	Próstata	Ratón	i.p.	6 dosis en días alternos en terapia aislada y combinada con Taxol.	Ciba-Geigy /Suiza	Disolución de lipiodol®	En administración aislada produjo reducción moderada del tumor y asociado con Taxol se verificó una acentuada reducción tumoral.	Li, 1999
8	Carcinoma de Ehrlich	Ratón	i.p.	7 dosis diarias	UFPE	Disolución etanólica a 35 %	Inhibición tumoral del 36,5 %. No se verificaron alteraciones en los órganos internos autopsiados.	Sousa, 2000
55-70	Mama	Ratón	i.p.	-	-	Disolución acuosa de HPβCD	Reducciones en los tumores superiores al 50 %.	Boothman, 2003
10 y 25	Ovario	Ratón	i.p.	Terapia aislada y combinada con Taxol en 6 dosis con intervalos de 24h entre ellas	-	Disolución de lipiodol® o de HPβCD	La terapia aislada presentó elevadas reducciones en el tumor. La terapia combinada reveló efecto sinérgico con resultados de reducción tumoral aún mejores. No se han verificado diferencias entre los vehículos utilizados.	Jiang, 2003
50	Mama	Ratón	i.p.	6 dosis en días alternos en terapia combinada con Taxol	-	Disolución de lipiodol®	Reducción drástica del tumor, sin repercusión en el peso de los animales comparados con el controle.	Jiang, 2003
50	Mieloma múltiple	Ratón	i.p.	6 dosis en días alternos		Disolución acuosa de HPβCD	Disminución estadística del tumor. Non hubo toxicidad en ningún de los animales, ni perdida de peso.	Jiang, 2003
50	Tumor sólido FSaII	Ratón	i.p.	Dosis única aislada y combinada con radioterapia	Sigma/ EUA	Disolución acuosa de HPβCD	La terapia aislada retardó el crecimiento del tumor y su terapia combinada con radiación logró un efecto sinérgico.	Park, 2005

Tabla 1.2. Recopilación de los estudios toxicológicos con βLAP en animales publicados hasta la fecha.

Vía	Animal	Proveedor de βLAP	Vehículo	Régimen de administración	Resultados y observaciones	Referencia
v.o.	Ratón	Ciba-Geigy/Suiza	Suspensiones acuosas	Dosis única	Dosis máxima tolerada (DMT) igual a 1250 $mg \cdot Kg^{-1}$	Schaffner-Sabba 1984
v.o.	Pollo	Ciba-Geigy/Suiza	Suspensiones acuosas	Dosis única	Dosis máxima tolerada (DMT) superior a 1250 $mg \cdot Kg^{-1}$	Schaffner-Sabba 1984
v.o.	Ratas	UFPE/Brasil	Suspensiones acuosas	Dosis única	La DL_{50} se situó por encima de la mayor dosis probada de 1600 $mg \cdot Kg^{-1}$ la cual provocó la muerte de 40 % de los animales. Hasta la dosis de 800 $mg \cdot Kg^{-1}$ ningún signo de toxicidad fue verificado.	Alves, 2002
i.p.	Ratón	Síntesis propia	Disolución acuosa de HPβCD	10 dosis distribuidas a lo largo de 4 semanas	Hasta las dosis de 50 $mg \cdot Kg^{-1}$ no hubo muertes o anomalías fisiológicas. La DL_{50} fue estimada entre 50-60 $mg \cdot Kg^{-1}$. Dosis superiores a 70 $mg \cdot Kg^{-1}$ presentan 100 % de mortalidad	Nasongkla, 2003
i.p.	Ratón	UFPE/Brasil	Disolución etanólica a 35 %	Dosis única	La dosis de 20 $mg \cdot Kg^{-1}$ fue letal para 83,3 % de los animales.	Sousa, 2000
i.p.	Ratón	-	Aceite de oliva	Dosis única	La DL_{50} fue estimada entre 201-207 $mg \cdot Kg^{-1}$. Fueron observados algunos efectos a nivel del SNC, pero las autopsias de los animales supervivientes no revelaron alteraciones anatomopatológicas.	Castro, 1998
i.p.	Rata	UFPE/Brasil	Suspensiones	Dosis diarias de 5 $mg \cdot Kg^{-1}$ durante 90 días.	Discreta leucopenia y anemia reversible sin alteraciones bioquímicas	Santos, 1988
i.p.	Rata	UFPE/Brasil	Suspensiones acuosas	Dosis única	La DL_{50} fue estimada en 80 $mg \cdot Kg^{-1}$	Ferreira de Santana, 1968
i.p.	Rata	UFPE/Brasil	Suspensiones acuosas	Ensayo crónico	Muerte de los animales a partir de la sexta administración, empleando la dosis de 9 $mg \cdot Kg^{-1}$	Ferreira de Santana, 1968
tópica	Conejos	UFRJ/Brasil	Disolución etanólica	Dosis única aplicada en la región dorsal	No hubo signos de irritabilidad dérmica hasta la máxima concentración evaluada (800 $mg \cdot Kg^{-1}$).	Pereira, 2006

Ensayos Clínicos

Estudios de Fase I

Terapia con βLAP en pacientes con tumores sólidos refractarios avanzados

Este estudio, iniciado en septiembre de 2003, se dirigió a evaluar la tolerancia al fármaco y a caracterizar su perfil farmacocinético tras su administración intravenosa.

En el ensayo intervinieron 18 pacientes, hombres y mujeres de mediana edad (58,5 años), con diferentes tipos de cáncer - pulmonar, sarcoma, colo-rectal, pancreático y otros - que no respondían a las terapias disponibles. Las dosis administradas se situaron entre 10 y 550 mg/m^2, con frecuencia semanal durante 9 meses.

Los resultados experimentales permiten concluir una farmacocinética lineal para βLAP, incluso para dosis superiores a 390 mg/m^2, que se caracteriza por un aclaramiento plasmático de 114 $L/h/m^2$ y un volumen aparente de distribución de 490 L/m^2. Tras la administración de una dosis de 390 mg/m^2 por infusión intravenosa durante 1h, la concentración plasmática de βLAP alcanzada fue de 2434 ng/mL y de 6,9 ng/mL a las 24 horas. La administración repetida de dosis semanales no produce acumulación del fármaco. El intervalo de dosis estudiado no fue suficiente para determinar la dosis máxima tolerada. Apenas se registraron efectos colaterales, que incluyen ligeras mialgias, reducción del apetito, anemia y fatiga (ArQule 2004; Shapiro y col., 2005; NCI, 2006a).

Terapia con βLAP en asociación con taxol en pacientes con tumores sólidos avanzados

En diciembre de 2004 se inició este ensayo con los objetivos de determinar la dosis máxima tolerada, caracterizar la farmacocinética y llevar a cabo una evaluación preliminar de la actividad antitumoral de βLAP en combinación con el taxol.

En el estudio participaron 16 pacientes aquejados de distintos tipos de tumores sólidos avanzados, que siguieron tratamientos protocolizados durante 8 semanas. Uno de ellos consiste en la administración intravenosa de 50 a 100 mg/m^2 de βLAP durante cinco días consecutivos y una dosis única de taxol al tercer día. El segundo de los protocolos evaluados consiste en una dosis única de βLAP asociada a la de taxol. Ambos ciclos de tratamiento se repiten cada 3 semanas.

La combinación de los dos fármacos no produce alteraciones de importancia en los parámetros farmacocinéticos de cada uno de ellos. La combinación de βLAP-taxol fue bien tolerada, si bien se detectaron casos de neutropenia y anemia. Finalmente, 12 de los 16 pacientes consiguieron cuadros clínicos de estabilidad o de mejora (Li y col., 2006; NCI, 2006b).

Estudio de Fase II

Terapia con βLAP en asociación con gemcitabina en pacientes con adenocarcinoma de páncreas

En este ensayo, llevado a cabo en enero de 2005, participaron 73 pacientes con una edad media de 63 años. El tratamiento consistió en ciclos semanales con infusiones intravenosas de βLAP de 400 mg/m^2 y de gemcitabina de 800 mg/m^2 repetidos cada cuatro semanas.

En una elevada proporción de pacientes se observaron regresiones en los tumores que confirman, de modo preliminar, la utilidad de la asociación. Los efectos adversos mas destacables de este tratamiento fueron anemia (54 % de los pacientes), hemolisis (17 %), fatiga (15 %), edema (7 %) y náuseas (5 %) (Khong y col., 2007; NCI, 2007a).

Terapia con βLAP en pacientes con leomiosarcoma metastásico avanzado

En febrero de 2006 se inició este ensayo con 54 pacientes con leomiosarcoma metastásico recurrente sometidos a terapias previas con fracaso. Los pacientes recibieron dosis semanales de βLAP de 450 mg/m^2 hasta toxicidad inaceptable.

Aunque varios pacientes experimentaron mejoras clínicas, uno de ellos falleció por la hemólisis producida por el tratamiento. En lo que se refiere a efectos secundarios, los más importantes fueron anemia (68 % de los pacientes), hiperbilirrubinemia (35 %), fatiga (35 %), náuseas (30 %), constipación (24 %), hemolisis (21 %), disnea (21 %) y vómitos (21 %) (Hartner y col., 2007; NCI, 2007b).

Terapia con βLAP en pacientes con carcinoma de cabeza y cuello avanzado

En este ensayo, iniciado en julio de 2006, intervinieron 59 pacientes con carcinoma metastático de cabeza y cuello que no respondieron a las terapias disponibles. Los pacientes recibieron cuatro administraciones semanales de βLAP de 450 mg/m^2.

Aunque el fármaco fue bien tolerado, se registraron los siguientes efectos colaterales: anemia acompañada de edema (11 % de los

pacientes), fatiga (5 %), disnea (4 %) y hiperbilirrubinemia (2 %). El estudio no se ha concluido por lo que los resultados finales se darán a conocer próximamente (Kawecki y col., 2007; NCI, 2007c).

1.6. SISTEMAS DE LIBERACIÓN DE βLAP

La práctica totalidad de las investigaciones llevadas a cabo con βLAP se han centrado en las áreas de farmacología y de química. Los alentadores resultados de los estudios preclínicos y, los muy recientes, de los ensayos clínicos, han sido determinantes para el inicio de los estudios sobre formulación de βLAP. En este sentido, cabe destacar los trabajos de Boothman y Gao dirigidos a obviar las principales limitaciones farmacológicas de βLAP, en especial su reducida biodisponibilidad. Así, se obtuvieron importantes incrementos en la solubilidad de βLAP como consecuencia de su complejación con ciclodextrinas, en particular con hidroxi-propil-β-ciclodextrina. Estos incrementos en la solubilidad del fármaco se reflejaron en una clara mejora de su biodisponibilidad en animales (Nasongkla y col., 2003).

Los estudios de Wang y colaboradores (2006; 2007), publicados recientemente, se centraron en el desarrollo de implantes poliméricos para liberación intratumoral de βLAP. Además, el empleo de diferentes ciclodextrinas permite una amplia modulación de la velocidad de cesión del fármaco, que da lugar a distintas cinéticas, relacionada con grado de complejación obtenido.

El avance más reciente en sistemas de liberación de βLAP, propone su incorporación a micelas. Los sistemas desarrollados con copolímeros PEG-PLA permiten la liberación *in vitro* de alrededor de un

50 % del fármaco en 18 h. Además, los ensayos llevados a cabo sobre líneas celulares, pusieron de manifiesto que la acción citotóxica de estos sistemas, es selectiva para las células cancerosas. Por otra parte, la citotoxicidad de βLAP no se ve modificada por su encapsulación en las micelas (Blanco y col., 2007).

1.7. REFERENCIAS

F. C. Alves. Desenvolvimento de formas farmacêuticas a base de beta-lapachona. Recife/Brazil: Programa de Pós-graduação em Ciências Farmacêuticas da UFPE; 2002.

Andrade-Neto VF, Goulart MOF, da Silva Filho,Jorge F., da Silva MJ, Pinto, Do Carmo FR, Pinto AV, et al. Antimalarial activity of phenazines from lapachol, β-lapachone and its derivatives against Plasmodium falciparum *in vitro* and Plasmodium berghei *in vivo*. Bioorg. Med. Chem. Lett. 2004;14(5):1145-1149.

Antunes RMP, Lima EO, Pereira MSV, Camara CA, Arruda TA, Catao RMR, et al. *In vitro* antimicrobial activity and determination of the minimum inhibitory concentration (MIC) of natural and synthetic compounds against bacteria and leveduriform fungi. Rev. Bras. Farmacogn. 2006;16(4):517-524.

ArQule. Arqule presents preliminary interim phase 1 date for ARQ 501 and announces combination study with Taxotere. Nota de prensa de Arqule. September, 2004.

Blanco E, Bey EA, Dong Y, Weinberg BD, Sutton DM, Boothman DA, et al. beta-Lapachone-containing PEG-PLA polymer micelles as novel nanotherapeutics against NQO1-overexpressing tumor cells. J. Control. Release 2007. en prensa.

Brandão MAF, Braga de Oliveira A, Snieckus V. Combined directed metalation-cross coupling strategies. A regiospecific route to heteroring-annelated ortho-naphthoquinones and a short synthesis of β-lapachone. Tetrahedron Lett. 1993;34(15):2437-2440.

Boothman DA, Trask DK, Pardee AB. Inhibition of potentially lethal DNA damage repair in human tumor cells by β-lapachone, an activator of topoisomerase I. Cancer Res. 1989;49(3):605-612.

Boothman D, Gao J, Nasongkla N, Pink J, inventors. Case Western Reserve University, USA, assignee. Lapachone delivery systems, compositions and uses related thereto. PCT Designated States: Designated States W: AE, AG, AL, AM, AT, AU, AZ, BA, BB, BG, BR, BY, BZ, CA, CH, CN, CO, CR, CU, CZ, DE, DK, DM, DZ, EC, EE, ES, FI, GB, GD, GE, GH, GM, HR, HU, ID, IL, IN, IS, JP, KE, KG, KP, KR, KZ, LC, LK, LR, LS, LT, L patent 2003090710. 2003 November 06.

Boveris A, Docampo R, Turrens JF, Stoppani AO. Effect of beta and alpha-lapachone on the production of H_20_2 and on the growth of Trypanosoma cruzi. Rev. Asoc. Argent. Microbiol. 1977;9(2):54-61.

Boveris A, Docampo R, Turrens JF, Stoppani AO. Effect of β-lapachone on superoxide anion and hydrogen peroxide production in Trypanosoma cruzi. Biochem. J. 1978;175(2):431-439.

Butle MS. Natural products to drugs: natural product derived compounds in clinical trials. Nat. Prod. Rep. 2005;22:162-195.

Carvalho PER. Espécies arbóreas brasileiras. 1st ed. Colombo: Embrapa; 2003.

Castro MS, Silva E, Oliveira A. Avaliação da toxicidade aguda da beta-lapachona. Proceedings of 50ª Reunião da Sociedade Brasileira para o Progresso da Ciência; Natal, Brasil. 1998: 1199-1199.

Cruz FS, Docampo R, Boveris A. Generation of superoxide anions and hydrogen peroxide from β-lapachone in bacteria. Antimicrobial Agents Chemother. 1978;14(4):630-633.

D`Albuquerque IL, Maciel MCN, Schuler AR, Araujo MCM, Maciel GM, Cavalcanti MSB, Martins DG, Lacerda AL. Preparação e primeiras observações sobre as propriedades antibióticas e antineoplásicas das naftoquinonas homólogas inferiores na série da 2-hidroxi-3-(3-metil-2-butenil)-1,4-naftoquinona (lapachol). Rev. Inst. Antibiot. 1972;12:31-40.

De Moura KCG, Salomao K, Menna-Barreto RFS, Emery FS, Pinto,Maria do Carmo F.R., Pinto AV, et al. Studies on the trypanocidal activity of semi-synthetic pyran[b-4,3]naphtho[1,2-d]imidazoles from β-lapachone. Eur. J. Med. Chem. 2004;39(7):639-645.

Di Gianni P, Franco M, Bustuoabad OD, Ruggiero R. β-Lapachona: una naftoquinona con actividad antitumoral in vivo. Bol. Acad. Nac. Med. B. Aires. 1997;75(1):145-52.

Docampo R, Lopes JN, Cruz FS, Souza W. Trypanosoma cruzi: ultrastructural and metabolic alterations of epimastigotes by beta-lapachone. Exp. Parasitol. 1977;42(1):142-149.

Ferreira de Santana C, Gonçalves de Lima O, D'Albuquerque IL, Lacerda AL, Martins DG. Antitumor and toxicological properties of an extract of wood from the trumpet bush, Tabebuia avellanedae. Rev. Inst. Antibiot. 1968;8(1-2):89-94.

Fieser LF. Naphthoquinone antimarials. XVI. Water-soluble derivatives of alcoholic and unsaturated compounds. J. Am. Chem. Soc. 1948;70:3232-3237.

Fonseca SGC, da Silva LBL, Castro RF, de Santana DP. Validation of the analytical methodology for the determination of lapachol in solutions by HPLC. Quimica Nova 2004;27(1):157-159.

García-Fernández L, Reyes F, Sánchez-Puelles J. The Marine Pharmacy: New Antitumoral Compounds from the Sea. Pharm. News 2002;9(6):495 - 501.

Gonçalves de Lima O, D`Albuquerque IL, Machado MP, Silva E, Pinto GP. Primeiras observações sobre a ação antimicrobiana do lapacho. An. Soc. Biol. Pe. 1956;14:129-135.

Gonçalves de Lima O, D`Albuquerque IL, Gonçalves de Lima C, Dália Maia MH. Substâncias antimicrobianas de plantas superiores. Rev. Inst. Antibiot.1962;4(1/2):3-17.

Gottleib OR, Mors WB. Potential utilization of Brazilian Wood Extractives. J. Agric. Food Chem. 1980;28:196-215.

Guiraud P, Steiman R, Campos-Takaki G, Seigle-Murandi F, Simeon de Buochberg M. Comparison of antibacterial and antifungal activities of lapachol and β-lapachone. Planta Med. 1994;60:373-374.

Hartner LP, Rosen L, Hensley M, Mendelson D, Staddon AP, Chow W, et al. Phase 2 dose multi-center, open-label study of ARQ 501, a checkpoint activator, in adult patients with persistent, recurrent or metastatic leiomyosarcoma (LMS). Proceedings of 2007 ASCO Annual Meeting; Chicago, USA. June 1-5, 2007: 20521.

Hooker SC, Shepard HW, Walsh JG, Connitt GH. Constitution of lapachol and its derivatives. V. The structure of Paterno's "isolapachone". J. Am. Chem. Soc. 1936;58:1190-1197.

Jiang Z, Reddy DG, inventors. Cyclis Pharmaceuticals, Inc., USA, assignee. Pharmaceutical compositions containing b-lapachone or derivatives or analogs. PCT Designated States: Designated States W: AE, AG, AL, AM, AT, AU, AZ, BA, BB, BG, BR, BY, BZ, CA, CH, CN, CO, CR, CU, CZ, DE, DK, DM, DZ, EC, EE, ES, FI, GB, GD, GE, GH, GM, HR, HU, ID, IL, IN, IS, JP, KE, KG, KP, KR, KZ, LC, LK, LR, LS, LT, L patent 2003011224. 2003 February 13.

Kawecki A, Adkins DR, Cunningham CC, Vokes E, Yagovane DM, Dombal G, et al. A phase II study of ARQ 501 in patients with advanced squamous cell carcinoma of the head and neck. Proceedings of 2007 ASCO Annual Meeting; Chicago, USA. June 1-5, 2007: 16509.

Khong HT, Dreisbach L, Kindler HL, Trent DF, Jeziorski KG, Bonderenko I, et al. A phase 2 study of ARQ 501 in combination with gemcitabine in adult patients with treatment naïve, unresectable pancreatic adenocarcinoma. Proceedings of 2007 ASCO Annual Meeting; Chicago, USA. June 1-5, 2007: 15017.

Krishnan P, Bastow KF. Novel mechanisms of DNA topoisomerase II inhibition by pyranonaphthoquinone derivatives - eleutherin, α-lapachone, and β-lapachone. Biochem. Pharmacol. 2000;60(9):1367-1379.

Krishnan P, Bastow KF. Novel mechanism of cellular DNA topoisomerase II inhibition by the pyranonaphthoquinone derivatives α-lapachone and β-lapachone. Cancer Chemother. Pharmacol. 2001;47(3):187-198.

Lewis WH, Okunade AL, Elvin-Lewis MPF. Pau d' Arco or Lapacho (Tabebuia). Encyclopedia of Dietary Supplements 2005:527-535.

Lemos TLG, Monte FJQ, Kellen A, Santos L, Fonseca AM, Santos HS, et al. Quinones from plants of northeastern Brazil: structural diversity, chemical transformations, NMR data and biological activities. Nat. Prod. Res. 2007;21(6):529-550.

Li CJ, Zhang LJ, Dezube BJ, Crumpacker CS, Pardee AB. Three inhibitors of type 1 human immunodeficiency virus long terminal repeat-directed gene expression and virus replication. Proc. Natl. Acad. Sci. U.S.A. 1993a;90(5):1839-1842.

Li CJ, Averboukh L, Pardee AB. β-Lapachone, a novel DNA topoisomerase I inhibitor with a mode of action different from camptothecin. J. Biol. Chem. 1993b;268(30):22463-22468.

Li CJ, Wang C, Pardee AB. Induction of apoptosis by β-lapachone in human prostate cancer cells. Cancer Res. 1995;55(17):3712-3715.

Li CJ, Li Y, Pinto AV, Pardee AB. Potent inhibition of tumor survival in vivo by β-lapachone plus taxol: combining drugs imposes different artificial checkpoints. Proc. Natl. Acad. Sci. U.S.A. 1999;96(23):13369-13374.

Li Y, Sun X, LaMont JT, Pardee AB, Li CJ. Selective killing of cancer cells by β-lapachone: Direct checkpoint activation as a strategy against cancer. Proc. Natl. Acad. Sci. U.S.A. 2003;100(5):2674-2678.

Li CJ, inventor. Arqule I, USA, assignee. Beta-lapachone and s-phase drug combinations for cancer treatment. PCT Designated States: Designated States W: AE, AG, AL, AM, AT, AU, AZ, BA, BB, BG, BR, BW, BY, BZ, CA, CH, CN, CO, CR, CU, CZ, DE, DK, DM, DZ, EC, EE, EG, ES, FI, GB, GD, GE, GH, GM, HR, HU, ID, IL, IN, IS, JP, KE, KG, KP, KR, KZ, LC, LK, LR, L patent 2005082354. 2005 September 09.

Li C, Nemunaitis J, Senzer N, Edelman G, Glasner S, Dombal G, et al. A phase Ib trial of ARQ 501, a selective checkpoint activator, in combination with docetaxel in patients with advanced solid tumors. Proceedings of 2006 ASCO Annual Meeting;Atlanta, USA. June 2-6, 2006: 13053.

Longhi, RA. Árvores e arvoretas do sul. 2nd ed. Porto Alegre: L&PM; 1995.

Lopes JN, Cruz FS, Docampo R, Vasconcellos ME, Sampaio MC, Pinto AV, et al. *In vitro* and *in vivo* evaluation of the toxicity of 1,4-

naphthoquinone and 1,2-naphthoquinone derivatives against Trypanosoma cruzi. Ann. Trop. Med. Parasitol. 1978;72(6):523-531.

Menna-Barreto RFS, Henriques-Pons A, Pinto AV, Morgado-Diaz JA, Soares MJ, De Castro SL. Effect of a β-lapachone-derived naphthoimidazole on Trypanosoma cruzi: Identification of target organelles. J. Antimicrob. Chemother. 2005;56(6):1034-1041.

Molina Portela MP, Stoppani AO. Redox cycling of beta-lapachone and related o-naphthoquinones in the presence of dihydrolipoamide and oxygen. Biochem. Pharmacol. 1996;51(3):275-283.

Moon D, Choi YH, Kim N, Park Y, Kim G. Anti-inflammatory effects of β-lapachone in lipopolysaccharide-stimulated BV2 microglia. Int. Immunopharmacol. 2007;7(4):506-514.

Mueller K, Sellmer A, Wiegrebe W. Potential Antipsoriatic Agents: Lapacho Compounds as Potent Inhibitors of HaCaT Cell Growth. J. Nat. Prod. 1999;62(8):1134-1136.

Nasongkla N, Wiedmann AF, Bruening A, Beman M, Ray D, Bornmann WG, et al. Enhancement of solubility and bioavailability of beta-lapachone using cyclodextrin inclusion complexes. Pharm. Res. 2003;20(10):1626-1633.

NCI. Food and Drug Administration gov Identifier NCT00075933. Clinical Trials of National Cancer Institute (USA). 2006a; Available at: http://clinicaltrials.gov/show/NCT00075933. Accessed July 10, 2007.

NCI. Food and Drug Administration gov Identifier NCT00099190. National Institute of Cancer (USA). Clinical Trials of National Cancer Institute (USA). 2006b; Available at: http://clinicaltrials.gov/show/NCT00099190. Accessed July 10, 2007.

NCI. Food and Drug Administration gov Identifier NCT00102700. National Institute of Cancer (USA). Clinical Trials of National Cancer Institute (USA). 2007a; Available at: http://clinicaltrials.gov/show/NCT00102700. Accessed July 10, 2007.

NCI. Food and Drug Administration gov Identifier NCT00310518. National Institute of Cancer (USA). Clinical Trials of National Cancer Institute (USA). 2007b; Available at: http://clinicaltrials.gov/show/NCT00310518. Accessed July 10, 2007.

NCI. Food and Drug Administration gov Identifier NCT00358930. National Institute of Cancer (USA). Clinical Trials of National Cancer Institute (USA). 2007c; Available at: http://clinicaltrials.gov/show/NCT00358930. Accessed July 10, 2007.

Neto GG, Morais RG. Recursos Medicinais de Espécies do Cerrado de Mato Grosso: Um estudo bibliográfico. Acta Bot. Bras. 2003;17(4):561-584.

Neves-Pinto C, Malta VRS, Pinto, Do Carmo FR, Santos RHA, Castro SL, Pinto AV. A Trypanocidal Phenazine Derived from β-Lapachone. J. Med. Chem. 2002;45(10):2112-2115.

Newman DJ, Gordon MC, Snaderb KM. The influence of natural products upon drug discovery. Nat. Prod. Rep. 2000;17:215-234.

OMS. Organización Mundial para la Salud. Report of the Scientific Working Group on Chagas Disease. Buenos Aires, Argentina. 17-20 April 2005.

Pardee AB, Li YZ, Li CJ. Cancer therapy with β-lapachone. Curr. Cancer. Drug Targets 2002;2(3):227-242.

Park HJ, Ahn K, Ahn S, Choi E, Lee SW, Williams B, et al. Susceptibility of cancer cells to β-lapachone is enhanced by ionizing radiation. Int. J. Radiat. Oncol. Biol. Phys. 2005;61(1):212-219.

Perdue RE, Jr., Hartwell JL. Search for plant sources of anticancer drugs. Morris Arboretum Bulletin 1969;20(3):35-53.

Pereira EM, Machado T, Leal IC, Jesus DM, Damaso CR, Pinto AV, et al. Tabebuia avellanedae naphthoquinones: activity against methicillin-resistant staphylococcal strains, cytotoxic activity and *in vivo* dermal irritability analysis. Ann. Clin. Microbiol. Antimicrob. 2006;22:5.

Perez-Sacau E, Soto-Delgado J, Estevez-Braun A, Ravelo AG. Synthesis of 9- and 10-membered macrolactones by selective ozonolysis of 1,4-diazaphenanthrene derivatives. Tetrahedron 2005;61(2):437-445.

Pinto AV, Pinto MCR, Gilbert B, Pellegrino J, Mello RT. Schistosoma mansoni: blockage of cercarial skin penetration by chemical agents. I. Naphthoquinones and derivatives. Trans. R. Soc. Trop. Med. Hyg. 1977;71(2):133-135.

Pinto CN, Dantas AP, De Moura KCG, Emery FS, Polequevitch PF, Pinto, Do Carmo F.R., et al. Chemical reactivity studies with naphthoquinones

from Tabebuia with anti-trypanosoma efficacy. Arzneimittelforschung 2000;50(12):1120-1128.

Planchon SM, Wuerzberger S, Frydman B, Witiak DT, Hutson P, Church DR, et al. Beta-lapachone-mediated apoptosis in human promyelocytic leukemia (HL-60) and human prostate cancer cells: a p53-independent response. Cancer Res. 1995;55(17):3706-3711.

Planchon SM, Pink JJ, Tagliarino C, Bornmann WG, Varnes ME, Boothman DA. β-Lapachone-induced apoptosis in human prostate cancer cells: involvement of NQO1/xip3. Exp. Cell Res. 2001;267(1):95-106.

Pink JJ, Planchon SM, Tagliarino C, Varnes ME, Siegel D, Boothman DA. NAD(P)H:quinone oxidoreductase activity is the principal determinant of β-lapachone cytotoxicity. J. Biol. Chem. 2000;275(8):5416-5424.

Santos ER. Avaliação hematológica e bioquímica do lapachol e da β-lapachona. Proceedings of X Simpósio de plantas medicinais do Brasil; São Paulo, Brasil. 1988:18-18.

Schaffner-Sabba K, Schmidt-Ruppin KH, Wehrli W, Schuerch AR, Wasley JW. beta-Lapachone: synthesis of derivatives and activities in tumor models. J. Med. Chem. 1984;27(8):990-994.

Schuerch AR, Wehrli W. β-Lapachone, an inhibitor of oncornavirus reverse transcriptase and eukaryotic DNA polymerase-a. Inhibitory effect, thiol dependency and specificity. Euro. J. Biochem. 1978;84(1):197-205.

Shapiro G, Supko JG, Ryan DP, Appelman L, Berkenblit A, Craig AR, et al. Eder Phase I trial of ARQ 501, an Activated Checkpoint Therapy

(ACT) agent, in patients with advanced solid tumors. Proceedings of 2005 ASCO Annual Meeting; Orlando, USA. 13-17 May, 2005: 3042.

Shiah SG, Chuang SE, Chau YP, Shen SC, Kuo ML. Activation of c-Jun NH2-terminal kinase and subsequent CPP32/Yama during topoisomerase inhibitor beta-lapachone-induced apoptosis through an oxidation-dependent pathway. Cancer Res. 1999;59(2):391-398.

M. R. Q. Sousa. Estudos dos efeitos da β-lapachona sobre células da linhagem Hep-2 carcinoma de Erlich e sarcoma 180. Recife/Brasil: Programa de Pos-graduação em Ciencias Biológicas da UFPE; 2000.

Wang F, Blanco E, Ai H, Boothman DA, Gao J. Modulating β-lapachone release from polymer millirods through cyclodextrin complexation. J. Pharm. Sci. 2006;95(10):2309-2319.

Wang F, Saidel GM, Gao J. A mechanistic model of controlled drug release from polymer millirods: Effects of excipients and complex binding. J. Controlled Release 2007;119(1):111-120.

Catedral de Santiago de Compostela

Capítulo 2

Objetivos

Los resultados de la revisión bibliográfica llevada a cabo ponen de manifiesto el indudable potencial terapéutico de β-lapachona (βLAP), que sigue siendo objeto de amplias investigaciones, tanto en el ámbito académico como en el industrial. Por otra parte, los resultados de los últimos ensayos clínicos hacen previsible su incorporación al arsenal terapéutico a corto plazo (capítulo 1).

Estos resultados alentadores contrastan con la escasa información disponible acerca de las propiedades físico-químicas, tecnológicas y biofarmacéuticas del fármaco, necesarias para su incorporación, en condiciones óptimas, a las formas de dosificación más adecuadas.

Partiendo de estos hechos, el trabajo a desarrollar se ha estructurado en dos etapas, que responden a dos objetivos concretos: estudios de preformulación de βLAP y desarrollo de una serie de aproximaciones tecnológicas – con evaluación de la utilidad de cada una de ellas – para la formulación del fármaco.

En la primera etapa se llevará a cabo una caracterización lo más completa posible de las propiedades físico químicas de βLAP con especial atención a la búsqueda y definición de posibles polimorfos (capítulo 3 y 4). También será objeto de una especial atención los estudios de estabilidad de βLAP, que comprenderán estabilidad en disolución y en estado sólido, con evaluación de los efectos de variables ambientales (luz y humedad relativa), de características del medio (pH) y de la complejación del fármaco con ciclodextrinas (capítulos 5 y 6). Esta etapa del estudio se completará con estudios de compatibilidad de βLAP con los excipientes de más amplia utilización en formas de dosificación sólidas (capítulo 7).

Para alcanzar el segundo de los objetivos, se evaluarán los efectos de la precipitación del fármaco sobre polímeros hidrofílicos (capítulo 8), de la microprecipitación por cambio de fase (capítulo 9) y de la formación de complejos de inclusión con ciclodextrinas (capítulo 10) sobre las propiedades de βLAP, en especial sobre los cambios producidos en su velocidad de disolución. Finalmente, se desarrollarán sistemas termosensibles útiles para la administración intratumoral de βLAP (capítulo 11), con liberación del fármaco modulada por la incorporación de aditivos cosolubilizantes.

Campus Universitario Sur, USC

Capítulo 3

Caracterización Físico-química de β-lapachona

3.1. INTRODUCCIÓN

En el desarrollo de una nueva entidad terapéutica es imprescindible acumular el máximo de información acerca del comportamiento de la molécula a lo largo de las etapas de investigación preclínica y clínica. La determinación de las características fisicoquímicas del fármaco innovador constituye un valioso instrumento para la definición de los límites de calidad y el establecimiento de criterios de seguridad y de eficacia terapéutica (ICH Q6A, 1999). Una exhaustiva y minuciosa búsqueda de puntos débiles e inconsistencias farmacéuticas, que se manifiestan en las condiciones habituales de desarrollo y de producción, debe prevenir y/o minimizar sus posibles efectos negativos sobre la calidad del producto final.

En relación con el estado sólido, el polimorfismo y el pseudo-polimorfismo son fenómenos que afectan a más de 50 % de los compuestos farmacéuticos (Marini y col., 2003). Las distintas formas polimórficas de un principio activo, pueden tener propiedades físicas y químicas diferentes. El punto de fusión, la reactividad química, la solubilidad aparente, la velocidad de disolución, la densidad y las propiedades mecánicas son ejemplos de ello y pueden afectar de forma significativa la calidad, seguridad y eficacia de los medicamentos.

La FDA recomienda que, durante el desarrollo de nuevos fármacos, se lleve a cabo la búsqueda de posibles formas polimórficas y solvatos, a través de procesos de cristalización en distintas condiciones. Además, aconseja un riguroso seguimiento del estado cristalino del

fármaco durante el procesado farmacéutico, el escalado y el periodo de almacenamiento (FDA, 2004).

El objetivo del presente capítulo es definir el perfil fisicoquímico de la β-lapachona [βLAP] a través de diferentes ensayos de caracterización, estableciendo correlaciones entre distintas propiedades de interés farmacéutico y prestando una especial atención a la búsqueda de posibles formas polimórficas de este principio activo.

3.2. MATERIALES Y MÉTODOS

Materiales

Se utilizaron dos lotes de β-lapachona [βLAP], L103 y L503, producidos en la Universidad Federal de Pernambuco/Brasil, además de patrones primarios de βLAP (083K1337) y de lapachol (00509KN) suministrados por Sigma®. Los disolventes y reactivos utilizados en los ensayos fueron de grado analítico o de elevado grado de pureza.

Resonancia magnética nuclear [NMR]

Se realizaron NMR monodimensionales, de 13C y de 1H y experimentos bidimensionales de *Heteronuclear Multiple Bond Correlation* [HMBC] y de *Heteronuclear Multiple Quantum Correlation* [HMQC] en un equipo Varian-Inova operando a 750 MHz. Se disolvió la βLAP en cloroformo deuterado y se referenciaron los espectros por la señal del disolvente (77 ppm para el 13C y 7,26 ppm para el 1H).

Estudio térmico

Las medidas de calorimetría diferencial de barrido [DSC] se llevaron a cabo por duplicado utilizando un calorímetro TA Q100 calibrado con indio. Se analizaron muestras de 3-4 mg, en cápsulas de aluminio tapadas, no herméticas, en atmósfera de nitrógeno con un flujo de 50 $mL \cdot min^{-1}$. Para la determinación del perfil térmico de βLAP se aplicaron distintas velocidades de calefacción y de enfriamiento.

Para la estimación de la pureza se realizaron ciclos de calefacción desde 30 ºC hasta 170 ºC, sobre muestras de entre 1 y 2 mg, con una velocidad de calefacción de 1 $ºC \cdot min^{-1}$ y se aplicó la ecuación de Van´t Hoff (TA Universal analysis 2000 V4.2E; USP 29, 2006).

Se llevaron a cabo medidas termogravimétricas en un equipo Shimadzu TGA 50, sobre muestras de aproximadamente 5 mg, en cápsulas de aluminio abiertas en un intervalo de temperaturas de 25 a 600 ºC a distintas velocidades de calefacción.

Se determinó el contenido en humedad de la βLAP por termogravimetría, empleando el equipo Shimadzu TGA 50, registrando la pérdida de peso que sufren las muestras al ser sometidas a un proceso de calentamiento a razón de 5 $ºC \cdot min^{-1}$ hasta 105 ºC y mantenidas a esta temperatura durante 2h.

Medidas espectrofotométricas y de dispersión de luz

Se obtuvieron los espectros de infrarrojos con trasformada de Fourier [FT-IR] utilizando un aparato Bruker, modelo IFS-66V, en un rango de barrido de 400-4000 cm^{-1} y con una resolución de 4 cm^{-1}. Las muestras fueron comprimidas con KBr en prensa hidráulica.

Los espectros Raman con trasformada de Fourier [FT-Raman] se obtuvieron en un equipo Bruker, modelo FRA 106 equipado con láser de Nd:Yag de 350 mW a longitud de onda de excitación de 1.064 nm.

La caracterización espectrofotométrica UV/visible se llevó a cabo utilizando una disolución de βLAP en etanol/agua (1:1) en un espectrofotómetro Agilent 8453 UV-visible con cubetas de cuarzo de 10 mm. Se registró el barrido ultravioleta-visible [UV-Vis] en el intervalo de 200 a 700 nm.

Difracción de Rayos-X de polvo [XRPD]

El ensayo se llevó a cabo en un equipo Philips PW 1710, utilizando monocromador de grafito con ánodo de Cu y radiación generada a 30 mA y 40 Kv, en el intervalo $2<2\theta<60$, con una velocidad de barrido de 0,02 $º2\theta \cdot s^{-1}$.

La determinación de la estructura cristalina de la βLAP fue llevada a cabo de forma inédita, tal como se recoge en la correspondiente separata que constituye el capítulo 4.

Análisis morfológico

La evaluación morfológica de las partículas de βLAP se llevó a cabo por microscopía electrónica de barrido [SEM] utilizando un aparato LEO-435VP conectado a un equipo de microanálisis y por microscopía óptica [OM] mediante un microscopio Olympus SZ60 conectado a una cámara de video. El procesado de la imagen de, aproximadamente, 600 partículas obtenida por OM se realizó utilizando el programa analySIS® versión 3.2 que permitió la determinación de los diámetros de Feret y la

obtención de las distribuciones de tamaño de partícula de los materiales evaluados que se caracterizaron a través de los valores de diámetro medio y desviación estándar [SD].

Superficie especifica

El área superficial específica se determinó mediante la técnica de adsorción de nitrógeno en un aparato micromeritics ASAP 2000, previa desgasificación de las muestras durante 24h a 50 ºC y 10^{-3} mmHg, aplicando el modelo propuesto por Brunauer, Emmett y Teller [BET] (Stanley-Wood, 1983). La porosidad (< 0,1 μm) se estimó también a partir de la isoterma de adsorción de nitrógeno (Stanley-Wood, 1983).

Densidad real

Se llevó acabo por picnometría de helio, por triplicado, utilizando un picnómetro Quantachrome MPY-2.

Coeficiente de reparto [P_{ow}]

El procedimiento experimental elegido para esta determinación siguió la normativa 123 de la OECD (OECD 123, 2003) que establece un método validado para fármacos poco hidrosolubles. La concentración de βLAP en la fase acuosa y octanólica fueron evaluadas por espectrofotometría UV-visible (Agilent 8453) a una longitud de onda de 257 nm. El P_{ow} fue determinado mediante la ecuación:

$$P_{ow} = \frac{C_o}{C_w}$$

donde, C_o es la concentración del fármaco en la fase octanólica y C_w es la concentración del fármaco en la fase acuosa. El coeficiente de reparto fue representado por su logaritmo en base 10.

Propiedades de flujo

Para su evaluación se ha acudido al empleo del aparato Hosokawa Powder Tester PT-E, determinando los índices de *flowability* y de *floodability* a partir de los parámetros compresibilidad [C], ángulo de reposo [AR], de caída [AC] y de espátula [AE], dispersibilidad [D] y uniformidad [U] (Thomson, 1984) de la βLAP, tal como fue suministrada.

Screening Polimórfico

La estrategia adoptada para el estudio de las posibles formas polimórficas de βLAP se basó en cuatro métodos de cristalización, frecuentemente utilizados para este tipo de determinaciones y que se describen a continuación (Hilfiker y col., 2003; Zhu y Sacchetti, 2004; Miller y col., 2005). Fueron empleados cinco disolventes de distintas polaridades: acetonitrilo [AN], etanol [EtOH], cloroformo [CLOF], hexanol [HEX] y piridina [PD].

Método anti-disolvente: se lleva a cabo a través de la adición de agua a una disolución saturada de βLAP en la proporción 2:1 (v/v). El precipitado formado es filtrado y secado en estufa a 40 ^{o}C durante 2h. *Cristalización por evaporación*: se basa en la evaporación del disolvente en una disolución saturada del fármaco a temperatura ambiente, hasta la formación de cristales. A continuación se procede a la separación de los cristales por filtración y su posterior secado en estufa a 40 ^{o}C durante 2h.

Cristalización por enfriamiento: consiste en mantener la disolución saturada de βLAP en nevera (4 ^{o}C) hasta crecimiento cristalino. Los cristales obtenidos se separan por filtración y se secan en estufa a 40 ^{o}C durante 2h. *Suspensión con ciclos de calefacción-enfriamiento*: Se añade exceso de fármaco a las disoluciones saturada de βLAP, sometiendo estos sistemas a continuos ciclos de enfriamiento y calefacción (2 y 40 ^{o}C) bajo agitación magnética durante 3 días. Los cristales obtenidos son filtrados y secados en estufa a 40 ^{o}C durante 2h.

Para cada uno de los disolventes seleccionados, se prepararon disoluciones saturadas de βLAP, a temperatura ambiente, incorporando un exceso de βLAP pulverizada, bajo agitación magnética durante 12h. A continuación, las disoluciones se filtraron y se emplearon en las distintas técnicas de cristalización.

Los cristales obtenidos fueron analizados mediante XRPD y DSC, según las recomendaciones de la FDA (FDA, 2004).

3.3. RESULTADOS Y DISCUSIÓN

Los resultados de los estudios de caracterización de βLAP que se presentan a continuación, se obtuvieron con el lote L503, una vez constatada la inexistencia de diferencias en pureza y cristalinidad del fármaco entre los dos lotes utilizados en este estudio.

Caracterización físico-química

NMR

La técnica de NMR permitió dilucidar la estructura molecular de la βLAP (Figura 3.1). Se asignaron las señales que se describen a continuación a partir de los espectros representados en las figuras 3.2. a 3.5.

1H: singlete (Hc) a 1,468 ppm; triplete (Hb) a 1,854 ppm; triplete (Ha) a 2,573 ppm; triplete (He) a 7,503 ppm; triplete (Hf) a 7,638 ppm; doblete (Hd) a 7,8 ppm y doblete (Hg) a 8,0 ppm.

13C: Ca a 16,169 ppm; Cc a 26,768 ppm; Cb a 31,621 ppm; C7 a 79,252 ppm; C4 a 112,729 ppm; Cd a 124,040 ppm; Cg a 128,566 ppm; C2 a 130,16 ppm; Ce a 130,631 ppm; C1 a 132,64 ppm; Cf a 134,736 ppm; C3 a 161,990 ppm; C5 a 178,568 ppm y C6 a 179,854 ppm.

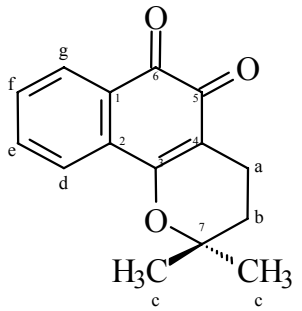

Figura 3.1. Asignación estructural de β-lapachona

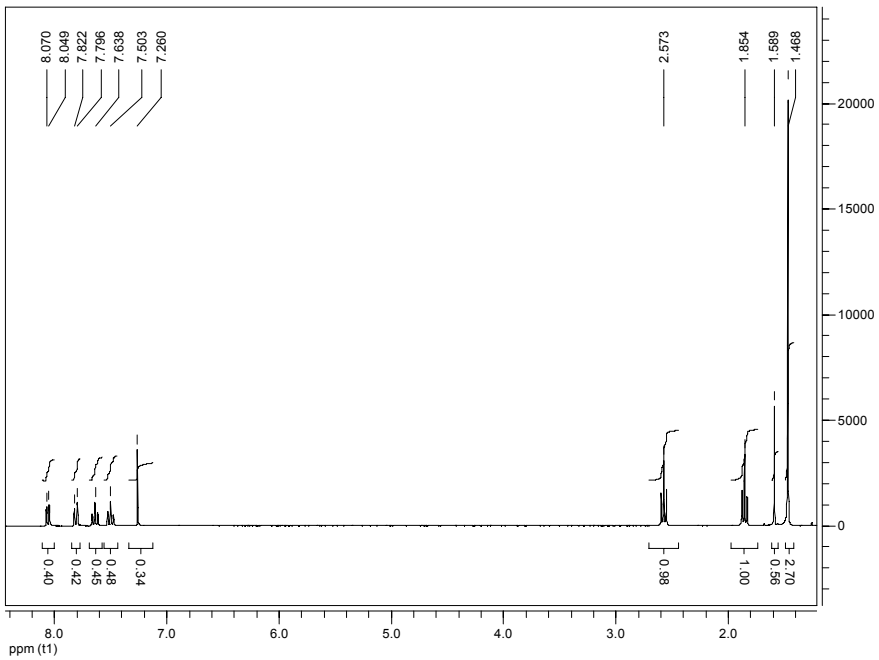

Figura 3.2. Espectro de NMR ^{1}H de la βLAP en cloroformo deuterado, referenciado por el disolvente.

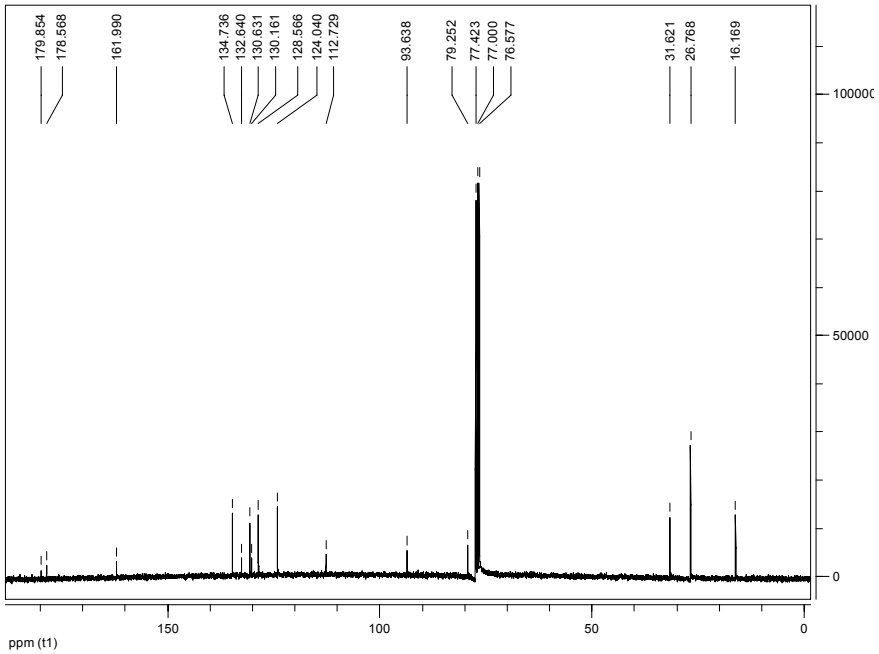

Figura 3.3. Espectro de NMR ^{13}C de βLAP en cloroformo deuterado, referenciado por el disolvente.

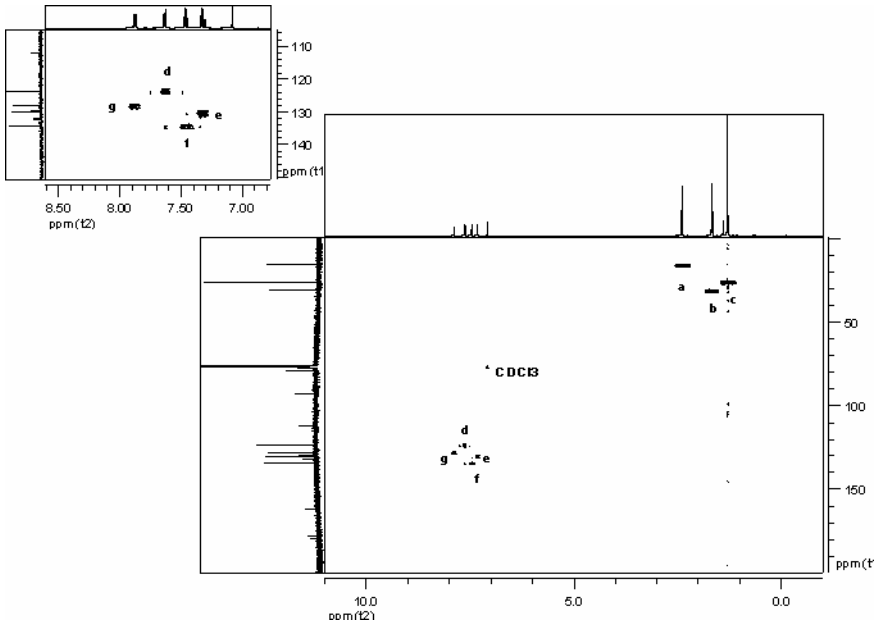

Figura 3.4. Representación del ^{1}H-^{13}C HMQC de βLAP en cloroformo deuterado, en detalle la región aromática.

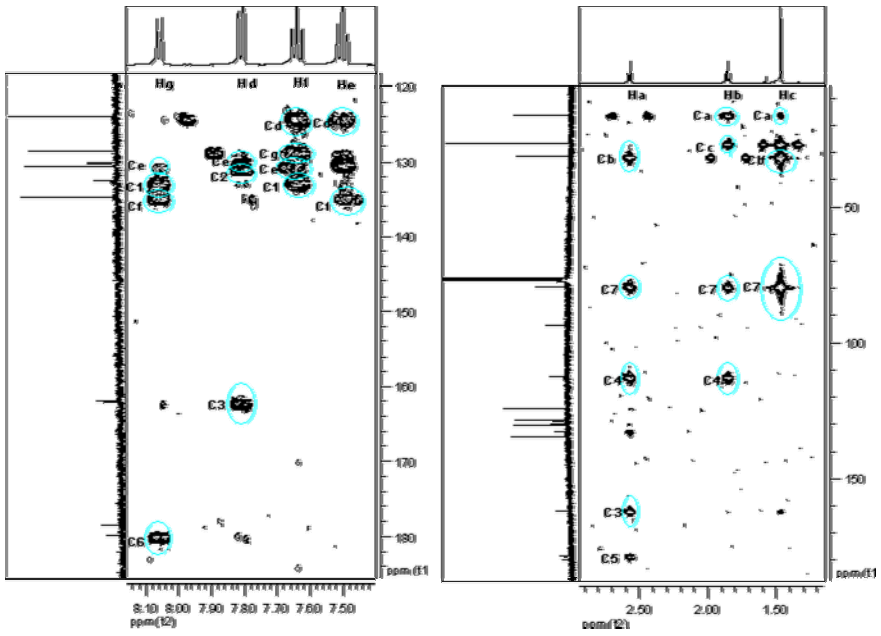

Figura 3.5. Representación del ^{1}H-^{13}C HMBC de βLAP en cloroformo deuterado, siendo A la región aromática y B la región alifática.

Estudio térmico

En la actualidad, los equipos de análisis térmico poseen una elevada sensibilidad, precisión y exactitud, lo que permite obtener información acerca de la cristalinidad del compuesto, de la existencia de polimorfos, de transformaciones físicas como fusión o sublimación, de transiciones vítreas, de procesos de deshidratación o de evaporación, de eventos químicos de pirólisis, de interacciones entre componentes y, también, de la pureza de los fármacos.

Los termogramas de calorimetría diferencial de barrido registrados a velocidades de calentamiento crecientes entre 1 y 30 $^{o}C \cdot min^{-1}$ mostraron un solo evento endotérmico para la βLAP, correspondiente a la fusión del fármaco (Figura 3.6). La entalpía asociada al proceso de fusión se incrementa con la velocidad de calentamiento de la muestra, a la vez que el pico se ensancha perdiendo resolución, como es habitual en este tipo de procesos.

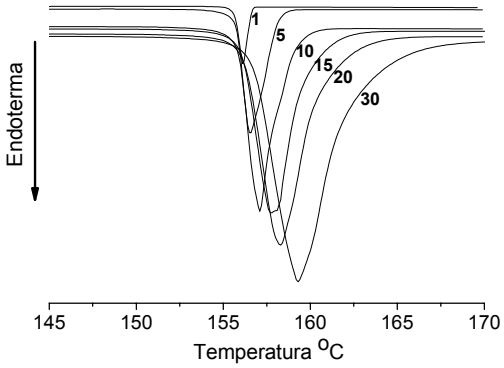

Figura 3.6. DSC de βLAP a velocidades de calefacción crecientes.

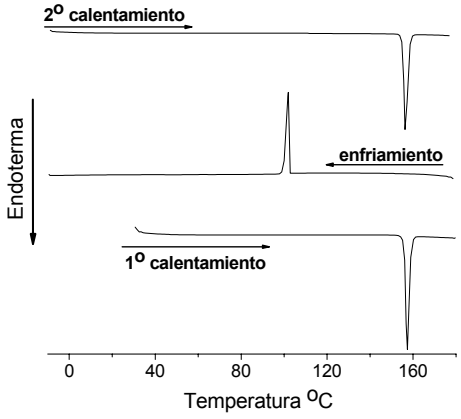

Figura 3.7. Termograma correspondiente a un ciclo de DSC de calefacción-enfriamiento de βLAP.

Adicionalmente, se determinó el perfil térmico DSC de βLAP, a través de la aplicación de ciclos de calefacción–enfriamiento a 10ºC·min^{-1} (Figura 3.7). Como puede observarse, la βLAP presenta un punto de fusión a 157,3 ± 0,16 ºC con una energía asociada de 103,17 ± 1,45 J·g^{-1}. Durante el enfriamiento se produce la cristalización del fármaco a 104,59 ± 2,63 ºC con entalpía de 78,48 ± 7.30 J·g^{-1}, como se demuestra por el pico de fusión registrado en el segundo calentamiento (Tabla 3.1).

Tabla 3.1. Resultados de DSC de βLAP tras calefacción hasta 180 ºC, enfriamiento hasta -10 ºC y nueva calefacción hasta 180 ºC. (Desviación estándar).

Fenómeno	***Rango de fusión ºC***	***Pico ºC***	***Entalpía J·g^{-1}***
Primera fusión	151-162	157,30 (0,16)	103,17 (1,45)
Cristalización	105-99	104,59 (2,63)	78,48 (7,30)
Segunda fusión	152-162	157,00 (0,16)	95,53 (2,14)

La pureza de una sustancia química es un concepto relativo y, desde un punto de vista farmacéutico, es necesario establecer unas especificaciones para este parámetro. En el caso de la βLAP, la determinación de la pureza es de especial interés, dado que aún se produce a pequeña escala, a partir de un extracto vegetal (multicomplejo conteniendo diversas estructuras orgánicas distintas) y que sus posibles impurezas de síntesis no están estudiadas a nivel toxicológico. El proceso de fabricación de este producto implica su cristalización a partir de un medio complejo, lo que podría dar lugar a la presencia de compuestos similares, como el lapachol (isómero y molécula precursora) (D´Albuquerque y col., 1972).

Planchon y colaboradores han señalado una importante repercusión de la presencia de impurezas en los estudios farmacológicos realizados con βLAP suministrada por el proveedor suizo Ciba-Geigy®

(Planchon y col., 1995). La deterrminación de la pureza de los dos lotes de βLAP analizados se llevó a cabo a partir de los datos de fusión obtenidos por DSC (Tabla 3.2). Los lotes analizados presentan una elevada pureza, incluso superior a la del patrón de Sigma®. Los resultados obtenidos sugieren que el proceso de fabricación seguido es reproducible.

Tabla 3.2. Resultados del análisis de pureza de βLAP, basado en la ecuación de Van´t Hoff.

Muestras	***Pureza (%)***	***Corrección (%)***
L503	99,99	0,00005
L103	99,99	0,00006
Patrón Sigma®	99,89	7,8

En la figura 3.8 se puede observar la clara separación de los picos de fusión de la βLAP y del lapachol, con degradación de las muestras por encima de los 200 ºC. Los DSC de los lotes de βLAP estudiados no indican la presencia de lapachol como impureza.

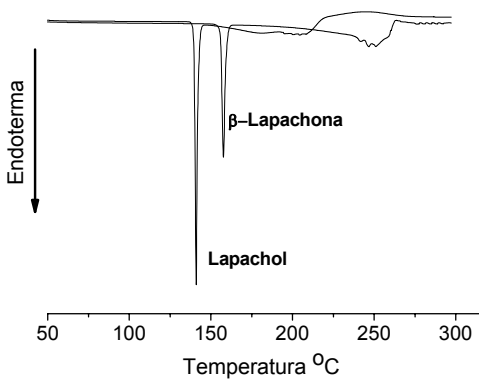

Figura 3.8. DSC de βLAP y de lapachol

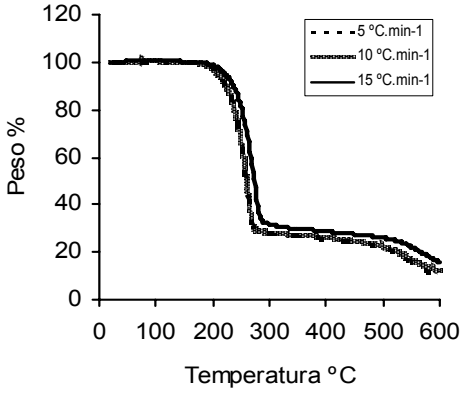

Figura 3.9. TGA de βLAP a distintas velocidades de calefacción.

La técnica de termogravimetría permite determinar los cambios de masa que experimenta la muestra cuando se somete a un proceso de calentamiento. Como puede observarse en la figura 3.9, en la que se presentan las curvas de TGA obtenidas a diferentes velocidades de calefacción, no se detecta una pérdida de peso significativa hasta alcanzar temperaturas cercanas a 230 ºC, a las que comienza a producirse la descomposición del fármaco, que se acompaña de una pérdida de masa del 70 %. La técnica termogravimétrica permitió, además, determinar la humedad de las muestras que en ambos casos resultó ser inferior al 0,5 %.

Medidas espectrofotométricas y de dispersión de luz

Los espectros de interacción de radiaciones UV, FT-IR o FT-Raman con las moléculas o los átomos de una sustancia resultan muy útiles para su análisis cualitativo y cuantitativo, por lo que son técnicas ampliamente utilizadas en el ámbito farmacéutico. De los tres señalados, el espectro ultravioleta de una sustancia es, sin duda, el menos específico.

El espectro UV/Visible de βLAP (Figura 3.10) coincide con el descrito en la literatura para este producto aislado a partir de extractos vegetales (Gonçalves de Lima y col., 1962) y presenta máxima absorción a 257 nm. La figura 3.10 recoge también el barrido para la misma disolución de βLAP sometida a degradación luminosa durante 24h. Como puede observarse, se produce un acentuado cambio en el espectro UV con desplazamiento del máximo de absorbancia hacia menores longitudes de onda. Los cambios observados en la banda principal del

espectro UV pueden servir como parámetro cualitativo a la hora de identificar fotodescomposición de βLAP.

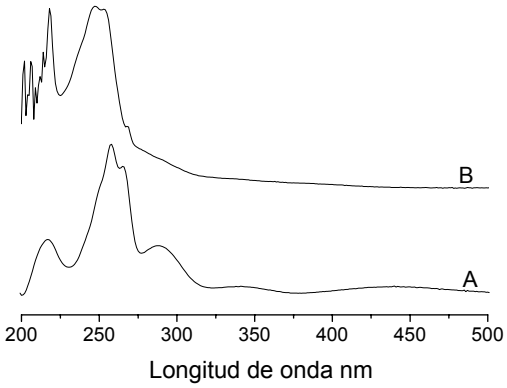

Figura 3.10. Espectro UV de βLAP antes (A) y después (B) de estrés luminoso.

Los espectros FT-IR y FT-Raman son únicos para cualquier compuesto. Pequeñas diferencias en la estructura producen cambios significativos en los espectros, por lo que ambas técnicas son utilizadas en el ámbito farmacéutico para identificación molecular. El espectro FT-Raman y FT-IR proporcionan información similar, aunque las contribuciones relativas de los grupos funcionales difieren para ambas técnicas (USP 29, 2006) por lo que se consideran complementarias. Como se puede apreciar en la Figura 3.11, los picos destacados en el espectro FT-Raman no siempre lo están en el espectro FT-IR. Los datos de asignación de picos por estas técnicas, junto con la identificación molecular inédita hecha a este nivel, son de gran utilidad para poner en evidencia interacciones fármaco-excipiente en sistemas farmacéuticos.

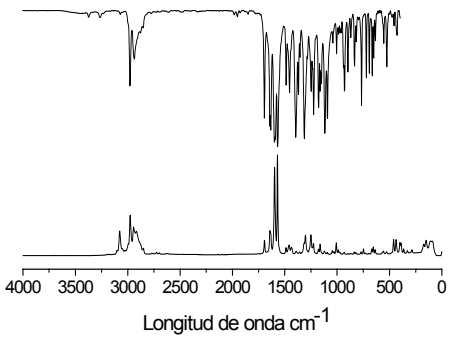

FT-IR (cm^{-1})	FT-Raman (cm^{-1})	Asignación
3069 (vw)	3076 (m)	CH aromático
2978 (s)	2978 (w)	CH aromático
2936 (m,b)	2945 (w,b)	CH alifático
1954 (vw)	-	harmónicas
1695 (vs)	1695 (vw)	C=0
1599 (m)	1599 (vs)	C–C aromático
1568 (m)	1570 (vs)	C–C aromático
1315 (vs)	1303 (vw)	C-O-C
1119 (vs)	1122 (vw)	C-O-C

Figura 3.11. Espectros FT-IR y FT-Raman de βLAP con asignación de picos en la tabla. Las bandas se clasifican por intensidad: muy fuerte (vs); fuerte (s); media (m); debil (w); muy debil (vw); ancha (b).

Difracción de Rayos-X de Polvo [XRPD]

Esta técnica permite un análisis sencillo, rápido y no destructivo, útil para la identificación de fármacos cristalinos, puesto que una forma cristalina produce, como consecuencia de la ordenación tridimensional de sus moléculas, un patrón de difracción de Rayos-X único.

Se obtuvo el difractograma de Rayos-X de βLAP, que no corresponde a ninguno de los compuestos referenciados en la base de datos del *Cambridge Crystallograpic Data Center*, incluso cuando se compara con estructuras cristalográficas de derivados de βLAP (Figuras 3.12 a 3.14).

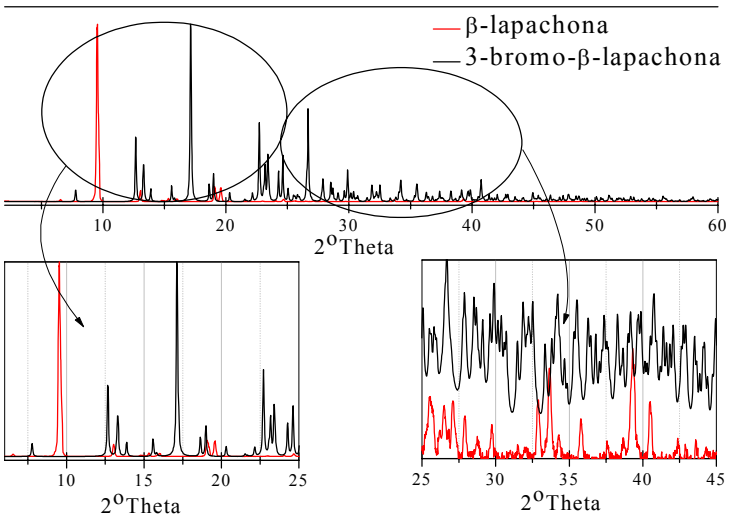

Figura 3.12. Comparación de difractogramas entre βLAP en rojo y 3-bromo-β-lapachona en negro.

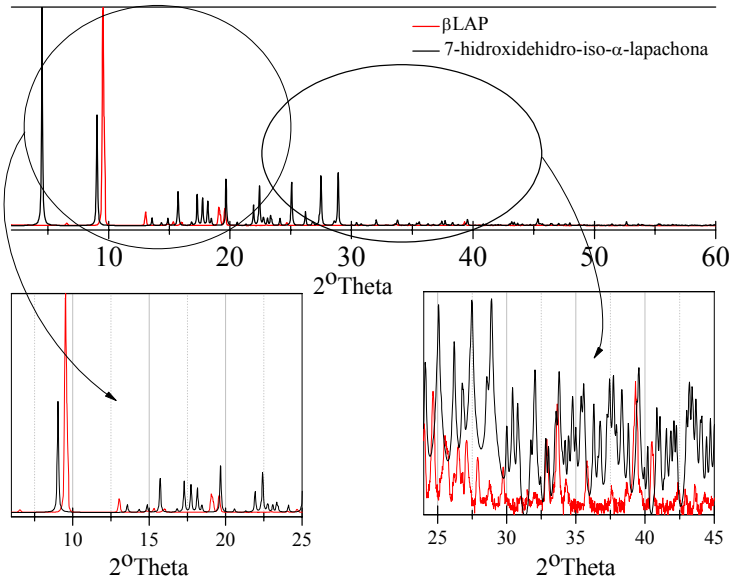

Figura 3.13. Comparación de difractogramas entre βLAP en rojo y 7-hidroxidehidro-iso-α-lapachona en negro.

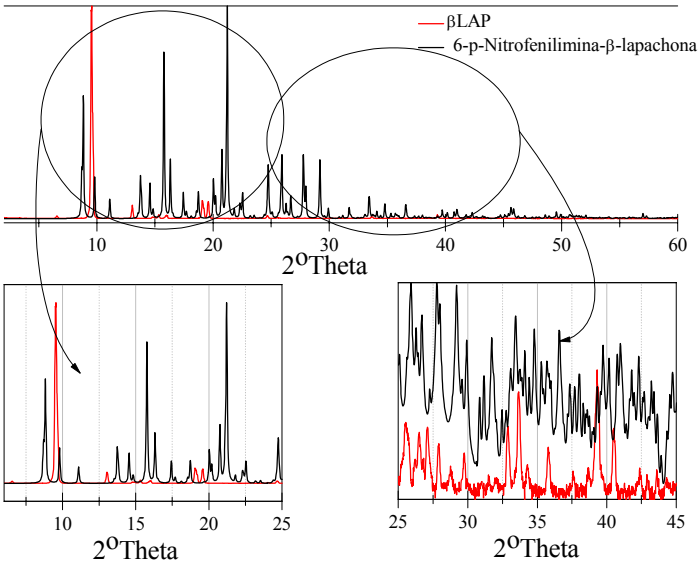

Figura 3.14. Comparación de difractogramas entre βLAP en rojo y 6-p-Nitrofenilimina-β-lapachona en negro

Con objeto de establecer las posibles variaciones en el patrón de difracción para este compuesto en función del tamaño de partícula, se comparó los XRPDs obtenidos con diferentes fracciones granulométricas del producto, con el difractograma teórico de βLAP, derivado a partir de los datos de difracción de monocristal. Como puede apreciarse en los difractogramas de la figura 3.15, aunque las posiciones de los picos coinciden en todos los casos con las del difractograma teórico, sus intensidades relativas varían en función del tamaño de partícula de la muestra, lo que puede ser atribuido a un fenómeno de orientación preferencial de los cristales. Una reducción en el tamaño de las partículas reduce este efecto, aproximándose el difractograma obtenido, al patrón teórico simulado.

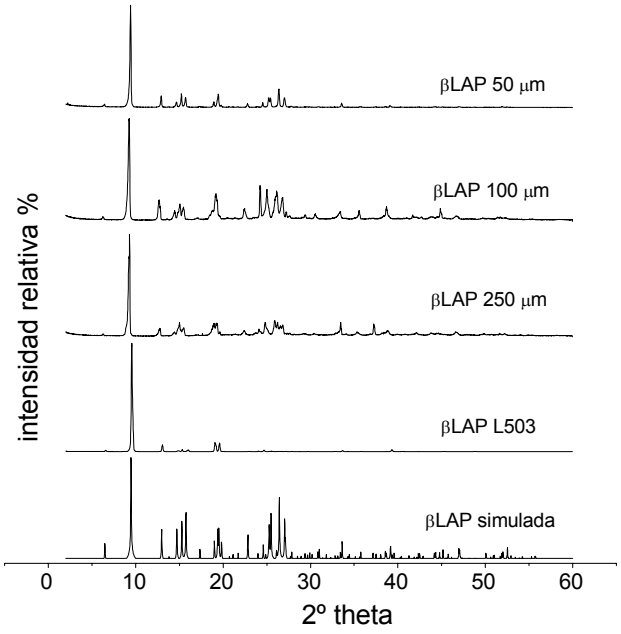

Figura 3.15. Comparación de XRPD de βLAP simulado y el experimental con diferentes fracciones granulométricas del producto

Análisis morfológico

Las fotomicrografias SEM de las partículas de βLAP y del patrón de Sigma® mostraron estructuras cristalinas predominantemente aciculares, con algunos cristales irregulares y muchos fragmentos cristalinos. A través de la técnica de microanálisis fue posible obtener información semicuantitativa de la constitución elemental de las muestras, lo que permitió detectar, tanto en los lotes UFPE como en el patrón Sigma®, contaminación por Ca y Si (Figura 3.16). Estos contaminantes pueden proceder del envase de vidrio en el que se ha acondicionado el material y no afectan a la pureza de éste, como se confirmó mediante DSC.

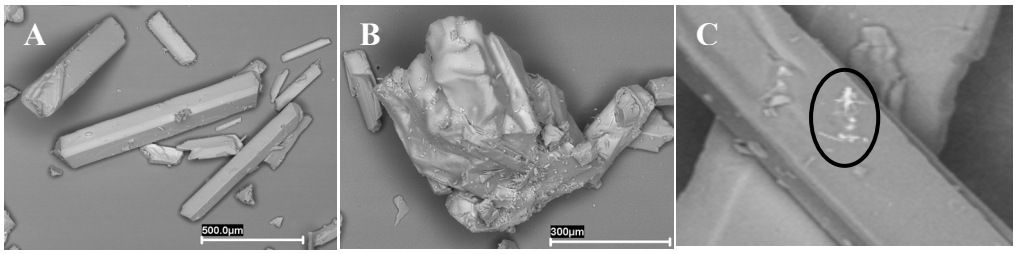

Figura 3.16. Fotomicrografías SEM de cristales típicos de la βLAP (A), cristales atípicos (B) y contaminación superficial en detalle (C).

La industria farmacéutica utiliza cada vez con mayor frecuencia las técnicas de análisis de imagen para la evaluación de la distribución granulométrica de materiales particulares. El tamaño de partícula condiciona en muchos casos el proceso de fabricación de las formas farmacéuticas y, además, puede tener una repercusión directa sobre la eficacia de los preparados en la medida en que puede influir sobre la biodisponibilidad y/o la estabilidad de los productos. En el caso de la βLAP, la velocidad de disolución, posible factor limitante en la absorción de este fármaco poco soluble en agua, está fortísimamente relacionada con su tamaño de partícula.

Para la caracterización de las distribuciones de tamaño de partícula de los lotes de βLAP se calcularon los diámetros de Feret, útiles para la evaluación de partículas no esféricas. Los datos obtenidos por análisis de imagen se ajustaron a una distribución logarítmico normal, lo que permitió determinar los valores de diámetro medio y de desviación estándar geométricas en 122,1 µm y 2,16, para el lote L103, y en 106,8 µm y 2,32, para el lote L503 (Figura 3.17). Como puede observarse, los valores de diámetro medio son considerables y no existen diferencias

importantes entre ambos lotes. Además, se trata de distribuciones muy abiertas debido al elevado número de fragmentos de cristal presentes en las muestras (Figura 3.18).

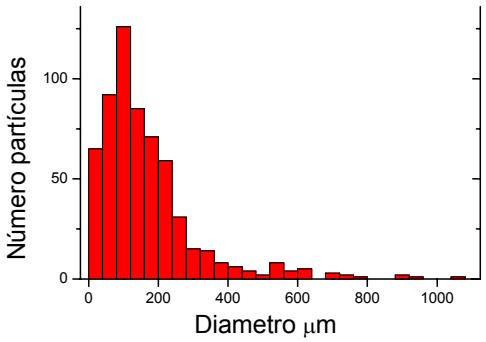

Figura 3.17. Distribución de tamaños de partícula de βLAP L503 por OM (diámetro medio de Feret).

Figura 3.18. Fotomicrografia OM de partículas de βLAP L503.

Superficie específica

Junto con el tamaño de partícula, la superficie específica del fármaco condiciona una serie de propiedades importantes como sus características de flujo y su velocidad de disolución. Se utilizó la aproximación BET para la determinación de la superficie específica obteniéndose un valor de 0,1593 $m^{2}{\cdot}g^{-1}$(Figura 3.19). Así mismo, debe destacarse reducida porosidad de las partículas estimada en $2{,}1{\cdot}10^{-3}$ $cm^{3}{\cdot}g^{-1}$.

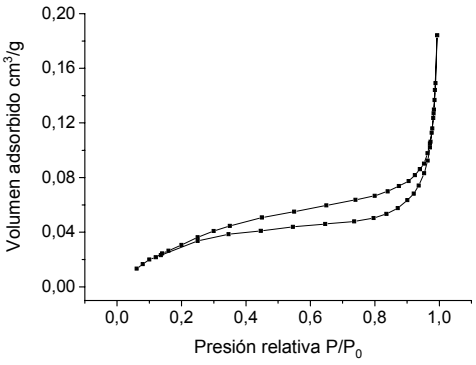

Figura 3.19. Curvas de adsorción y desorción de βLAP según el modelo BET.

Densidad real

La densidad de un polvo puede adoptar distintos valores según la técnica empleada en su determinación. La densidad determinada por picnometría de helio, utilizada en este estudio, denominada densidad real o picnométrica, equivale a la densidad verdadera de un material a menos que contenga espacios vacíos impenetrables, o poros cerrados que sean inaccesibles al gas empleado en el picnómetro.

El valor de densidad real obtenido para la βLAP es de 1,311 ± 0,050 $g \cdot cm^{-3}$, que coincide con la estimación realizada a partir de los datos de difracción de rayos X de monocristal que resultó ser de 1,309$g \cdot cm^{-3}$ (capítulo 4), lo que confirma la inexistencia de poros ciegos en los cristales de βLAP analizados. El valor de densidad real resulta de interés no solo para identificar una entidad química, sino para detectar la presencia de posibles polimorfos, ya que el valor de este parámetro depende de la estructura cristalina y del grado de cristalinidad del producto.

Coeficiente de reparto

El coeficiente de reparto es un indicador de la liposolubilidad de un fármaco, es decir de la facilidad con que atraviesa las membranas biológicas y se determina midiendo su reparto entre el agua y un disolvente orgánico. El método más habitual para la determinación del coeficiente de reparto de fármacos es el del matraz agitado, existiendo diversas variantes del mismo. Este método tiene el inconveniente de sobreestimar la concentración de fármaco en la fase acuosa si se produce la emulsificación parcial del disolvente orgánico (octanol), lo que puede resultar relevante cuando los valores de coeficiente de reparto son elevados.

El método de agitación moderada propuesto por la OECD (OECD 123, 2003) para la determinación de coeficientes de reparto, reduce la posibilidad de formación de microgotas y está particularmente indicado para sustancias altamente hidrófobas. Se basa en la aplicación de una turbulencia controlada en medio termostatizado que promueve el intercambio entre las fases sin provocar la emulsificación del disolvente orgánico. Para la βLAP se obtuvieron valores de P_{ow} de 324,978, con un coeficiente de variación inferior al 10 %. Los valores de log P_{ow} = 2,512, unidos a la reducida hidrosolubilidad del fármaco permiten situarlo, dentro de la clasificación biofarmacéutica, en fármaco tipo II (Amidon y col., 1995), es decir, fármaco poco hidrosoluble que atraviesa fácilmente las membranas biológicas.

Propiedades de flujo

Aunque los valores de algunos de los índices calculados son característicos de un material de flujo deficiente (elevados valores angulares), el cálculo de los parámetros propuestos por Carr (Carr, 1965), tal como se recoge en la tabla 3.3, clasifica a la βLAP como un material de características de flujo intermedias, que puede requerir el empleo de dispositivos y/o de substancias auxiliares para promover el desplazamiento de sus partículas.

Tabla 3.3. Valores de los parámetros de flujo utilizados para la determinación del índice de *flowability*.

Ángulo de Reposo	*Compresibilidad*	*Ángulo de Espátula*	*Uniformidad*	*Flowability*
40 ^{o}	24,3 %	60 ^{o}	6	**Normal**

La evaluación de la tendencia a dispersión del material durante su flujo se evaluó a través del índice de *floodability*, que resultó ser elevado (Tabla 3.4), lo que hace recomendable su manipulación en campana de extracción.

Tabla 3.4. Valores de los parámetros de flujo utilizados para la determinación del índice de *floodability*.

Grado de Flowability	*Ángulo de caída*	*AR - AC*	*Dispersabilidad*	*Floodability*
Normal	30 ^{o}	10 ^{o}	13,5 %	**Relativamente elevado**

Screening Polimórfico

El resultado del screening polimórfico se resume en la tabla 3.5. No se ha encontrado ningún indicio de formación cristalina diferente de la forma inicial de βLAP (polimorfo I). La inmiscibilidad entre el hexanol y el

cloroformo con el agua impidieron la obtención de cristales por el método de anti-disolvente.

Tabla 3.5. Resultados del screening polimórfico.

	Anti-disolvente	***Evaporación***	***Enfriamiento***	***Suspensión***
Acetonitrilo	Polimorfo I	Polimorfo I	Polimorfo I	Polimorfo I
Etanol	Polimorfo I	Polimorfo I	Polimorfo I	Polimorfo I
Hexanol	-	Polimorfo I	Polimorfo I	Polimorfo I
Cloroformo	-	Polimorfo I	Polimorfo I	Polimorfo I
Piridina	Polimorfo I	Polimorfo I	Polimorfo I	Polimorfo I

Los resultados de los análisis térmicos y de los difractogramas de polvo de las muestras están representados en las figuras 3.20 a 3.27. Los cristales de βLAP obtenidos en las distintas condiciones experimentales exhibieron similar perfil térmico, presentando el pico de fusión a 157 ^{o}C ± 0,5 ^{o}C. Además, no se aprecian diferencias importantes en los picos de XRPD que justifiquen la presencia de otra fase cristalina, lo que confirma la estabilidad de la celdilla ortorrómbica original de βLAP.

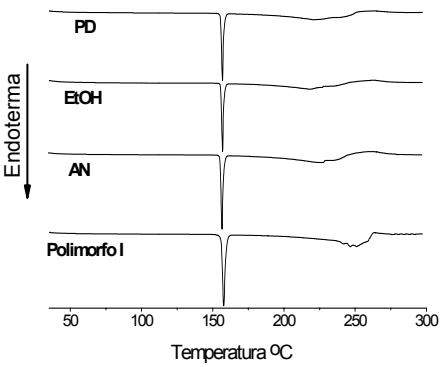

Figura 3.20. DSC de βLAP obtenido por el método de anti-disolvente

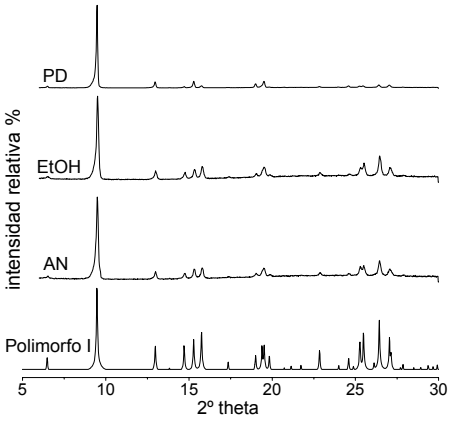

Figura 3.21. XRPD de βLAP obtenido por el método de anti-disolvente.

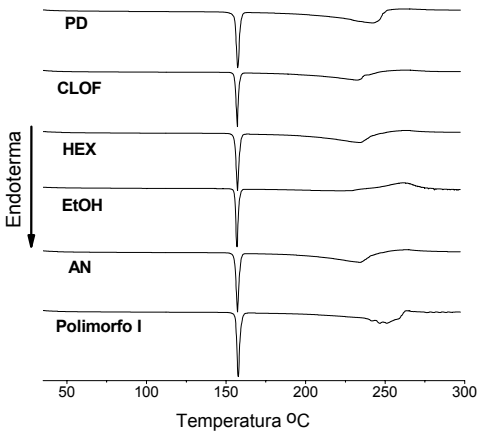

Figura 3.22. DSC de βLAP obtenido por el método de evaporación.

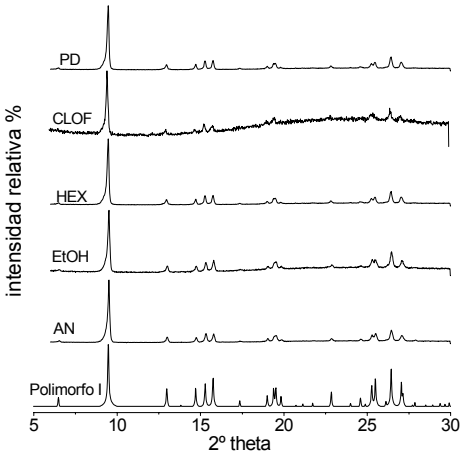

Figura 3.23. XRPD de βLAP obtenido por el método de evaporación.

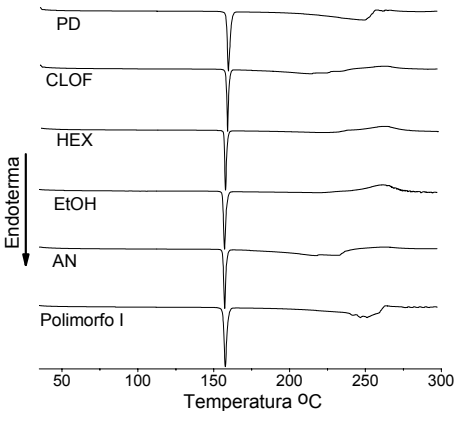

Figura 3.24. DSC de βLAP obtenido por el método de enfriamiento.

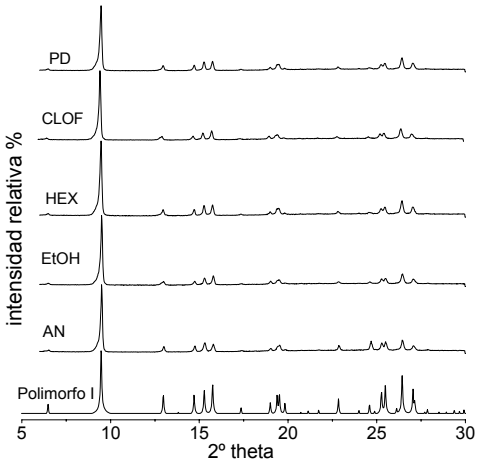

Figura 3.25. XRPD de βLAP obtenido por el método de enfriamiento.

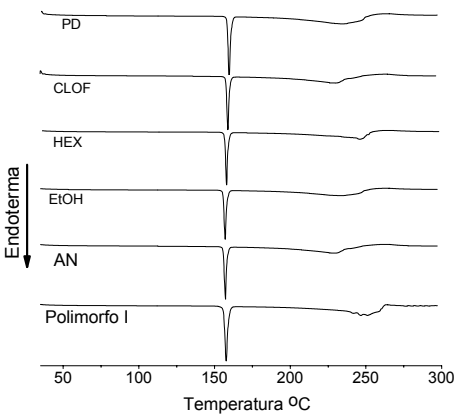

Figura 3.26. DSC de βLAP obtenido por el método de suspensión.

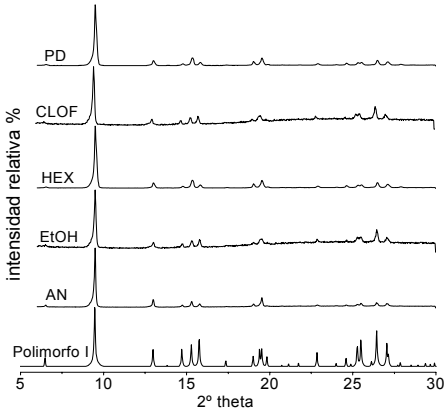

Figura 3.27. XRPD de βLAP obtenido por el método de suspensión.

3.4. CONCLUSIONES

De manera general, la caracterización fisicoquímica realizada aporta una valiosa información, en su mayor parte inédita, acerca de la βLAP lo que permitirá disponer, en el futuro, de elementos de comparación en cuanto a su identificación, valoración y variabilidad entre lotes.

Una única forma cristalina de βLAP se ha identificado en el estudio, tras diferentes procesos de crecimiento cristalino con disolventes de distintas polaridades. Los cristales ortorrómbicos de color naranja cuentan con una celdilla unidad bastante estable, lo que permite suponer un escalado no problemático, desde este punto de vista, para la producción industrial de βLAP.

3.5. REFERENCIAS

Amidon GL, Lennernas H, Shah VP, Crison JR. A theoretical basis for a biopharmaceutic drug classification: the correlation of in vitro drug product dissolution and in vivo bioavailability. Pharm. Res. 1995;12(3):413-420.

Carr R. Chemical engineering. New York: McGraw-Hill; 1965.

D`Albuquerque IL, Maciel MCN, Schuler AR, Araujo MCM, Maciel GM, Cavalcanti MSB, et al. Preparação e primeiras observações sobre as propriedades antibióticas e antineoplásicas das naftoquinonas homólogas inferiores na série da 2-hidroxi-3-(3-metil-2-butenil)-1,4-naftoquinona (lapachol). Rev. Inst. Antibiot. 1972;12:31-40.

FDA. Guidance for Industry ANDAs: Pharmaceutical Solid Polymorphism. Guideline from U.S. Department of Health and Human Services. Food and Drug Administration. December. 2004.

Gonçalves de Lima O, D`Albuquerque IL, Gonçalves de Lima C, Dália Maia MH. Substâncias antimicrobianas de plantas superiores. Rev. Inst. Antibiot.1962;4(1/2):3-17.

Hilfiker R, Berghausen J, Blatter F, Burkhard A, De Paul SM, Freiermuth B, et al. Polymorphism – Integrated approach from high-throughput screening to crystallization optimization. J. Therm. Anal. Calorim. 2003;73:429-440.

ICH Q6A. Specifications: test procedures and acceptance criteria for new drug substances and new drug products. The tripartite harmonised ICH guideline. October. 1999.

Marini A, Berbenni V, Moioli S, Bruni G, Cofrancesco P, Margheritis C, et al. Drug-excipient compatibility studies by physico-chemical techniques. The case of indomethacin. J. Therm. Anal. Calorim. 2003;73(2):529-545.

Miller JM, Collman BM, Greene LR, Grant DJW, Blackburn AC. Identifying the stable polymorph early in the drug discovery – Development process. Pharm. Dev. Tech. 2005;10:291-297.

OECD 123, Guideline 123. Partition Coefficient n-Octanol/Water (POW) Slow-Stirring Method for Highly Hydrophobic Chemicals. Organisation for Economic Co-operation and Development September 2002 update November 2003.

Planchon SM, Wuerzberger S, Frydman B, Witiak DT, Hutson P, Church DR, et al. Beta-lapachone-mediated apoptosis in human promyelocytic leukemia (HL-60) and human prostate cancer cells: a p53-independent response. Cancer Res. 1995;55(17):3706-3711.

Stanley-Wood NG. Enlargement and compaction of particulate solids. London: Butterworths; 1983.

Thomson FM. Handbook of powder science and technology. New York: Fayed; 1984.

USP 29. United States Pharmacopeial Oficial. 29ed. Rockville; 2006.

Zhu H, Sacchetti M. Solubilization and solid-state characterization of poorly soluble 5-α reductase inhibitor. Drug. Dev. Ind. Pharm. 2004;20(6):573-580.

Rúa da Calderería, Santiago de Compostela

Capítulo 4

β-Lapachone

Autores: Marcílio S. S. Cunha-Filho[1], Ramón Martínez-Pacheco[1], Mariana Landín[1] and Bruno Dacunha-Marinho[2]

[1]Departamento de Farmacia y Tecnología Farmacéutica, Facultad de Farmacia, Universidad de Santiago de Compostela, Santiago de Compostela, Spain
[2]ED. CACTUS, Unidade de Raios X, Universidad de Santiago de Compostela, Santiago de Compostela, Spain

Revista: Acta Crystallographica Seccion C. 2006. 62;o473-o475.

4.1. ABSTRACT

The most remarkable aspect of the crystal structure of the title compound (systematic name: 3,4-dihydro-2,2-dimethyl-2Hnaphtho[1,2-b]pyran-5,6-dione), $C_{15}H_{14}O_3$, is that a π-stacking interaction is present between the two naphthalene ring systems of symmetry-related molecules. Apart from these π-π interactions, different molecules are held together by weak C-H…O hydrogen-bonding interactions.

4.2. COMMENT

The title compound, (I), is a naphthoquinone which can be isolated on a small scale from South American trees of the families Bigoniaceae and Verbenaceae (Burnett and Thomson, 1968). It can be produced chemically on a large scale from lapachol, following the procedures developed by Hooker (1892). These consist of cyclization in sulfuric acid by nucleophilic attack on the O atom of the lapachol isoprenyl side chain, followed by further recrystallizations (Hooker et al., 1936).

A research group at the Federal University of Pernambuco, Brazil, first noted the activity of (I) against several micro-organisms (Lima et al., 1962; D'Alburquerque, 1968) and tumour cells (Ferreira de Santana et al., 1968; D'Alburquerque et al., 1972). In recent years, compound (I) has become very interesting as a potential agent against several diseases. It has antifungal, antiviral, antipsoriatic and anti-inflammatory activities (Guiraud et al., 1994; Li et al., 1993; Mueller et al., 1999). It is also active against parasites such as Tripanosoma cruzi, the etiologic agent of Chagas disease (Pinto et al., 2000). But it is its antineoplastic activity that has generated the greatest expectations of this molecule.

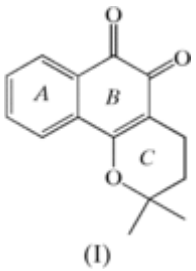

(I)

In vitro and *in vivo* studies have shown that (I) inhibits conventional therapy-resistant tumours, particularly malignant neoplasms with a slow cell cycle, such as prostate, colon and some ovarian and breast cancers (Planchon et al., 1995; Li et al., 2003; Park et al., 2005). 300 research articles and nearly 40 patents have been published on the subject in the last 15 years. Thus, its excellent pharmacological potential suggests that this drug could shortly be included in the therapeutic arsenal.

In this paper, we report the molecular and crystal structures of (I) (Figure 4.1). Some X-ray data from structural derivatives of (I) have previously been reported (De Simone et al., 2002; Reibenspies et al., 1989; Di Chenna et al., 2001). It should be noted that the most similar structure already reported, 3-bromo-β-lapachone (De Simone et al., 2002), presents the benzo and quinone rings lying in the same plane, and the heterocycle is in a distorted half-chair conformation. In the present case, the structure of (I) also has benzo and quinine rings, designated A and B, respectively. A Cremer & Pople (1975) analysis of the six-membered non-planar ring (ring C) gives ring-puckering parameters φ = 248.4 (3)^{o} and θ = 52.4 (2)°, and a puckering amplitude *Q* = 0.4497 (19) Å. Thus, the conformation of the ring is between the half-chair (H) and envelope (E) symmetrical forms.

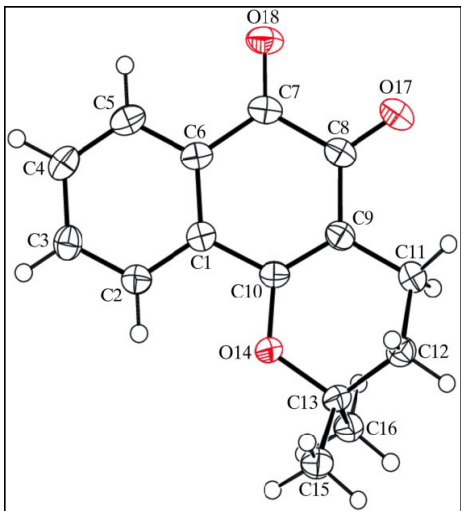

Figure 4.1. The molecule of (I), showing the atom-labelling scheme. Displacement ellipsoids are drawn at the 50% probability level and H atoms are shown as small spheres of arbitrary radii.

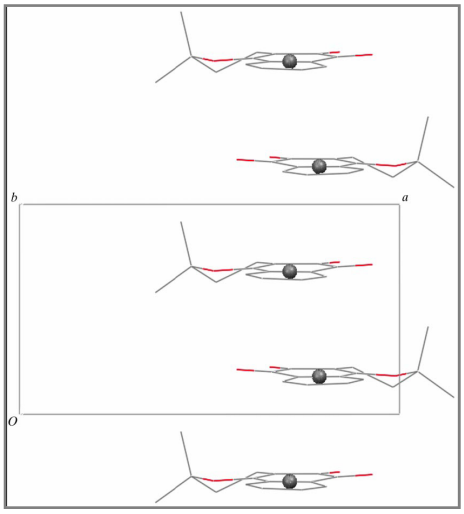

Figure 4.2. Five adjacent symmetry-related molecules of (I), linked by π - stacking interactions along the *c* axis. Also shown (grey spheres) are the calculated centroids of the planar rings.

The main differences between the reported analogues and compound (I) seem to be the strategy of self-assembly through weak intermolecular interactions. In the case of (I), the two planar rings in the molecule at (*x*, *y*, *z*) stack above the symmetry-related rings of the molecule at (-*x* + 3/2, *y* - 1/2, *z*), with distances of 3.659 and 3.509 Å between the centroids of rings *A* and *B*, respectively, a perpendicular distance between the rings of 3.432 Å, and centroid offsets of 1.270 and 0.731 Å, respectively. Figure 4.2 shows this stacking interaction, which generates stacked molecules running almost parallel to the [010] direction. The supramolecular structure also contains a weak intermolecular C-H···O hydrogen bond between atoms O17 and O18 and aromatic and non-aromatic H atoms of symmetry-related molecules.

Table 4.1 and 4.2 presents the geometric parameters of these weak interactions.

Table 4.1. Selected geometric parameters (Å, °).

C9-C10	1.365 (2)	O14-C10	1.339 (2)
C9-C11	1.500 (2)	O14-C13	1.483 (2)
C11-C12	1.524 (2)	O17-C8	1.229 (2)
C13-C12	1.516 (2)	O18-C7	1.212 (2)
C9-C11-C12	109.28 (14)	C13-C12-C11	112.47 (14)
C10-O14-C13	119.70 (12)	O14-C13-C12	110.00 (13)

Table 4.2. Weak hydrogen-bond geometry.

D…A	D…A†	D-H…A‡
C11…O17^{i}	3.507 (2)	142
C12…O17^{iii}	3.340 (2)	143
C12…O17^{iv}	3.539 (2)	165
C16…O18^{ii}	3.334 (2)	125
C3…O18^{iii}	3.492 (2)	147

† Distance between donor and acceptor atoms. ‡ Angle between donor, H and acceptor atoms. Symmetry codes: (i) –x+3/2, y+1/2, z; (ii) x-1/2, -y+1/2, -z+1; (iii) –x+3/2, y-1/2, z; (iv) x-1/2, y, -z+3/2.

As reported previously, the strategy of self-assembly through these weak interactions is of central importance for efficient and specific biological reactions, and for the design of new supramolecules possessing interesting structural and physical or chemical properties. As an example, we have found that by changing the crystal growing conditions of this molecule we can dramatically modify its dissolution rate (Landin et al., 2005). This could be explained according to the different preferred orientations achieved. Further studies will be reported in subsequent publications.

4.3. EXPERIMENTAL

Compound (I) was used as supplied, from a batch produced by the Federal University of Pernambuco, Brazil, following the procedure of Hooker et al. (1936), and purified by ethanolic recrystallizations. Its ^{1}H and ^{13}C NMR spectra were completely assigned by two-dimensional NMR experiments using two-dimensional ^{1}H-detected heteronuclear one-bond (HMQC) and multiple-bond (HMBC) techniques, as follows: ^{1}H NMR ($CDCl_3$, 750 MHz): δ1.468 (*s*, 6H, CH_3), 1.854 (*t*, 2H, CH_2), 2.573 (*t*, 2H, CH_2), 7.503 (*t*, 1H, Ar), 7.638 (*t*, 1H, Ar), 7.796-7.822 (*d*, 1H, Ar), 8.049-8.070 (*d*, 1H, Ar); ^{13}C NMR ($CDCl_3$, 750 MHz): δ16.169 (*s*), 26.768 (*s*), 31.621 (*s*), 79.252 (*s*), 112.729 (*s*) 124.040 (*s*), 128.566 (*s*), 130.16 (*s*), 130.631 (*s*), 132.64 (*s*), 134.736 (*s*), 161.990 (*s*), 178.568 (*s*), 179.854 (*s*).

The purity of (I) was confirmed by high-performance liquid chromatography (HPLC) (Waters M600, photodiode array detector) and differential scanning calorimetry (DSC Q100, TA Instruments, Delaware, USA). HPLC results showed a purity of approximately 100%. No impurities or degradation products were detected. DSC thermograms showed a single peak at 430 K, corresponding to the characteristic melting point of the drug (Krishna et al., 2004), with an enthalpy of 109 J g^{-1}.

H atoms were positioned geometrically and treated as riding, with C-H = 0.95-0.99 Å with U_{iso}(H) = 1.2U_{eq}(C) or 1.5U_{eq}(methyl C).

Data collection: *COLLECT* (Nonius, 1999); cell refinement: *SCALEPACK* (Otwinowski and Minor, 1997); data reduction: *XPREP* (Bruker, 2006); program(s) used to solve structure: *SIR97* (Altomare et al., 1999); program(s) used to refine structure: *SHELXL97* (Sheldrick, 1997); molecular graphics: *ORTEP-3 for Windows* (Farrugia, 1997) and *MERCURY* (Macrae et al., 2006); software used to prepare material for publication: *WinGX* (Farrugia, 1999) and *PLATON* (Spek, 2003).

Crystal data

- $C_{15}H_{14}O_3$
- M_r = 242.26
- Orthorhombic, *P b c a*
- *a* = 12.8995 (6) Å
- *b* = 6.8681 (3) Å
- *c* = 26.6419 (13) Å
- *V* = 2360.34 (19) Å^3
- *Z* = 8
- D_x = 1.363 Mg m^{-3}
- D_m = 1.3113(49) Mg m^{-3}
- D_m measured by helium-air pycnometer
- Cu *K*α radiation
- μ= 0.77 mm^{-1}
- *T* = 120 (2) K
- Prism, orange
- 0.31 × 0.13 × 0.13 mm

Data collection

- Nonius KappaCCD 2000 area-detector diffractometer
- φ and ω scans
- Absorption correction: multi-scan (*SADABS*; Sheldrick, 2006) T_{min} = 0.775, T_{max} = 0.905
- 2300 measured reflections
- 2300 independent reflections
- 2001 reflections with *I* > 2(*I*)
- R_{int} = 0.062
- θ_{max} = 69.4^o

Refinement

- Refinement on F^2
- $R[F^2 > 2\sigma(F^2)] = 0.061$
- $wR(F^2) = 0.170$
- $S = 1.12$
- 2077 reflections
- 166 parameters
- H-atom parameters constrained
- $w = 1/[\sigma^2(F_o^2) + (0.1016P)^2 + 0.9714P]$ where $P = (F_o^2 + 2F_c^2)/3$
- $(\Delta/\sigma)_{max} = 0.001$
- $\Delta\rho_{max} = 0.28$ e Å^{-3}
- $\Delta\rho_{min} = -0.30$ e Å^{-3}
- Extinction correction: *SHELXL97* (Sheldrick, 1997)
- Extinction coefficient: 0.0048 (9)

4.4. ACKNOWLEDGEMENTS

Authors thank LAFEPE, Brazil, and Professor Dr Pedro Jose Rolim Neto, Federal University of Pernambuco, Brazil, for their kind gifts of the title compound. This work was supported by the Spanish Government (grant Nº. SAF2002-03440) and by the Programme Alban, the European Union Programme of High-Level Scholarships for Latin America (scholarship Nº E04D043994BR).

4.5. REFERENCES

Altomare, A., Burla, M. C., Camalli, M., Cascarano, G. L., Giacovazzo, C., Guagliardi, A., Moliterni, A. G. G., Polidori, G. & Spagna, R. (1999). J. Appl. Cryst. 32, 115-119.

Bruker (2006). XPREP. Version 2006/1. Bruker AXS Inc., Madison, Wisconsin, USA.

Burnett, A. & Thomson, R. (1968). J. Chem. Soc. C, 7, 850-853.

Cremer, D. & Pople, J. A. (1975). J. Am. Chem. Soc. 97, 1354-1358.

D'Alburquerque, L. (1968). Rev. Inst. Antibiot. (Recife), 8, 73-88.

D'Alburquerque, L., Maciel, M., Schuler, A., De Araujo, C., Maciel, G. & Cavalcanti, M. (1972). Rev. Inst. Antibiot. (Recife), 12, 31-40.

De Simone, C. A., Malta, V. R. S., Pereira, M. A., Bispo, J. R. S., Pinto, A. V. & Pinto, M. C. F. R. (2002). Acta Cryst. E58, o296-o297.

Di Chenna, P. H., Benedetti-Doctorovich, V., Baggio, R. F., Garland, M. T. & Burton, G. (2001). J. Med. Chem. 44, 2486-2498.

Farrugia, L. J. (1997). J. Appl. Cryst. 30, 565.

Farrugia, L. J. (1999). J. Appl. Cryst. 32, 837-838.

Ferreira de Santana, C., Goncalves de Lima, O., D'Albuquerque, L., Lacerda, A. & Martins, D. (1968). Rev. Inst. Antibiot. (Recife), 8, 89-94.

Guiraud, P., Steiman, R., Campos-Takaki, G., Seigle-Murandi, F. & Simeon de Buochberg, M. (1994). Planta Med. 60, 373-374.

Hooker, S., Shepard, H., Walsh, J. & Connitt, G. (1936). J. Am. Chem. Soc. 58, 1190-1197.

Hooker, S. C. (1892). J. Chem. Soc. 6, 611-651.

Krishna, V., Lamba, J. & Singh, P. (2004). J. Indian Chem. Soc. 81, 1039-1044.

Landin, M., Cunha Filho, M. S. S. & Martinez-Pacheco, R. (2005). Proceedings of the Conference on Optimising Drug Delivery and Formulation, Evaluation of Drug-Delivery Systems, Issues and Perspectives, November 20-23, Versailles, France, pp. 85-96.

Li, C., Zhang, L., Dezube, B., Crumpacker, C. & Pardee, A. (1993). Proc. Natl Acad. Sci. USA, 90, 1839-1842.

Li, Y., Sun, X., La Mont, J., Pardee, A. & Li, C. (2003). Proc. Natl Acad. Sci. USA, 100, 2674-2678.

Lima, O., D'Albuquerque, L., de Lima, C. & Dalia, M. (1962). Rev. Inst. Antibiot. (Recife), 4, 3-17.

Macrae, C. F., Edgington, P. R., McCabe, P., Pidcock, E., Shields, G. P., Taylor, R., Towler, M. & van de Streek, J. (2006). J. Appl. Cryst. 39, 453-457.

Mueller, K., Sellmer, A. & Wiegrebe, W. (1999). J. Nat. Prod. 62, 1134-1136.

Nonius (1999). COLLECT. Version 5.0. Nonius BV, Delft, The Netherlands.

Otwinowski, Z. & Minor, W. (1997). Methods in Enzymology, Vol. 276, Macromolecular Crystallography, Part A, edited by C. W. Carter Jr & R. M. Sweet, pp. 307-326. New York: Academic Press.

Park, H., Ahn, K., Ahn, S., Choi, E., Lee, S. & Williams, B. (2005). Int. J. Radiat. Oncol. Biol. Phys. 61, 212-219.

Pinto, C., Dantas, A., De Moura, K., Emery, F., Polequevitch, P. & Pinto-Maria, F. (2000). Arzneim. Forsch. (Drug. Res.), 50, 1120-1128.

Planchon, S., Wuerzberger, S., Frydman, B., Witiak, D., Hutson, P. & Church, D. (1995). Cancer Res. 55, 3706-3711.

Reibenspies, J. H., Williams, H. J., Ortiz, C., Scott, A. I., Suarez, M. & Dominguez, X. A. (1989). J. Crystallogr. Spectrosc. Res. 19, 597-599.

Sheldrick, G. M. (1997). SHELXL97. University of Göttingen, Germany.

Sheldrick, G. M. (2006). SADABS. Version 2006/1. University of Göttingen, Germany.

Spek, A. L. (2003). J. Appl. Cryst. 36, 7-13.

Rúa das Hortas, Santiago de Compostela

Capítulo 5

Stability and degradation kinetics of the investigational antitumoral drug β-lapachone in solid state

Autores: Marcílio S. S. Cunha-Filho[1], Ramón Martínez-Pacheco[1] and Mariana Landín[1]

[1]Departamento de Farmacia y Tecnología Farmacéutica, Facultad de Farmacia, Universidad de Santiago de Compostela, Santiago de Compostela, Spain

Manuscript submitted to J. Pharm. Biom. Anal.

5.1. ABSTRACT

β-lapachone (βLAP) is a promising antitumoral drug under extensive investigation and on clinical trial at the moment in. In this work, the stability study of βLAP in solid state has been carried out. For this purpose, a precise and accurate HPLC method, selective against a synthesis impurity (lapachol) and thermal and photo degradation products, has been developed and validated. The effect of the relative humidity (RH) and light on physical and chemical stability of βLAP was studied following a factorial design (2x2). Samples were characterized by HPLC, DSC, TGA, X-ray powder diffraction and optical microscopy. The study has revealed the photo sensitivity behaviour of βLAP and a forceful interaction between the RH and illumination disclosing important consequences in physical and chemical stability of βLAP.

Keywords: β-lapachone; solid-state stability; HPLC method; relative humidity; illumination

5.2. INTRODUCTION

β-lapachone (βLAP, Fig. 5.1) can be obtained on a large scale through acid cyclization of lapachol, a natural product extracted from *Tabebuia avellanedae* Lor. following the method developed by Hooker and co-workers [1,2]

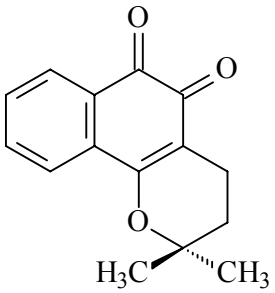

Fig. 5.1. Chemical structure of βLAP

Over the last few years βLAP has been reported to possess a wide range of pharmacological properties including antiviral, anti-inflammatory, anti-trypanosomic activities [3,4,5] being outstanding its chemotherapic potential in cancer treatment [6,7]. *In vitro* and *in vivo* studies have shown that βLAP inhibits conventional therapy-resistant tumors, particularly the proliferation of neoplasm of slow cell cycle like prostate, pancreatic, colon and some ovarian and breast cancer [8,9]. Clinical trials of phase I and II have recently been launched on this molecule with encouraged results [10].

In spite of its interesting potential, a stability study of βLAP in solid state has not yet been reported. However, the study of factors affecting

stability and the degradation kinetics, such as light and humidity, provide essential information to the establishment of the shelf-life, the storage conditions, the re-test period and the pharmaceutical formulation development setting [11, 12].

A fundamental requirement for a stability study is the development of an assay method selective enough to analyse the drug and its degradation products. Bearing this in mind, the high performance liquid chromatography would be the choice method [13, 14].

On this basis, the objective of the present work is to carry out an accelerated stability study of βLAP in solid state evaluating the effect of environment variables, light and relative humidity on the degradation process rate. In order to do this, a HPLC method was developed and validated to prove an acceptable suitability, reliability and feasibility for the quantitative assay of the drug in the presence of impurities or degradation products.

5.3. EXPERIMENTAL

Materials

β-lapachone (Batch L503; 3,4-dihydro-2,2-dimethyl-2H-naphthol-[1,2-b]pyran-5,6-dione; $C_{15}H_{14}O_3$; MW 242.3) was supplied by Laboratorio Farmacêutico do Estado de Pernambuco, LAFEPE (Brazil) with purity estimated by DSC and HPLC in 99.9 %. Reference standard of β-lapachone (083K1337) and lapachol (00509KN) was purchased by Sigma-Aldrich (Germany). Methanol HPLC was obtained from Merck

(Germany). The solutions were prepared using pure water set by using Millipore Milli Q Plus quantification system (USA).

Chromatography conditions

βLAP assays were performed on a high performance liquid chromatograph, Waters M600, equipped with a C18 cartridge column (125 mm x 45 mm x 5 µm) (Waters, USA) based on a previously reported method [15]. The mobile phase consisted of a mixture of methanol/water 65 % (v/v). The isocratic flow rate was 1 $mL \cdot min^{-1}$ at room temperature. The injection volume was 20 µL. Chromatographic detection was set at 253 nm with a photodiode array detector. The βLAP test concentration was 40 $\mu g \cdot mL^{-1}$ with a retention time around 5.5min. The mobile phase and samples were filtered using a 0.45 µm nylon membrane (Waters, USA).

A System Suitability test was evaluated by obtaining the chromatographic parameters; capacity factor (K), number of the theoretical plates (N) and tailing factor (T) [16].

Validation of the High Performance Liquid Chromatography (HPLC) method

The validation of analytical methodology was carried out according to the ICH and AEFI guidelines [16, 17, 18] as described as follows:

Selectivity

In order to test the selectivity of the method against photo and thermal degradation products and also against a synthetic precursor,

lapachol, βLAP at test concentration (40 µg.mL-1) with and without those impurities were evaluated in six replicates. The results were expressed as *Discrepancy* according to follow equation. The concentration values were compared using the T-Student test (α = 0.05).

$$\text{Discrepancy}\ (\%) = \frac{(C_f - C_i)}{Ci} \times 100$$

where C_i is the average response without the impurity and C_f is the average response with the impurity.

The photo degradation product (PDP) was obtained by exposing an aqueous solution of βLAP (30 $\mu g \cdot mL^{-1}$) to light, according to ICH guideline Q1B [19], until complete decomposition. The thermal degradation product (TDP) was produced by keeping a solution of βLAP (30 $\mu g \cdot mL^{-1}$) in phosphate buffer (pH 10), in an oven at 50 ^{o}C until complete decomposition. The addition of those solutions to the βLAP test concentration was equivalent to 10 % degraded βLAP. The lapachol was added to the βLAP test solution at a concentration of 4 $\mu g \cdot mL^{-1}$.

Linearity

A total of three calibration curves were prepared, in a range of 50-150 % from the test concentration of βLAP (40 $\mu g \cdot mL^{-1}$). Linearity was analyzed by the regression line equation calculated by the least-squares method and the proportionality test throughout the Student t-test [18]. The response factors were calculated and analysed.

Precision and accuracy

Precision was considered at three levels. *Repeatability of instrumental system* (RI), which was studied by ten consecutive analyses,

replicates of the same sample of βLAP (40 $\mu g \cdot mL^{-1}$); *repeatability of method* (RM), based on the analysis of six determinations of βLAP (40 $\mu g \cdot mL^{-1}$) and *intermediate precision* (IP), established by the random analysis of three determinations of βLAP (40 $\mu g \cdot mL^{-1}$) prepared by two different analysts, using two instruments on different days. Moreover, relative standard deviation (RSD) of peak area was calculated.

Accuracy was evaluated using the same range of linearity in triplicate, at five concentration levels. *Recovery* (%) was calculated and evaluated by Student t-test (α = 0.05).

Detection limit (DL) and Quantification limit (QL)

The results of the linearity test in the drug concentration range 1-3 $\mu g \cdot mL^{-1}$ were used to calculate DL and QL as follows:

$$DL\ or\ QL = E + \frac{F \cdot SD}{slope \times \sqrt{n}}$$

where, *E* = intercept of the linearity test; *F* = factor that is 3 for DL and 10 for QL; *SD* = standard deviation; *n* = replicates number.

Solid drug stability study

A factorial design (2x2) was used to study the effect of the relative humidity (RH) at two levels (0 and 75 %), by storing samples of βLAP at 40 ºC in silica gel or in an environment of saturated solution of NaCl [20] respectively, and the illumination, at two levels (darkness and light) (Table 5.1). The light sources were selected following ICH Q1B specifications [19], and applied using a modified oven equipped with two white fluorescent lamps (Hitachi F8T5, Japan) and two emission mercury UV

lamps (370 nm) (Philips 08F8T5/BLB, Holland). Overall illumination (1800lx) and radiation UV (0.0078 $W \cdot m^{-2}$) were measured by a luximeter (HD9221, Delta Corp., Italy) equipped with a probe (P912151).

Samples of βLAP were conditioned in aluminium pans, about 15mg per pan (5.5 mm Ø, 1.5 mm thickness) [19], and stored at 40 ± 2 ^{o}C under the described conditions. Chemical and physical characterization of the samples was carried out at different times of storage (1, 3 and 6 months).

The quantification of the effects of the studied variables light and relative humidity on the βLAP stability was carried out by ANOVA and stepwise linear regression using Statgraphics® plus version.

Table 5.1. Sample names as regard as the storage conditions.

	RH [%]	
	0	**75**
Darkness	D0	D75
Light	L0	L75

Characterization of solid systems

Optical Microscopy (OM) studies

The morphological characteristics of the samples were analysed using an Olympus SZ60 (Opelco, Japan) microscope connected to a video camera Olympus DP12 (Opelco, Japan).

X-Ray Powder Diffraction (XRPD)

The X-Ray Powder Diffraction patterns were collected using Copper radiation (40 Kv, 30 mA), on a Philips PW 1729 diffractometer

(Philips corp., Netherlands) with Bragg-Brentano geometry, in the 2<2θ<60 range with a step size of 0.02º and counting time of 2 s per step.

Differential Scanning Calorimetry (DSC)

Samples weighing 1-2 mg were placed in open aluminium pans and heated from 30 to 170 ºC at a rate of 1 ºC·min^{-1} using a temperature modulated DSC Q100 calorimeter (TA Instruments, USA). Nitrogen was used as the purge gas at a flux rate of 50 mL·min^{-1}. The calibration of temperature and heat flow was performed with standard indium samples. In order to estimate the purity of βLAP the Van't Hoof equation was used (TA Universal analysis 2000 V4.2E) [16].

Thermogravimetric Analysis (TGA)

Moisture contents (MC) of the aged βLAP samples were determined on a Thermogravimetric analyser TGA 2950 (TA Instruments, USA) to measure weight loss by approx. 5 mg sample after 2h at a temperature of about 105 ºC.

5.4. RESULTS AND DISCUSSION

HPLC method

System suitability

The system suitability test was defined based on the results obtained in several chromatograms during validation. Capacity factor (K), theoretical plates (N) and tailing factor (T) (Table 5.2) were consistent throughout the validation study, the values being lower than the

acceptable limits [18]. Therefore, this method can be applied to routine, stability studies with no problems.

Table 5.2. HPLC suitability system parameters. *K* = capacity factor; *N* = number of theoretical plates and *T* = tailing factor.

	K	N	T
Results range	4,0-5,8	4000-5500	1,1-1,5
Limits [16]	>2,0	>2000	≤2,0

Selectivity

Selectivity evaluates the analytical method capacity to distinguish between the drug and impurities with similar chemical structure. For this purpose, samples of βLAP solution and mixtures of βLAP with different impurities were analysed. Figure 5.2 presents the chromatograms of the different combinations. As it can be seen, the method is selective towards the lapachol, which would be an impurity from the βLAP synthesis process, and also the unknown thermal and photo degradation products. The impurities elute a different retention time and do not interfere with βLAP as demonstrated by the resolution values (R) (Fig. 5.2). The interference of the impurities was evaluated by the discrepancy parameter (Table 5.3), the values being close to 0.5 % in all cases. Student t-test showed no significant statistical differences between βLAP in single solutions and mixtures of drug-impurities. Those variations can be attributed to random errors.

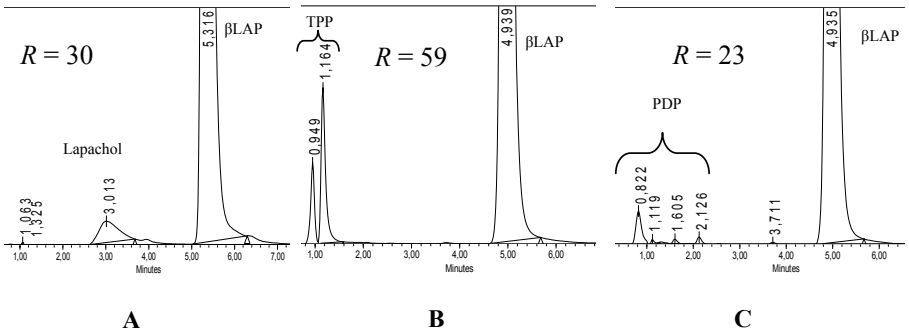

Fig. 5.2. Chromatograms obtained from selectivity study of βLAP at 40 $\mu g \cdot mL^{-1}$ and interferences at 4 $\mu g \cdot mL^{-1}$ (A = Lapachol; B = Thermal degradation products and C = Photodegradation products) with its respective resolution (R) values.

Table 5.3. Selectivity data of the developed HPLC method. (Relative standard deviation). PDP (photo degradation products), TDP (Thermo degradation products).

	βLAP [μg·mL^{-1}]	***Discrepancy [%]***
βLAP	39.55 (0.8)	-
βLAP + Lapachol	39.35 (0.3)	-0.32
βLAP + PDP	39.72 (1.0)	+0.44
βLAP + TDP	39.78 (1.0)	+ 0.59

Linearity

Linearity was determined as the ratio of the peak area (A) and concentration of βLAP (C) in the range of 20-60 $\mu m \cdot mL^{-1}$. The parameters of the regression were: A = 112967.C – 13944; correlation coefficient r = 0.9991 with d.f.=14, F=7078.5, α>0.01. The slope was significantly different from zero and the intercept was statistically equal to zero. Coefficient of variation of response factors was 1.8 % lower than the limit 5 % [18].

Precision and accuracy

Precision results are shown in the Table 5.4. Relative standard deviations (RSD) of peak areas lower than 2 % assess the RI, RM and IP.

Table 5.4. Precision data of the developed HPLC method. RI (*Repeatability of Instrumental system),* RM (*Repeatability of Method)* and IP (*Intermediate Precision)*

	RI (n=10)	***RM*** (n=6)	***IP Analyst A***		***IP Analyst B***	
			Day1 (n=3)	**Day2** (n=3)	**Day1** (n=3)	**Day2** (n=3)
Mean Peak Area	4309480	4357720	4348841	4309055	4235936	4280216
RSD [%]	0.18	0.64	0.17	1.12	1.50	0.56
Mean RSD [%]			**1.37**			

Recovery calculated from experimental determinations was 100.05 % with a relative standard deviation of 0.45 %, lower than the established limits [18]. Student t-test confirmed the accuracy of the method.

Detection Limit (DL) and Quantification Limit (QL)

Detection limit and quantification limit for the βLAP assay were 0.04 and 0.07 $\mu g \cdot mL^{-1}$ respectively. These values fit the method not only to the stability assays but also to more rigorous level of drug sensitivity requirements such as the cleaning validations and dissolutions assays.

Stability in solid state

Chemical decomposition and important physical changes were observed in some βLAP solid-state samples in regard to the storage conditions. OM photomicrographs (Fig. 5.3) showed no changes for samples maintained in darkness (D0 and D75). However, the surface

particles exposed to light (L0 and L75) became darker with time, especially when stored at 75 % RH (L75).

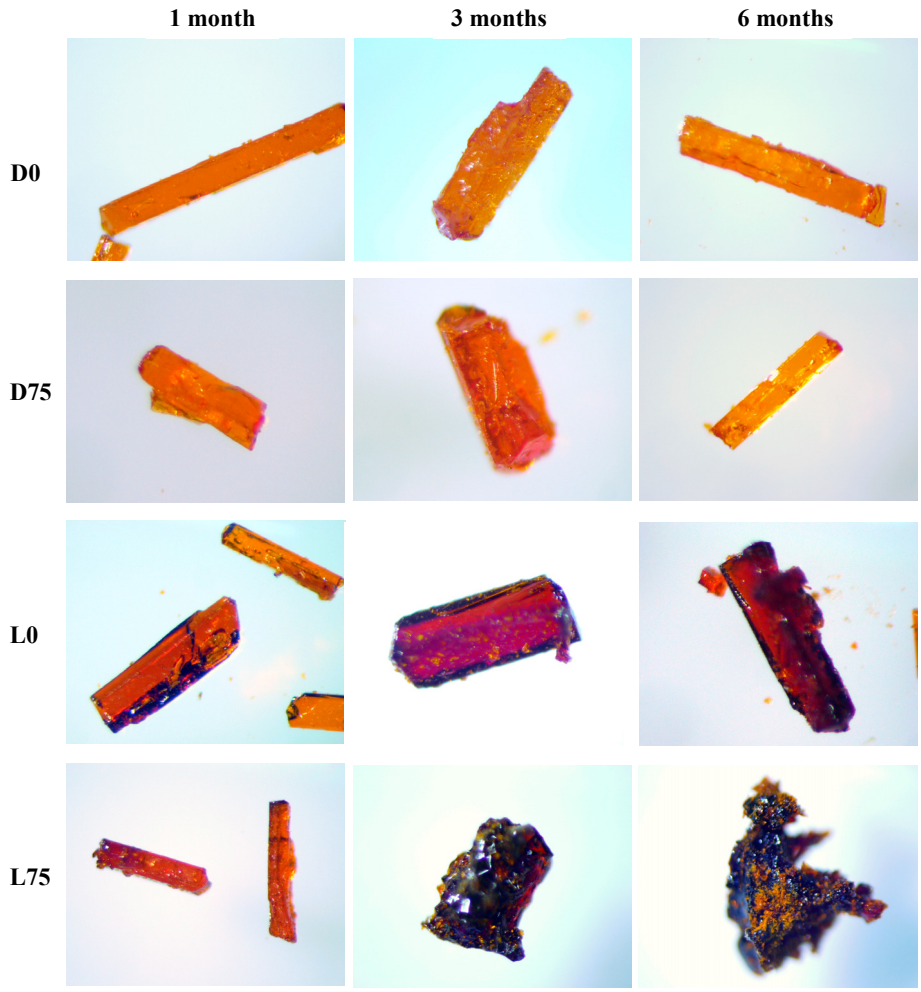

Fig. 5.3. βLAP photographs by OM in different conditions of illumination and RH using a 94.5x magnification.

X-ray techniques are a very powerful tool for monitoring solid-solid transitions [21]. XRPD patterns of βLAP show no important changes after storage (Fig. 5.4), maintaining the original polycrystalline diffraction pattern and exhibiting a main sharp peak at 9.5 º2θ with other secondary peaks at 13.05, 19.05, 19.59, 24.67 and 39.31 º2 θ [22]. Some small changes in the relative intensity of the peaks could be explained by a favoured orientation variation on the analyzed crystallites. However, a high pitch on the base line of the L75 sample after 6 months storage (Fig. 5.4) can be interpreted as reduction in crystallinity of this sample justifying OM results.

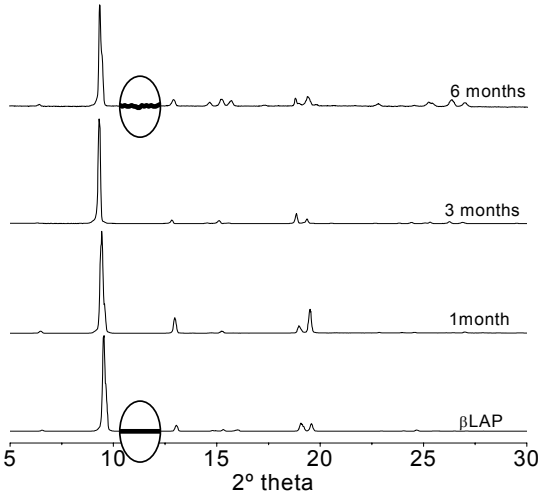

Fig. 5.4. X-ray diffraction patterns of βLAP after 1, 3 and 6 months stored under illumination and 75 % RH (sample L75).

HPLC, DSC and TGA results (Table 5.5) are conclusive on chemical degradation in the solid state. HPLC results present important variability as a consequence of the degradation being a superficial phenomenon as showed by OM and XRPD. Despite the conditioning in aluminium pans, which assumed a more homogeneous exposure of the

samples to light [23], the presence of inhomogeneous layers justifies the high standard deviations of some HPLC measurements.

Table 5.5. βLAP remaining by HPLC method and DSC and TG results for different time of storage.

Sample		βLAP[a] [% ± SD]	Purity[b] [%]	DSC			TGA
				Peak [^{0}C]	Range [^{0}C]	ΔH [Jg^{-1}]	MC [%]
βLAP	As supplied	100.4 ± 0.5	99.99	156.0	154.1-156.7	99.0	< 0.3
D0	1 month	101.8 ± 4.2	99.99	155.9	153.3-156.6	102.0	< 0.3
	3months	99.2 ± 3.2	99.98	156.0	153.8-156.7	99.8	< 0.3
	6 months	96.1 ± 1.8	99.97	155.9	154.3-156.6	101.3	< 0.3
D75	1 month	99.4 ± 0.3	99.99	155.9	154.2-156.6	104.0	< 0.3
	3months	96.4 ± 1.8	99.98	156.0	154.4-156.6	97.3	< 0.3
	6 months	96.6 ± 3.0	99.98	155.9	154.1-156.7	105.0	< 0.3
L0	1 month	100.5 ± 3.3	99.43	155.3	146.0-156.3	87.9	< 0.3
	3months	97.2 ± 0.3	-	154.7	143.8-156.2	72.9	< 0.3
	6 months	91.6 ± 1.6	-	-	-	-	0.97
L75	1 month	98.1± 1.3	97.97	155.98	135.6-159.3	85.3	1.54
	3months	79.5 ± 0.4	-	-	-	-	2.01
	6 months	47.7 ± 0.4	-	-	-	-	3.00

[a]HPLC analysis (n=3); [b]DSC analysis (Van´t Hoff method)

Purity values obtained by DSC agree with HPLC βLAP percentages up to around 3 % drug degradation, which is the limit established by the pharmacopoeias for DSC purity determinations [16]. Higher impurity values give unreliable thermal assessment.

Figure 5.5 shows DSC profiles of the samples, after one and 6 months storage. As can be seen samples maintained in the darkness (D0 and D75) do not show important modifications in the melting peak of βLAP. On the contrary, the irradiated samples (L75 and L0) do suffer a great displacement and broadening after one month storage or even the disappearance of the fusion peak after 6 months storage (L75, Fig. 5.5).

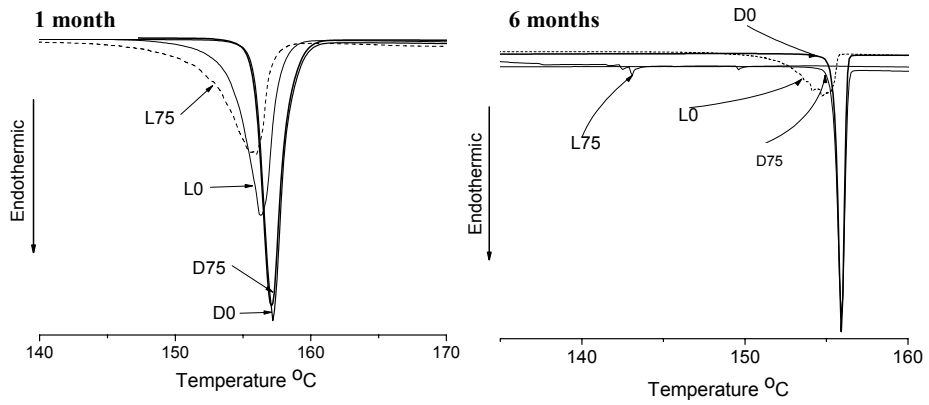

Fig. 5.5. DSC thermograms of βLAP after 1 and 6 months stored under different conditions of illumination and RH.

The environmental relative humidity is a decisive factor in the solid-state degradation process. Water condenses on the crystal surface forming a drug saturated solution film, where hydrolysis or other decomposition reactions can take place [24]. From our TGA results (table 5.5), not a single but synergic effect of RH and irradiation, pointed out by different authors [25], promotes the reaction of βLAP with water making degradation products more hygroscopic than the drug.

The analysis of variance of the parameter percentage of βLAP remaining after six months storage showed a statistical significant effect of the variables, RH, light and their interaction. The stepwise linear regression allows the calculation of the equation of corresponding surface response (Fig. 5.6). The effect of relative humidity (RH) and light (L) on the stability of βLAP is described by the following equation ($r = 0.9978$; $\alpha<0.05$).

$$\beta LAP\,(\%) = 96.13 - 2.04 \cdot 10^{-3} \cdot L - 3.16 \cdot 10^{-3} \cdot \mathrm{RH} - 3.39 \cdot 10^{-4} \cdot L \cdot \mathrm{RH}$$

The surface response (Fig. 5.6) denotes the great impact of the interaction between the light and relative humidity on the degradation rate of βLAP.

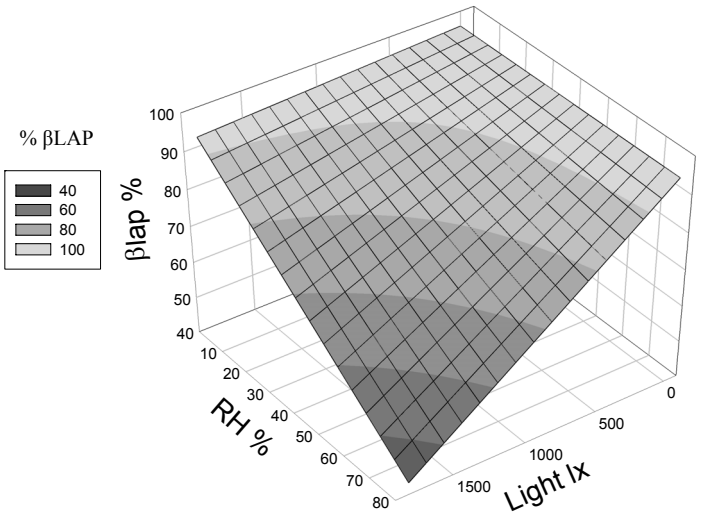

Fig. 5.6. Response surface of βLAP remaining for the sample L75 after 6 months storage.

The large degradation obtained after six months storage for the L75 sample allowed the kinetic analysis of degradation in those conditions. Figure 5.7 shows the βLAP remaining vs. time fitting pseudo-zero order kinetics in agreement with Leeson-Mattocks theory for solid state degradation in high relative humidity environments [26]. It is assumed that every decomposed drug molecule is rapidly replaced by a dissolving one. The degradation rate is kept constant as far as the concentration of the drug saturated solution film is maintained.

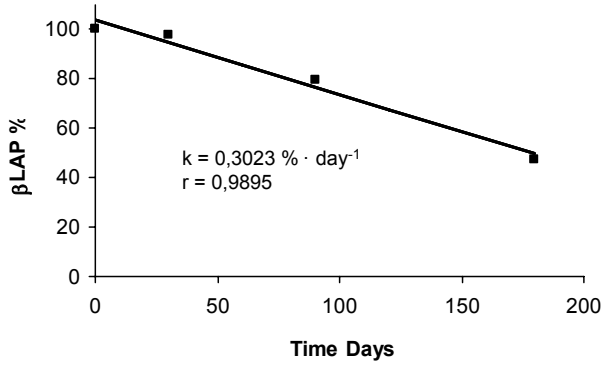

Fig. 5.7. The kinetic plot of the βLAP decomposition in solid state, under illumination and 75 % RH (sample L75).

5.5. CONCLUSIONS

A simple, rapid, accurate, precise and selective analytical method has been developed and validated. Selectivity of the βLAP HPLC method against lapachol and unknown βLAP thermal and photodegration products was demonstrated. Degradation of βLAP depends strongly on storage conditions, the interaction between light and relative humidity being the most important factor. In the solid state the interaction between those variables promotes a pseudo-zero order kinetic degradation associated to changes in colour, crystallinity and thermal behaviour of the product. Information presented herein can be used for the definition of the optimal βLAP handling and storage conditions.

5.6. ACKNOWLEDGEMENTS

Authors thank LAFEPE, Brazil, and Professor Dr Pedro Jose Rolim Neto, Federal University of Pernambuco, Brazil, for their kind gift of the βLAP. This work was supported by Xunta de Galicia (PGIDIT04BTF203011PR) and the Programme Alβan, the European Union Programme of High Level Scholarships for Latin America, scholarship nº E04D043994BR.

5.7. REFERENCES

[1] C.F. Santana, O. Golçalves de Lima, L. D`Albuquerque, A.L. Lacerda, D.G. Martins, Rev. Inst. Antibiot. 8 (1968) 89-94.

[2] S.C. Hooker, H.W. Shepard, J.G. Walsh Jr., G.H. Connitt, J. Am. Chem. Soc. 58 (1936) 90-1197.

[3] C.J. Li, L.J. Zhang, B.J. Dezube, C.S. Crumpacker, A.B. Pardee, Proc. Natl. Acad. Sci. 90 (1993) 1839-1842.

[4] D. Moon, Y.H. Choi, N.D. Kim, Y.M. Park, G.Y. Kim, Int. Immunopharmacol. 7 (2007) 506-514.

[5] M. Dubin, S.H. Villamil, A.O.M. Stoppani, Medicina 61 (2001) 343-350.

[6] Y. Li, S. Sun, J.T. LaMont, A.B. Pardee, C.J. Li, Proc. Natl. Acad. Sci. 100 (2003) 2674-2678.

[7] M. Ough, A. Lewis, E.A. Bey, J. Gao, J.M. Ritchie, W. Bornmann, D.A. Boothman, L.W. Oberley, J.J. Cullen, Cancer Biol. Ther. 4 (2005) 95-102.

[8] C.J. Li, Y. Li, A.V. Pinto, A.B. Pardee, Proc. Natl. Acad. Sci. 96 (1999) 13369-13374.

[9] M. Suzuki, M. Amano, J. Choi, H.J. Park, B.W. Williams, K. Ono, C.W. Song, Radiat. Res. 165 (2006) 525-531.

[10] G.I Shapiro, J.G. Supko, D.P. Ryan, L. Appelman, A. Berkenblit, A.R. Craig, S. et al., Proceedings of 2005 ASCO Annual Meeting. Orlando, USA. May 13-17 (2005) 3042.

[11] B.R. Matthews, Drug Dev. Ind. Pharm. 25 (1999) 831-856.

[12] P. Kovariková, M. Mokrý, J. Klimes, K. Vávrová, J. Pharm. Biomed. Anal. 40 (2006) 105-112.

[13] M. Zajac, A. Jelinska, L. Dobrowolski, Oszczapowicz, J. Pharm. Biomed. Anal. 32 (2003) 1181-1187.

[14] P. Pérez-Lozano, E. García-Montoya, A. Orriols, M. Miñarro, J.R. Ticó, J.M. Suñe-Negre, J. Pharm. Biomed. Anal. 42 (2006) 192-199.

[15] M.S.S.Cunha-Filho, F.C. Alves, G.M.C. Alves, D.B. Monteiro, F.P. Medeiros, P.J. Rolim-Neto, Rev. Bras. Farm. 86 (2005) 39-43.

[16] USP 29, The United States Pharmacopoeia, 29th, United States Pharmacopoeial Convention, Rockville, 2006.

[17] ICH Q2 (R1), Validation of analytical procedures: text and methodology, Internation Conference on Harmonization, Geneva, 2005.

[18] Validación de métodos analíticos, Monografías AEFI, Girona, Marzo, 2001.

[19] ICH Q1B, Photostability testing of new drug substances and products, Internation Conference on Harmonization, Geneva, 1996.

[20] H. Nyqvist, Int. J. Pharm. Tech & Prod. 4 (1983) 47-48.

[21] M. Bartolomei, J. Pharm. Biomed. Anal. 24 (2000) 81-93.

[22] M.S. Cunha-Filho, M. Landin, R. Martinez-Pacheco, B. Dacunha-Marinho, Acta Crystallogr.C 62 (2006) o473-5.

[23] W. Aman, K. Thoma, Pharmazie 12 (2003) 877-880.

[24] S. Yoshioka, V.J. Stella, Stability of drugs and dosage forms, Kluwer Academic, New York, 2000.

[25] H. Kaur, T.T. Mariappan, S. Singh, Pharm. Tech. 27 (2003) 52-56.

[26] J.T. Carstensen, Drug Stability, principles and practices, Marcel Dekker, New York, 1990.

Praza da Quintana, Santiago de Compostela

Capítulo 6

Stability Study of the Investigational Antitumoral β-lapachone in Solution

Autores: Marcílio S. S. Cunha-Filho[1], José Fernando Rosa dos Santos[1], Ana Estévez-Braun[2,3], Elisa Pérez-Sacau[2,3], Ramón Martínez-Pacheco[1] and Mariana Landín[1]

[1]Departamento de Farmacia y Tecnología Farmacéutica, Facultad de Farmacia, Universidad de Santiago de Compostela, Santiago de Compostela, Spain.

[2]Instituto Universitario de Bio-Orgánica "Antonio González", Avda. Astrofísico Francisco Sánchez Nº 2, La Laguna, Tenerife, Spain.

[3]Instituto Canario de Investigación del Cáncer (http://www.icic.es)

Manuscript in preparation

6.1. ABSTRACT

β-lapachone [βLAP] is a natural anticancer drug that selectively induces apoptosis by a novel mechanism of directly activation checkpoint regulators. βLAP has been studied in clinical trials, demonstrating acceptable toxicity and encouraging signs of efficacy. The aim of the present study was to investigate the stability of βLAP in solution and evaluate the effect of light, cyclodextrin complexation with randomized methyl-β-cyclodextrin [RMβCD] and pH on the kinetics of the degradation process and its mechanisms. Molecular modelling was also used as an auxiliary method to understand the influence of inclusion complex formation on the drug decomposition process. Two different degradation routes were found for βLAP: hydrolysis in the darkness generating as the main degradation product hydroxylapachol and photolysis under the light giving phthalates subproducts. Pseudo first-order rate constants were determined for βLAP in aqueous solutions. The light accelerates the drug degradation in 140-fold. The inclusion complex βLAP-RMβCD has different effects on the two degradation routes, a chemopreventive effect on the hydrolysis in the darkness and the opposite effect on the photolysis. The simulated inclusion complex that included the methylated ring inside the RMβCD should protect the βLAP ether bond against the hydrolytic process. The drug suffers an alkaline hydrolysis and its stability pH range is 2-4.

Keywords: β-lapachone; anticancer; stability; cyclodextrin; molecular modelling.

6.2. INTRODUCTION

β-lapachone [βLAP] is a naphthoquinone, originally isolated from a South American tree called Ipê Roxo (Tabebuia avellanedae Lor.) and has been extensively used by popular medicine.[1]

Numerous investigations suggest its potential therapeutic application against several diseases, including malaria, viral and bacterial infections, psoriases, schistosomiasis, and trypanosomiasis,[2-7] being outstanding its chemotherapic potential in cancer treatment.[8,9]

In vitro and *in vivo* studies have shown that βLAP inhibits selective antitumor activity in a broad range of conventional therapy-resistant tumours, particularly the proliferation of neoplasm of slow cell cycle like prostate, pancreatic, colon and some ovarian and breast cancer.[8,10,11] βLAP act by a novel mechanism of directly activation checkpoint regulators inducing apoptosis.[9] Synergistic action of βLAP with taxol and ionization radiation has been described as effective against tumors.[12-14] Clinical trials of phase I and II have recently been launched on this molecule with encouraging results.[15-17]

βLAP is poorly soluble in water (0.03 $mg \cdot mL^{-1}$) which raises problems to reach target plasma levels needed for optimal therapeutic efficacy. Some attempts have been made to avoid solubility problems through the use of CDs.[18-20]

In a previous work, the βLAP degradation in solid state has been investigated and the synergic effect of humidity and light on the stability has been established.[21] However, the degradation mechanism of βLAP is not fully understood and the identity of the degradation products, which is

important in predicting possible side effects and toxicity has not yet been reported.

On this basis, the objective of the present work was to study the stability of βLAP in solution and evaluate the effect of some variables as light and pH on the kinetics of the degradation process and to determine the pathway/s of degradation of the molecule. Additionally, the effect of randomized methyl-β-CD [RMβCD] on the stability of the βLAP in solution was studied supported by molecular modelling.

6.3. EXPERIMENTAL

Materials

β-lapachone [βLAP] (3,4-dihydro-2,2-dimethyl-2H-naphthol[1,2-b]pyran-5,6-dione; $C_{15}H_{14}O_3$; MW 242.3) was supplied by Laboratorio Farmacêutico do Estado de Pernambuco/LAFEPE (Recife, Brazil) with purity estimated by DSC and HPLC is 99.9 %. Randomized methyl-β-CD [RMβCD] (degree of molar substitution 0.57) was kindly donated by Roquette (Barcelona, Spain). The solvents and reagents used were high purity grade. Deuterium chloroform [$CDCl_3$] was purchased from Sigma-Aldrich (St. Louis, USA).

High Performance Liquid Chromatography [HPLC] assay

βLAP analysis was carried out following the previous reported validated method for stability studies on a high performance liquid chromatograph Waters M600 equipped with a C18 cartridge column (125

mm x 45 mm x 5 µm) (Waters, Milford, USA).[21] Mobile phase consisted of a mixture methanol/water (65/35, v/v) in an isocratic flow rate of 1mL·min^{-1} at room temperature. The injection volume was 20 µL. Chromatographic detection was set at 253 nm with a photodiode array detector. The βLAP test concentration was 40 µg·mL^{-1}. Mobile phase and samples were filtered using a 0.45 µm nylon membrane (Waters, Milford, USA).

Stability in solution

βLAP aqueous solution (30 µg·mL^{-1}) prepared from a stock ethanolic solution (20 mg·mL^{-1}) were conditioned in closed glass ampoules and stored at 40 ± 2 ^{o}C under two conditions of illumination (darkness and light). Light stress conditions were selected following ICH Q1B specifications,[22] and applied using a modified oven equipped with two white fluorescent lamps (Hitachi F8T5, Tokyo, Japan) and two emission mercury UV lamps (370 nm) (Philips 08F8T5/BLB, Eindhoven, Nederland). Total brightness (1800 lx) and radiation UV (0.0078 W·m^{-2}) were measured using a luximeter model HD9221 (Delta corp., Padua, Italy) equipped with a probe model P912151 (Delta corp., Padua, Italy).

Additionally, the influence of the presence of a randomized methyl-β-ciclodextrin [RMβCD] at concentration of 5 % (w/v) on the drug stability in solution was evaluated.[23]

At different storage times the percentage of βLAP remaining was determined in triplicate by HPLC. Pseudo-first order rate constants for the βLAP degradation [k] were determined from slopes given by the linear plots of natural logarithm of the percentage of βLAP remaining against time. Half-life [$t_{1/2}$] was determined by the equation:

$$t_{1/2} = \frac{0.693}{\text{slope}}$$

Purification and Identification of the degradation products of β LAP

The solutions of βLAP under degradation in the presence or absence of light showed the formation of several compounds under TLC chromatography. After removal the solvent under vacuum the corresponding residues were purified by preparative-TLC using Dichloromethane/Methanol (9:1) as eluent. The identification of the isolated products was carried out by 1H NMR, 13C NMR and EIMS analysis and by comparison with the data published in the chemical literature. 1H and 13C NMR spectra were recorded in $CDCl_3$ on a Bruker at 300 and 750 MHz, respectively, with TMS as the internal reference (Rheinstetten, Germany). The 2D NMR experiments were conducted on a Bruker WP-400 SY NMR spectrometer in $CDCl_3$ at 400 MHz (Rheinstetten, Germany). High- and low-resolution mass spectra were obtained on a VG Autospec spectrometer (Manchester, UK). Macherey-Nagel polygram Sil G/UV254 and preparative TLC SIL G-100UV254 foils were used for TLC.

Effect of pH

Following Connors and co-workers protocol,[24] a series of 30 $\mu g \cdot mL^{-1}$ βLAP solutions were prepared by adjusting pH values to the range 2 to 10. Buffer solutions were: acid phthalate (pH 2-4), neutralized phthalate (pH 4-6), phosphate (pH 6-8) and alkaline borate (pH 8-10). The ionic strength was adjusted to 0.74 by addition of NaCl. Samples were conditioned in closed glass ampoules and stored in darkness at

40ºC ± 2 ºC. At different times the percentage of βLAP remaining was determined in triplicate by HPLC. All pH measurements were made at 25°C with a digital Crison pH meter (model GLP 22, Barcelona, Spain). Observed first-order rate constants were calculated from slopes of linear plots of natural logarithm of the percentage of βLAP remaining against time.

Molecular modelling

The geometry optimization of the βLAP-RMβCD inclusion complexes was performed in vacuum and in the presence of water molecules using MM2 force field as implement in HiperChem (release 6.03 for windows). The presence of water was simulated by placing the solute molecules into a 20x20x20 Å box with 195 water molecules and a minimum distance of 2.0 Å between solute and water molecules, in a total amount of. The most stable complex conformation was considered through the lowest interaction energy.[25,26]

Statistical analysis

The study of variables effects, light and cyclodextrin addition on the βLAP stability was carried out by analyses of variance [ANOVA] and the stepwise linear regression using Statgraphics version plus® allows the calculation of corresponding surface response.

6.4. RESULTS AND DISCUSSION

βLAP stability in solution

Stability molecular study

Saturated aqueous solutions of βLAP (Figure 6.1B) present an intense orange colour related to the naphthoquinone structure that progressively became colourless as a consequence of the exposure to the light (Figure 6.1A). However, samples stored in darkness became red when they achieved a high level of decomposition (Figure 6.1C).

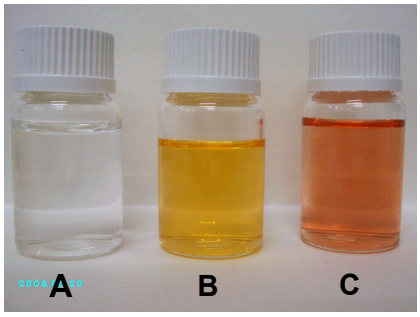

Figure 6.1. βLAP solutions before storage (B) and after storage at light (A) and darkness (C) after a month at 40°C.

The chromatograms of solutions A and C are presented in Figure 6.2. Under the HPLC conditions selected in the present study, βLAP elutes at about 5 min. Irradiated βLAP solution (Figure 6.2A) shows the appearance of multiple and earlier small peaks (0.8-3min). The thermal decomposition βLAP stored in the darkness (Figure 6.2C) presents a new major earlier peak (1.1min).

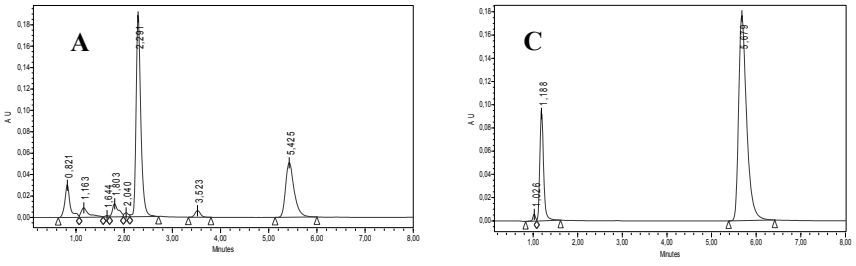

Figure 6.2. HPLC cromatograms of βLAP solutions after storage under the light (A) and in the darkness (C) after a month at 40°C.

Those facts, together with the βLAP naphthoquinone structure suggest the existence of two different degradation routes, hydrolysis, in the darkness, and photolysis under the light. On the purpose of establishing the degradation mechanisms and identifying the degradation products we have studied the crude obtained after elimination of the solvent under light irradiation and storage in the darkness.

71 mg of the dry sample stored in the darkness under pH 10 was chromatographed on two preparative-TLC using dichloromethane /methanol (9:1) as solvent. The major product was isolated as an amorphous red wine solid (31 mg), which showed a molecular formula of $C_{15}H_{16}O_4$ in HRMS. The main differences in the 1H NMR spectrum with respect to βLAP were the chemical shifts of the aromatic and the aliphatic hydrogens. The 13C NMR spectrum revealed the presence of a 1,4-naphthoquinone system instead of 1,2-naphthoquinone moiety as appear in βLAP. All these data suggested that the product isolated is hydroxylapachol (Figure 6.3) which has been previously obtained by synthesis from 2-hydroxy-1,4-naphthoquinone or from 2-hydroxy-3-(3-oxobutyl)-1,4-naphthoquinone by reductive acetylation and treatment with

MeMgI.[27,28] This compound showed low activity against carcinoma walker 256.[29]

The light samples (Figure 6.2C) presented, as indicated by the chromatogram, a complex composition of phthalates that are been studied at the moment.

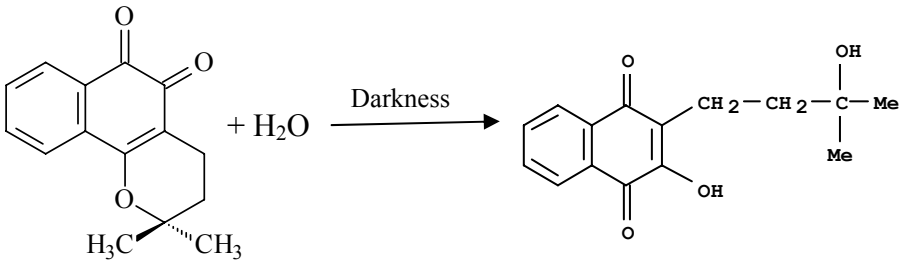

β-LAPACHONE HYDROXYLAPACHOL

Figure 6.3. Proposed hydrolysis for βLAP.

Kinetic stability study

Table 6.1 summarizes the fitting of βLAP remaining to pseudo-first-order kinetics in the conditions studied. As it can be seen, the βLAP exposure to the light accelerates the drug degradation in 140-fold. The half-life of the saturated βLAP solution is one year at 40 ºC in the darkness but just two and a half days when it is stored under the light.

A strategy for enhancing the low solubility of βLAP (0.038 $mg \cdot mL^{-1}$) is based on the complexation of the drug with cyclodextrins.[18-20] The βLAP-RMβCD complexes have a high constant formation and consequently, RMβCD is a potent solubility enhancer.[20] There is no data in the literature about the effect of complexation on the βLAP chemical stability.

According to the constant degradation rate, the βLAP stability is improved upon inclusion into the cavity when the solution is stored in the darkness (Table 6.1, $t_{1/2}$ =1386 days) but the opposite effect is observed when the samples are stored under the light being the $t_{1/2}$ equal to 12 hours (Table 6.1). Similar effects have been described by other authors for drugs as α-tocoferol that experiment a cyclodextrin photo-induced degradation when use hydroxipropyl-β-CD or hydroxipropyl-γ-CD but showed a protection effect against the decomposition in absence of light.[30]

Table 6.1. Kinetic analysis of βLAP remaining in aqueous solution. Pseudo-first-order degradation rate constant [*k*], correlation coefficient [*r*] and half-life [$t_{1/2}$] at 40 °C.

RMβCD %	Light lx	$k\ 10^{-3} day^{-1}$	*r*	$t_{1/2}$ day
0	0	2.1	0.9990	330
0	1800	280.0	0.9909	2.5
5	0	0.5	0.9919	1386
5	1800	1428.6	0.9986	0.5

The ANOVA pointed out the statistical relevance of the light, CD concentration and the interaction between those variables on the degradation rate constant of βLAP. Response surface plotted in Figure 6.4 illustrates the stimulating effect of the RMβCD on the light drug

decomposition, in contrast to the protector effect for hydrolysis decomposition.

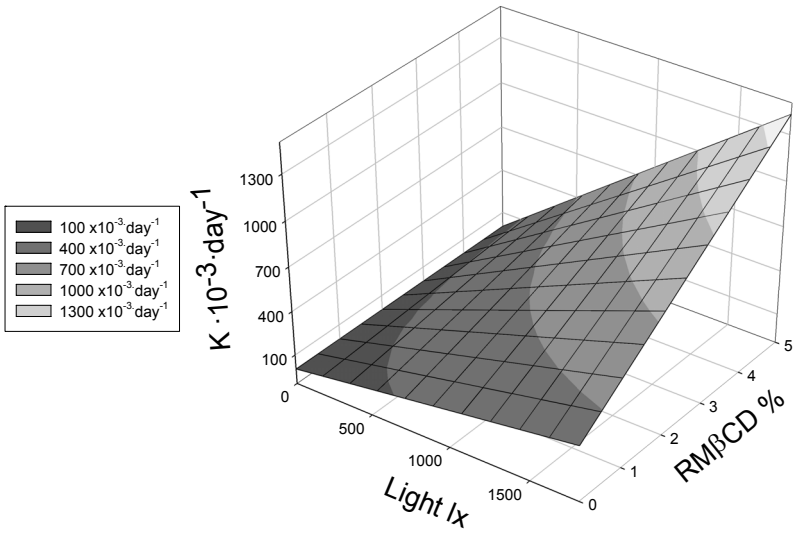

Figure 6.4. Stability degradation constant (*k*) of βLAP surface response.

The combined analysis of the effect of variables, light [L] and concentration of CD [RMβCD] on the βLAP degradation first-order rate constant (k) using stepwise regression allows obtaining the following equation:

$k = 2.1 + 0.155 \cdot [L] - 0.320 \cdot [RM\beta CD] + 0.128 \cdot [L] \cdot [RM\beta CD]$

The effect of cyclodextrins on drug stability is conditioned by the drug concentration and/or the formation of inclusion complexes of different nature.[31] Molecular modelling (Figure 6.5) indicate a more stable conformation of βLAP-RMβCD inclusion complexes 1:1 stoiquiometry than 1:2 stoiquiometry (see table 6.2 and table 6.3) in agreement with our previous experimental studies.[20] The good fit of βLAP in the cavity of

RMβCD could explain its high capacity in increasing drug aqueous solubility make it possible four conformations 1:1 with equivalent enthalpy values both in vacuum and aqueous medium (Table 6.2). In aqueous medium the conformation A is slightly more stable. The methylated group of βLAP included by the broad side of cyclodextrin (Figure 6.5, conformation A) led less interference of electronegative cyclodextrin carbonyl groups conferring more stability to the complex.

Table 6.2. Calculated enthalpy for the formation 1:1 βLAP-RMβCD stoiquiometry complexes.

	Included group	ΔH (Kcal·mol^{-1})	
	βLAP-CD	vacuum	aqueous medium
A	methyl-broad	111,1	-466.7
B	benzene-broad	111,0	-451.5
C	benzene-narrow	115,7	-453.6
D	methyl-narrow	115,0	-451.6

Table 6.3. Calculated enthalpy for the formation 1:2 βLAP-RMβCD stoiquiometry complexes.

Included group	ΔH (Kcal·mol^{-1})	
CD-βLAP-CD	vacuum	aqueous medium
broad-benzene/methyl-narrow	203,5	-193,6
broad-benzene/methyl-broad	178,2	-217,1
narrow-benzene/methyl-broad	184,3	-191,1
narrow-benzene/methyl-narrow	201,5	-171,7

Based on this, the conformation A and D, specially the first one, probably the most frequent inclusion complex conformation (Figure 6.5), included the methylated ring inside of cyclodextrin and protects the βLAP ether bond against the hydrolytic process. Moreover, the rapprochement of CDs unsubstituted hydroxyls groups to the electronegative atoms of

βLAP naphthoquinone group, in particular B and C conformations (Figure 6.5) can favour light decomposition of naththoquinone groups.[32]

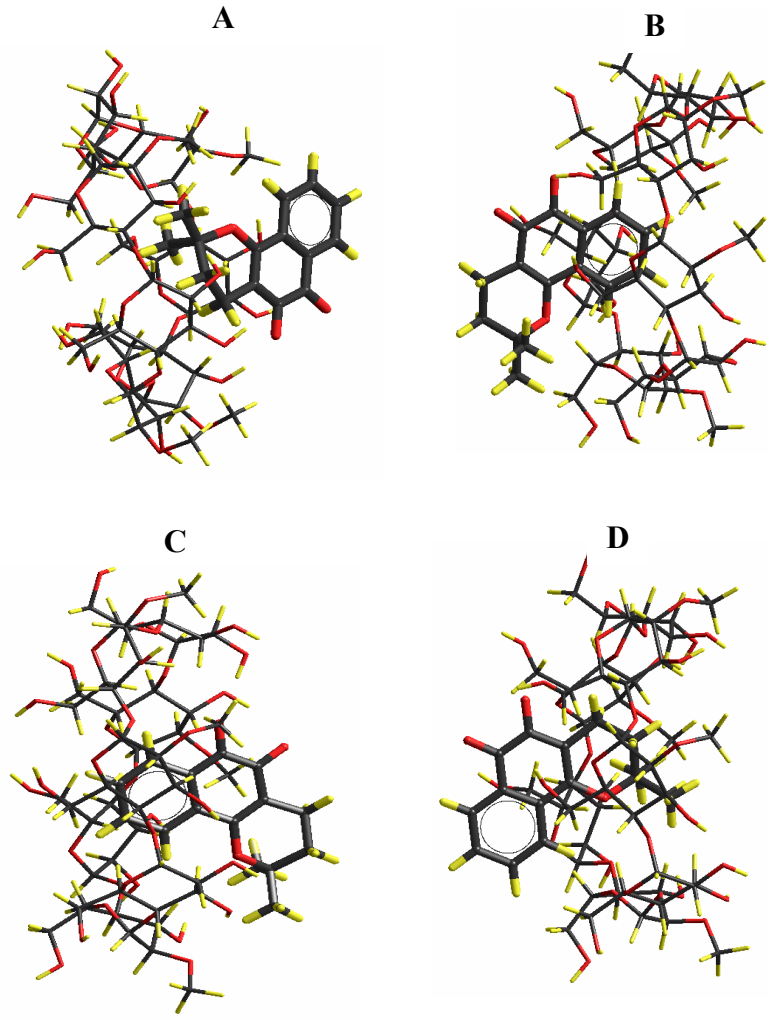

Figure 6.5.Posible structures of β-lapachone-RMβCD by MM2.

Effect of pH

The stability of drug in aqueous medium is strongly dependent on the pH value. Most of degradation routes are catalysed by hydroxyl or protons groups. So, it is very important the establishment of the drug behavior at different pHs in pre-formulation studies. For drugs of oral use, it is especially relevant the knowledge of its behaviour in the range of gastrointestinal tract pH.[33]

βLAP remaining in solution over a range of pH values (2 to 10) was monitored by HPLC. Data fit pseudo-first-order kinetics (Table 6.4). The log pseudo-first-order constants at various pH values are plotted in Figure 6.6. The obtained pH degradation profile is characteristic of a non ionic drug whose degradation is catalyzed by hydroxyl groups. The range of βLAP maximum stability in aqueous solution is between pH 2-4, prevailing a no hydroxyl catalytic process. The kinetic of degradation fit the following predictive model:

$$K_{obs} = 4.997 \cdot 10^{-4} + 582.6 \cdot [OH^-]^{0.8412}$$

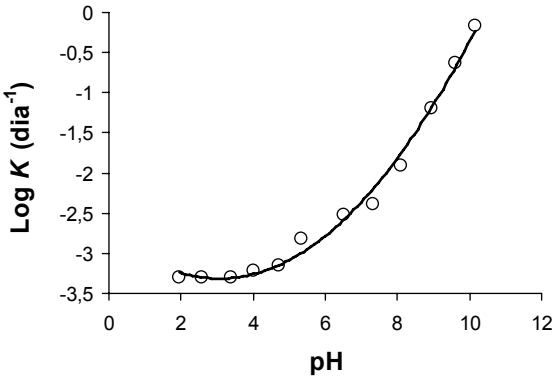

Figure 6.6. The pH rate profile of βLAP at 40°C.

Table 6.4. Kinetic analysis of βLAP pH profile at 40°C. Pseudo-first-order degradation correlation coefficient (*r*) and half-life ($t_{1/2}$).

pH	*r*	$t_{1/2}$ day
1,94	0,9817	1386
2,56	0,9800	1386
3,40	0,9987	1386
4,00	0,9897	1155
4,72	0,9754	990
5,33	0,9701	462
6,50	0,9998	231
7,32	0,9922	169
8,09	0,9938	55
8,93	0,9981	11
9,40	0,9975	3
10,00	0,9965	1

6.5. CONCLUSIONS

βLAP in solution has two different degradation routes: hydrolysis in the darkness and photolysis under the light. The hydrolysis gives as the main degradation product hydroxylapachol. The photolysis gives a complex mixture of degradation products that are under investigation.

The inclusion complex βLAP-RMβCD has different effects on the two degradation routes, a chemopreventive effect on the hydrolysis in the darkness and the opposite effect on the photolysis. The drug suffers an alkaline hydrolysis being the most stable range of pH between 2 and 4.

These studies provide important information as regards the optimal storage conditions and formulation of βLAP in solution.

6.6. ACKNOWLEDGEMENTS

Authors thank LAFEPE and Professor Pedro Jose Rolim Neto for their kind gift of the βLAP and Roquette Freres for the generous donation of cyclodextrins. This work was supported by Xunta de Galicia (PGIDIT04BTF203011PR) and the Programme Alβan, the European Union Programme of High Level Scholarships for Latin America, scholarship nº E04D043994BR.

6.7. REFERENCES

1. Gonçalves de Lima O, D`Albuquerque IL, Machado MP, Silva E, Pinto GP. 1956. Primeiras observações sobre a ação antimicrobiana do lapacho. An Soc Biol Pe 14:129-135.
2. Perez-Sacau E, Soto-Delgado J, Estevez-Braun A, Ravelo AG. 2005. Synthesis of 9- and 10-membered macrolactones by selective ozonolysis of 1,4-diazaphenanthrene derivatives. Tetrahedron 61(2):437-445.
3. Li CJ, Zhang LJ, Dezube BJ, Crumpacker CS, Pardee AB. 1993. Three inhibitors of type 1 human immunodeficiency virus long terminal repeat-directed gene expression and virus replication. Proc Natl Acad Sci USA 90(5):1839-1842.
4. Gonçalves de Lima O, D`Albuquerque IL, Gonçalves de Lima C, Dália Maia MH. 1962. Substâncias antimicrobianas de plantas superiores. Rev Inst Antibiot 4(1/2):3-17.
5. Mueller K, Sellmer A, Wiegrebe W. 1999. Potential Antipsoriatic Agents: Lapacho Compounds as Potent Inhibitors of HaCaT Cell Growth. J Nat Prod 62(8):1134-1136.
6. Moon D, Choi YH, Kim N, Park Y, Kim G. 2007. Anti-inflammatory effects of β-lapachone in lipopolysaccharide-stimulated BV2 microglia. Int Immunopharmacol 7(4):506-514.
7. Docampo R, Lopes JN, Cruz FS, Souza W. 1977. Trypanosoma cruzi: ultrastructural and metabolic alterations of epimastigotes by beta-lapachone. Exp Parasitol 42(1):142-149.

8. Pardee AB, Li YZ, Li CJ. 2002. Cancer therapy with β-lapachone. Curr Cancer Drug Targets 2(3):227-242.

9. Li Y, Sun X, LaMont JT, Pardee AB, Li CJ. 2003. Selective killing of cancer cells by β-lapachone: Direct checkpoint activation as a strategy against cancer. Proc Natl Acad Sci USA 100(5):2674-2678.

10. Pink JJ, Planchon SM, Tagliarino C, Varnes ME, Siegel D, Boothman DA. 2000. NAD(P)H: quinone oxidoreductase activity is the principal determinant of β-lapachone cytotoxicity. J Biol Chem 275:5416-5424.

11. Ough M, Lewis A, Bey EA, Gao J, Ritchie JM, Bornmann W, et al. 2005. Efficacy of beta-lapachone in pancreatic cancer treatment: exploiting the novel, therapeutic target NQO1. Cancer Biol Ther 4(1):95-102.

12. Boothman DA, Trask DK, Pardee AB. 1989. Inhibition of potentially lethal DNA damage repair in human tumor cells by β-lapachone, an activator of topoisomerase I. Cancer Res 49(3):605-612.

13. Li CJ, Li Y, Pinto AV, Pardee AB. 1999. Potent inhibition of tumor survival in vivo by β-lapachone plus taxol: combining drugs imposes different artificial checkpoints. Proc Natl Acad Sci USA 96(23):13369-13374.

14. Park HJ, Ahn K, Ahn S, Choi E, Lee SW, Williams B, et al. 2005. Susceptibility of cancer cells to β-lapachone is enhanced by ionizing radiation. Int J Radiat Oncol Biol Phys 61(1):212-219.

15. Shapiro G, Supko JG, Ryan DP, Appelman L, Berkenblit A, Craig AR, et al. Eder Phase I trial of ARQ 501, an Activated Checkpoint Therapy (ACT) agent, in patients with advanced solid tumors. Proceedings of 2005 ASCO Annual Meeting; Orlando, USA. 13-17 May, 2005: 3042.

16. Hartner LP, Rosen L, Hensley M, Mendelson D, Staddon AP, Chow W, et al. Phase 2 dose multi-center, open-label study of ARQ 501, a checkpoint activator, in adult patients with persistent, recurrent or metastatic leiomyosarcoma (LMS). Proceedings of ASCO Annual Meeting; Chicago, USA. June 1-5, 2007: 20521.

17. Kawecki A, Adkins DR, Cunningham CC, Vokes E, Yagovane DM, Dombal G, et al. A phase II study of ARQ 501 in patients with advanced squamous cell carcinoma of the head and neck. Proceedings of 2007 ASCO Annual Meeting; Chicago, USA. June 1-5, 2007: 16509.

18. Nasongkla N, Wiedmann AF, Bruening A, Beman M, Ray D, Bornmann WG, et al. 2003. Enhancement of solubility and bioavailability of beta-lapachone using cyclodextrin inclusion complexes. Pharm Res 20(10):1626-1633.

19. Wang F, Blanco E, Ai H, Boothman DA, Gao J. 2006. Modulating β-lapachone release from polymer millirods through cyclodextrin complexation. J Pharm Sci 95(10):2309-2319.

20. Cunha-Filho M, Dacunha-Marinho B, Torres-Labandeira JJ, Martínez-Pacheco R, Landín M. 2007. Characterization of β-Lapachone and Methylated β-Cyclodextrin Solid-state Systems. AAPS PharmSciTech 8:Article 60.

21. Cunha Filho M, Martínez-Pacheco R, Landín M. 2008. Stability and degradation kinetics of the investigational antitumoral drug β-lapachone in solid state. Submitted.

22. ICH Q1B, Photostability testing of new drug substances and products, Internation Conference on Harmonization, Geneva, 1996.

23. Tonnesen HH, Masson M, Loftsson T. 2002. Studies of curcumin and curcuminoids. XXVII. Cyclodextrin complexation: solubility, chemical and photochemical stability. Int J Pharm 244:127-135.

24. Connors, K. 1986. Chemical stability of pharmaceuticals: A handbook for pharmacists. John Wiley & Sons. pp. 847.

25. Lipkowitz KB. 1998. Applications of Computational Chemistry to the Study of Cyclodextrins. Chem Rev 98(5):1829-1873.

26. Pose-Vilarnovo B, Perdomo-Lopez I, Echezarreta-Lopez M, Schroth-Pardo P, Estrada E, Torres-Labandeira JJ. 2001. Improvement of water solubility of sulfamethizole through its complexation with b- and hydroxypropyl-b-cyclodextrin. Characterization of the interaction in solution and in solid state. Eur J Pharm Sci 13(3):325-331.

27. Pettit GR, Houghton, LE. 1971. Synthesis of hydroxyhydrolapachol and lapachol. J Chem Soc 3:509-11.

28. Cassis R, Tapia R, Valderrama J. 1977. Studies on quinones. IV. Synthesis of hydroxylapachol and related products. Anales de Quimica, 73(12):1512-13.

29. Subramanian S, Ferreira MMC. 1998. Structure-activity relationship study of lapachol and some derivatives of 1,4-naphthoquinones against carcinosarcoma Walker 256. Struct Chem 9:47-57.

30. Iaconinoto A, Chicca M, Pinamonti S, Casolari A, Bianchi A, Scalia S. 2004. Influence of cyclodextrin complexation on the photodegradation and antioxidant activity of a-tocopherol. Pharmazie 59(1):30-33.

31. Voulgari A, Benaki D, Michaleas S, Antoniadou-Vyza E. 2007. The effect of β-cyclodextrin on tenoxicam photostability, studied by a new

liquid chromatography method; the dependence on drug dimerisation. J Incl Phenom 57:141-146.

32. Fromming K, Szejtli, J. 1994. Cyclodextrin in Pharmacy. Kluwer: Academic/Plenum Publishers, pp 219.

33. Yoshioka S, Stella VJ. 2000. Stability of drugs and dosage forms. Kluwer: Academic/Plenum Publishers, pp 268.

Alameda, Santiago de Compostela

Capítulo 7

Compatibility of the antitumoral β-lapachone with different solid dosage forms excipients

Autores: Marcílio S. S. Cunha-Filho[1], Ramón Martínez-Pacheco[1] and Mariana Landín[1]

[1]Departamento de Farmacia y Tecnología Farmacéutica, Facultad de Farmacia, Universidad de Santiago de Compostela, Santiago de Compostela, Spain

Revista: J. Pharm. Biom. Anal. 2007. Manuscript in press. doi:10.1016/j.jpba.2007.08.016

7.1. ABSTRACT

The objective of the present study was to evaluate the compatibility of the β-lapachone (βLAP), an antitumoral drug in clinical phase, with pharmaceutical excipients of common use including diluents, binders, disintegrants, lubricants and solubilising agents. Differential Scanning Calorimetry (DSC) was used for a first screening to find small variations in peak temperatures and/or their associated enthalpy for six drug/excipient combinations (magnesium stearate, sodium estearyl fumarate, dicalcium phosphate dihydrate, mannitol, randomized methyl-β-cyclodextrin and hydroxipropil-β-cyclodextrin), which indicate some degree of interaction. Additional studies using Fourier Transformed Infrared Spectroscopy (FTIR), Optical Microscopy (OM) and Heating-Cooling DSC (HC-DSC) confirmed the incompatibility of βLAP with magnesium stearate and dicalcium phosphate dihydrate. Those excipients should be avoided in the development of solid dosage forms.

Keywords: β-lapachone; Compatibility; Excipient; Differential Scanning Calorimetry.

7.2. INTRODUCTION

The β-lapachone (βLAP) is an antitumoral drug in clinical phase that presents good perspectives for its incorporation in the therapies in the near future. βLAP is obtained on a small scale from South American trees of the families Bigoniaceae and Verbenaceae [1]. On a larger scale it can be produced following the method developed by Hooker and co-workers in 1892 through cyclization of lapachol in sulphuric acid [2].

Recent studies have demonstrated that βLAP possesses a potent antineoplasic activity. *In vitro* and *in vivo* studies have shown that βLAP inhibits conventional therapy-resistant tumours, particularly the malignant neoplasm of slow cell cycle like prostate, colon and some ovarian and breast cancer [3-5]. Despite its interesting potential applications, preformulation studies have not yet been performed.

The study of drug-excipient compatibility is an important stage in the development of a solid dosage form as their incompatibility can alter the stability and/or the biovailability of drugs, thereby, affecting its safety and/or efficacy. Two types of chemical incompatibilities have been described between excipients and drugs: those corresponding to intrinsic chemical drug degradation such hydrolysis or oxidation but without significant direct covalent chemical reactions, and those corresponding to covalent reaction between the drug and the excipient [6].

Throughout the different methods reported on drug-excipient compatibility studies, DSC has been shown to be a rapid, sensitive and simple technique used in routine experiments. Small variations in peak temperature or associated enthalpy are interpreted as an indication of

interaction and possible incompatibility. Despite the advantages of DSC there are certain limitations. The extrapolation of findings obtained at high temperatures, are not always in agreement with the drug real situation in the formulation [7,8]. Therefore, the DSC results must be interpreted carefully and some complementary techniques, such as infrared spectroscopy, microscopy or X-ray diffractometry can be useful in avoiding misleading conclusions [9].

In the present study the compatibility of βLAP with twelve different pharmaceutical excipients of common use in the development of solid dosage forms was evaluated. Five cyclodextrins have also been included because βLAP has an extremely low hydrosolubility and, recently, cyclodextrins have been shown to be useful in overcoming this problem [10-12].

7.3. EXPERIMENTAL

Materials

βLAP was a gift from UFPE, Brazil (batch L503) with a purity of 99.9 % by HPLC and DSC. Following excipients were purchased from commercial sources and used as such. Microcrystalline cellulose PH 101 (MCC, Guinama, Spain), pregelatinized maize starch (starch, Guinama, Spain), lactose monohydrated (lactose, Guinama, Spain), magnesium stearate (MGST, Guinama, Spain), sodium estearyl fumarate (PRUV, Juliá-Parrera, Spain), talc (talc, Guinama, Spain), hydroxipropilmethyl cellulose K100LV Premium (HPMC, Guinama, Spain), polyvinyl pyrrolidone (PVP, BASF, Germany), dicalcium phosphate dihydrate

emcompress (DCPD, United Mendell, UK), medium-viscosity carboxymethyl cellulose (CMC, Sigma, España), sodium croscarmellose (explocel, FMC, USA), mannitol (mannitol, AstraZeneca, Spain). The cyclodextrins β-cyclodextrin (βCD) and randomized methyl-β-cyclodextrin (RMβCD, molar substitution 0.5) were donated by Roquette, France; the hydroxipropil-β-cyclodextrin (HPβCD, molar substitution 2.7) was facilitated by Janssen Pharmaceutica, Belgium; the α-cyclodextrin (αCD) was provided by Wacker, Germany and the sulfobutylether-β-cyclodextrin (SBβCD, molar substitution 1.0) was donate by Cydex, EUA.

Study protocol

The flow diagram (Fig. 7.1) presents the protocol used for the βLAP-excipient compatibility evaluation. Firstly, DSC measurements on binary βLAP-excipient mixtures were selected for rapid screening. Investigation on mixtures showing interactions or changes in the thermal profile of components were completed with Fourier Transformed Infrared Spectroscopy (FTIR), Optical Microscopy (OM) and Heating-Cooling DSC studies (HC-DSC).

Sample preparation

βLAP-excipient physical mixtures in a ratio of 1:1 (w/w) were prepared by mixing in a Turbula WAB T2C (Switzerland) for 15 min. This proportion was chosen to maximize the probability of interactions between materials. Those samples have been denoted as PM.

PM samples were stored in an oven at 40 ºC and 75 % relative humidity in closed containers using sodium chloride saturated solutions for a month [13]. Those stressed samples have been denoted as SM.

Additionally, the drug, some excipients and its mixtures were subjected to thermal stress by heating up to 160ºC at a rate of 10ºC·min^{-1}. This treatment was proven to be non destructive for the isolated materials, which maintained their physical and chemical entity when cooling. Those samples have been denoted as TSM.

Differential Scanning Calorimetry (DSC)

Samples weighing 3-4 mg were placed in open aluminium pans and heated from 30 to 300 ºC at a rate of 10 ºC·min^{-1} using a temperature modulated DSC Q100 calorimeter (TA Instruments, USA). Nitrogen was used as purge gas at a flux rate of 50 mL·min^{-1}. The calibration of temperature and heat flow was performed with standard indium samples. Heating-cooling DSC (HC-DSC) studies were carried out at a rate of 10ºC·min^{-1} following the sequence 30-170-30-300 ºC.

Optical Microscopy (OM)

The morphological characteristics of the samples were analysed using an Olympus SZ60 (Opelco, Japan) microscope connected to a video camera Olympus DP12 (Opelco, Japan). The images were processed using Analysis® version 3.2.

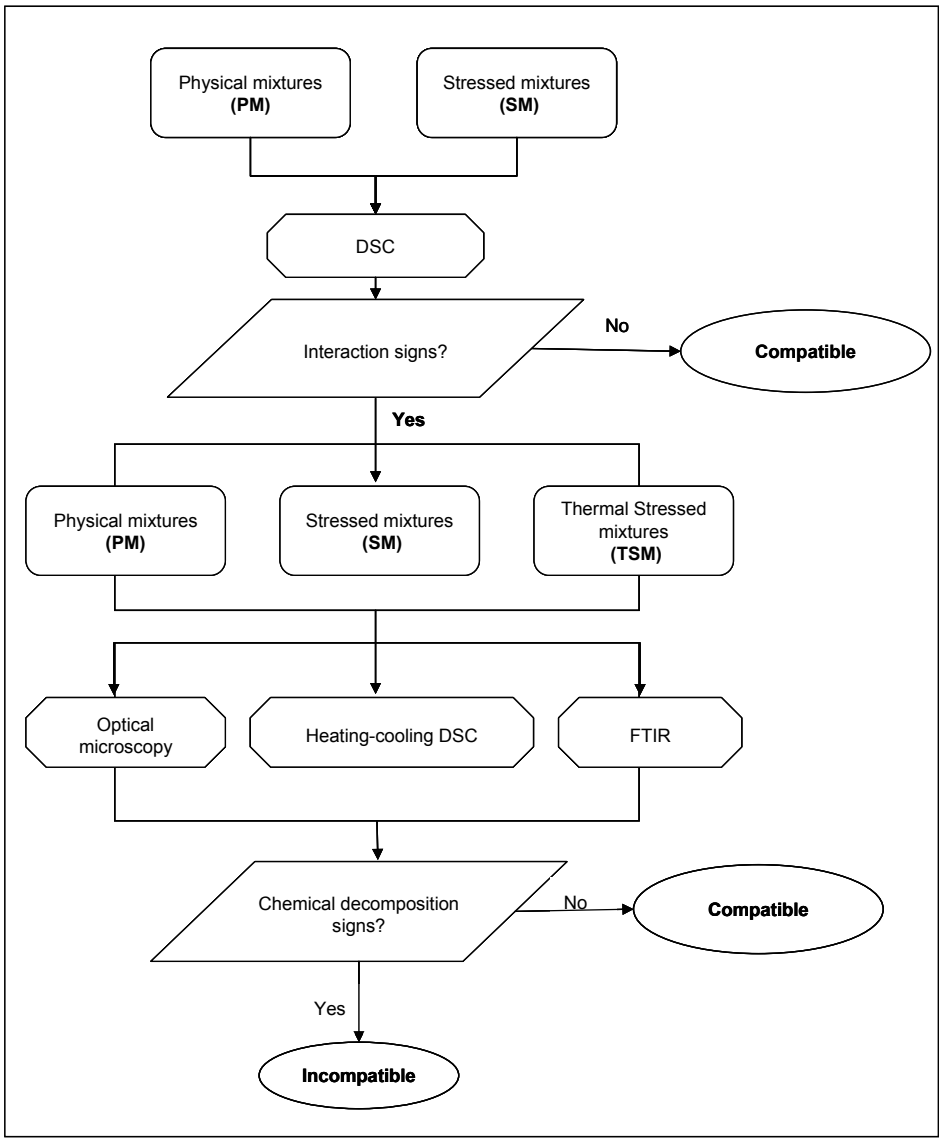

Fig. 7.1. Strategy for the βLAP-excipient compatibility study.

7.4. RESULTS AND DISCUSSION

Drug-excipient compatibility first DSC screening

DSC data of the βLAP and excipient thermal events in single or PM and SM binary systems are presented in Table 7.1 and Table 7.2.

The βLAP DSC curve (Table 7.1) displays two events; a sharp endotherm at 157.3 ºC, due to the drug melting with an associated enthalpy of 104.0 $\pm$ 1.5 $J \cdot g^{-1}$ and the drug decomposition after 230 ºC. This profile is characteristic of an anhydrous crystalline substance. The melting βLAP event is highly repeatable even when βLAP is blended with the different excipients (peak shifts higher than 0.5 ºC are in bold type in Table 7.1). Variations in the enthalpy values for the binary mixtures can be attributed to some heterogeneity in the small samples used for the DSC experiments (3-4mg) [7, 9].

Some excipient endothermic events are melting (lactose, mannitol, MGST or PRUV) or dehydration phenomena (lactose, DCPD) but the most are broad peaks associated to their loss of adsorbed water (Table 7.2) with inherent important variations in their enthalpies, particularly for the SM samples which have been stored at 40 ºC and 75 % RH. A careful analysis of excipient thermal behaviour is required in order to avoid misinterpretations. Bold type indicates important changes in the excipient DSC profiles in Table 7.2.

Thermograms obtained by DSC analysis of individual components were compared with those of the mixtures, before (PM) and after its storage at 40 ºC and 75 % RH (SM). Of the 17 commonly used excipients tested only six showed interactions with βLAP. The profiles of the

mixtures were an overlapping of the thermograms of the single components for MCC, starch, lactose, talc, HPMC, PVP, CMC, explocel, αCD, βCD and SBβCD, which is accepted as compatibility evidence between materials [15]. Changes in βLAP events and/or excipient DSC profiles in the binary systems (PM) could be detected in two diluents, DCPD and mannitol; two lubricants, MGST and PRUV and two solubilising agents HPβCD and RMβCD. Those variations are slightly accentuated with ageing at 40 ºC and 75 % relative humidity (SM).

Table 7.1. Thermal data from DSC of βLAP melting event, in single and PM and SM binary systems studied.

Raw Material	PM			SM		
	Range (ºC)	T_{peak} [a] (ºC)	ΔH (J g^{-1})	Range (ºC)	T_{peak} [a] (ºC)	ΔH (J g^{-1})
Single βLAP	152-162	157.3	104.0			
+ DCPD	**154-162**	**154.9**	**155.5**	**154-161**	**154.8**	**145.1**
+ lactose	153-162	157.6	55.1	153-162	157.1	62.4
+ mannitol	**152-160**	**156.5**	57.2	**152-160**	**156.0**	50.0
+ MCC	152-162	157.5	49.5	151-162	157.5	74.3
+ starch	153-162	157.4	58.7	153-162	157.0	68.9
+ CMC	153-162	157.3	65.3	152-162	157.3	65.6
+ HPMC	152-162	157.3	53.9	152-162	157.2	71.6
+ PVP	152-162	157.4	34.4	152-162	157.6	51.8
+ explocel	153-162	157.3	47.8	153-162	157.3	66.5
+ MGST	151-161	**156.8**	41.2	**151-160**	**156.7**	44.0
+ PRUV	**148-164**	**153.3 155.1**	60.3	**147-162**	**153.0 156.1**	87.6
+ talc	152-162	156.9	58.4	152-162	157.1	51.7
+ αCD	152-162	157.7	51.1	153-162	157.4	59.1
+ βCD	152-162	157.8	65.6	152-162	157.3	53.1
+ HPβCD	152-162	157.2	40.5	153-161	**156.8**	58.8
+ RMβCD	152-162	157.4	55.0	152-162	**156.8**	65.5
+ SBβCD	153-163	157.9	65.0	153-163	157.9	65.8

[a] Peak temperature

Table 7.2. Thermal data from DSC of excipients studied and PM and SM binary systems.

	Excipient events			**PM**			**SM**		
	range (ºC)	**T_{peak} [a] (ºC)**	**ΔH (J g^{-1})**	**range (ºC)**	**T_{peak} [a] (ºC)**	**ΔH (J g^{-1})**	**range (ºC)**	**T_{peak} [a] (ºC)**	**ΔH (J g^{-1})**
DCPD	117-170 172-204	150.8 191.1	101.4 310.0	-	-	-	-	-	-
lactose	110-156 195-223	143.6 217.7	146.4 153.1	110-150 195-223	143.7 217.6	55.6 54.1	110-150 195-221	144.0 217.2	53.5 35.3
mannitol	155-177	168.9	307.0	**161-173**	**167.4**	137.6	**161-172**	**167.1**	177.7
MCC	30-147	77.8	175.2	30-123	61.9	83.9	30-105	60.4	55.6
Starch	30-184	102.0	395.1	30-148	94.2	162.7	30-140	74.8	134.6
CMC	30-196	96.3	510.7	30-120	72.1	128.0	30-122	75.1	163.0
HPMC	30-122	75.8	177.9	30-98	58.5	78.2	30-95	60.8	82.5
PVP	30-151	92.9	428.0	30-123	74.7	227.9	30-127	76.7	221.8
explocel	30-183	87.6	407.9	30-140	78.3	177.8	30-127	70.5	129.5
MGST	30-132	73.0 103.7	205.5	30-122	73.7 103.4	112.2	**56-81** **90-122**	**72.5** **113.0**	**11.1** **73.6**
PRUV	72-117 117-147 197-205	110.2 135.2 200.4	131.9 80.2 30.8	72-113 **113-124** **124-144**	108.7 **117.9** **131.1**	60.4 **10.2** **38.8**	**75-110** **111-123** **124-139**	**103.3** **117.2** **129.9**	**21.3** **8.8** **21.5**
talc	-	-	-	-	-	-	-	-	-
αCD	30-155	75.5	411.8	30-143	73.5	200.5	30-140	72.0	204.5
βCD	30-145	107.8	339.4	30-125	97.8	178.4	30-125	105.7	200.1
HPβCD	30-150	88.0	260.9	30-135	79.6	166.6	30-120	70.2	116.5
RMβCD	30-145	91.6	277.5	30-130	79.7	149.6	30-127	78.6	177.2
SBβCD	30-196	88.8	383.9	30-140	73.1	87.9	30-147	63.5	127.3

[a]Peak temperature

Mixtures of βLAP with mannitol and DCPD have shown changes, among diluents studied, in both drug and excipients DSC events (Figs. 7.2 and 7.3). Mannitol is an excipient with a well-defined thermal profile characterized by a melting peak at 168.9 ºC indicative by its crystalline and anhydrous state (Fig. 7.2) [16]. Binary blending βLAP-mannitol (PM and SM) present shifts in melting peaks of drug and mannitol, as have been pointed out for other drugs such as amoxicilline, paracetamol or vitamin D [17-19].

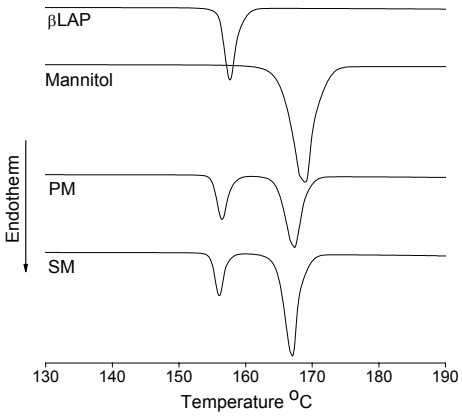

Fig. 7.2. DSC analysis of βLAP, mannitol and βLAP-mannitol combinations.

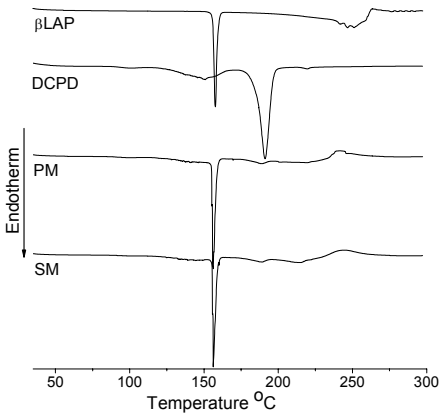

Fig. 7.3. DSC analysis of βLAP, DCPD and βLAP-DCPD combinations.

The DCPD DSC profile is associated with the loss of water of hydration from this material and the formation of anhydrous dicalcium phosphate. The dehydration process occurs in two stages at 150.8 and 191.1 ºC (associated enthalpies 100 and 310 $J \cdot g^{-1}$ respectively) in agreement with different authors (Table 7.2), the contribution of which depends on the DCPD variety and its particle size [20,21]. As it can be observed (Fig. 7.3), mixing βLAP with DCPD caused a shift in the melting

peak of the drug and the disappearance of the DCPD characteristic events. Additionally, the enthalpy associated 155.5 $J \cdot g^{-1}$ (Table 7.1), is lower than that corresponding to the addition of the thermal phenomena of components (about 250 $J \cdot g^{-1}$). These results suggest a robust interaction between components.

The MGST has been shown to be incompatible with an important number of drugs, such as glibenclamide or aspirin [22,23]. This excipient presents two molecules of water hydration (5.5 % of weight approx.). The dehydration process occurs in several steps at over 70 ºC. Additionally, it presents a melting peak at approximately 120 ºC, which sometimes appears at lower temperatures or even superimposes the dehydration events as a consequence of the product being a mixture of magnesium palmitate and stearate [9,24,25]. Our DSC results agree with previous information (Fig. 7.4 and Table 7.2), MGST showing a wide endotherm with two events at 73.0 and 103.7 ºC. The PM mixture thermogram presents a slight shift in the βLAP melting peak and a reduction in the associated enthalpy (Table 7.1). No changes can be denoted in the MGST events. However, the stressed sample (SM), exhibits important modifications regarding the MGST thermogram (Table 7.2). Those variations can be attributed to the modifications associated to the MGST ageing ($MGST_{aged}$) at the above conditions (40 ºC and 75 % RH) as it can be seen in the $MGST_{aged}$ DSC profile (Fig. 7.4). The hydration of MGST seems to increase the interaction with βLAP, which could affect on the drug stability negatively.

Mixtures of βLAP and PRUV also exhibit diverse variations in the thermal behaviour of both products (Fig. 7.5 and Table 7.2). The PRUV DSC profile is characterized by three endothermic events at 110 ºC, 135ºC and 200 ºC [26]. The PM mixtures show important variations in the

positions of the three events. In this respect, peaking at 110 ºC it seems to split into two; the peak at 135 ºC shifts to a lower temperature (131 ºC) and the one at 200 ºC disappears completely (Table 7.2). Additionally, a widening in drug melting peak can be observed. Those differences are maintained in the SM samples. The slight hygroscopic nature of both, βLAP and PRUV, justifies this behaviour [16].

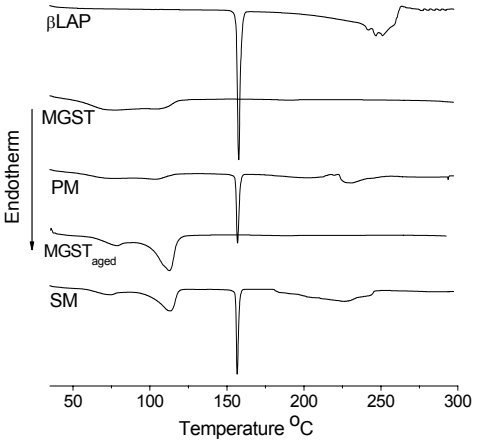

Fig. 7.4. DSC analysis of βLAP, MGST and βLAP-MGST combinations.

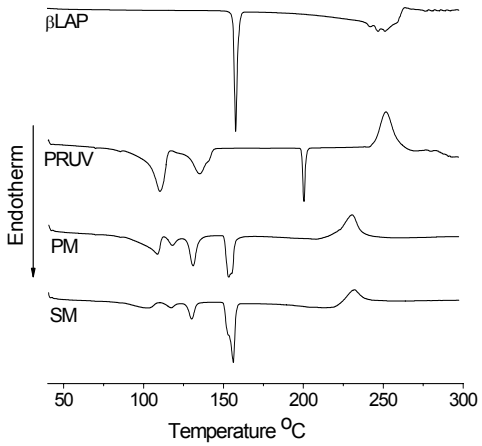

Fig. 7.5. DSC analysis of βLAP, PRUV and βLAP-PRUV combinations.

Cyclodextrins (CDs) are cyclic oligosaccharides with lipophilic inner cavities and hydrophilic outer surfaces capable of interacting with a large variety of drugs giving non-covalent inclusion complexes [27]. βLAP can form inclusion complexes with different cyclodextrins giving an improvement in its solubility and dissolution rate [10,12]. Variations in the raw material thermal profiles or even the disappearance of the fusion peak of the drug in combinations of drug-cyclodextrin are often interpreted as an evidence of an inclusion complex formation.

Cyclodextrins exhibit a broad endothermic effect ranging between 30 ºC and 149 ºC associated with water loss from inside the cavity (Table 7.2). Among the cyclodextrins studied, only HPβCD and RMβCD (Fig. 7.6 and 7.7) show small modifications in the thermal profiles of the stressed samples (SM), mainly shifting at the melting peak of the drug and in the enthalpies associated to loss of water from the CDs which could be indicative of the interactions. The βLAP-RMβCD mixtures (Fig. 7.6) show, additionally, an extra exothermic event at 178 ºC, which was really small quantitatively (associated enthalpy 8 $J \cdot g^{-1}$) but was consistent. This could be associated to a strong interaction between the RMβCD and the melted drug and subsequently, the βLAP entrance into the empty CD cavity in an energetic favoured process that decreases the energy of the system. The RMβCD has been shown as the most useful βCD derivative in improving βLAP solubility [12].

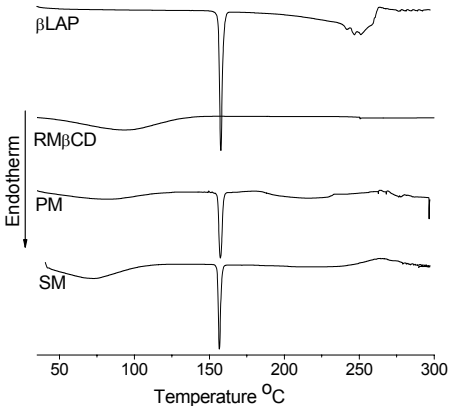

Fig. 7.6. DSC analysis of βLAP, RMβCD, βLAP-RMβCD combinations.

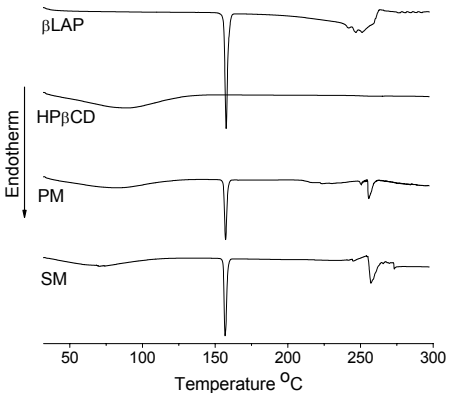

Fig. 7.7. DSC analysis of βLAP, HPβCD, βLAP-HPβCD combinations.

FTIR, OM and HC-DSC compatibility confirmatory assays

Neither mannitol nor PRUV incompatibility with βLAP was confirmed from those additional experiments. No significant changes in the FTIR characteristic bands of the pure substances can be detected, even after heating at 160 ºC (TSM samples). HC-DSC experiments show, on cooling, two exothermal events corresponding to the drug and excipient crystallization process. On the second heating, the endothermal events of the first heating remain unchanged. No sign of decomposition was detected by optical microscopy (as an example see mannitol-βLAP mixtures, Fig. 7.8). Results are in agreement with other author findings for mannitol [7,9,19] and PRUV [26]. The interaction detected by thermal methods can be explained on the basis of the proximity of the melting events of both components without significant physicochemical stability problems.

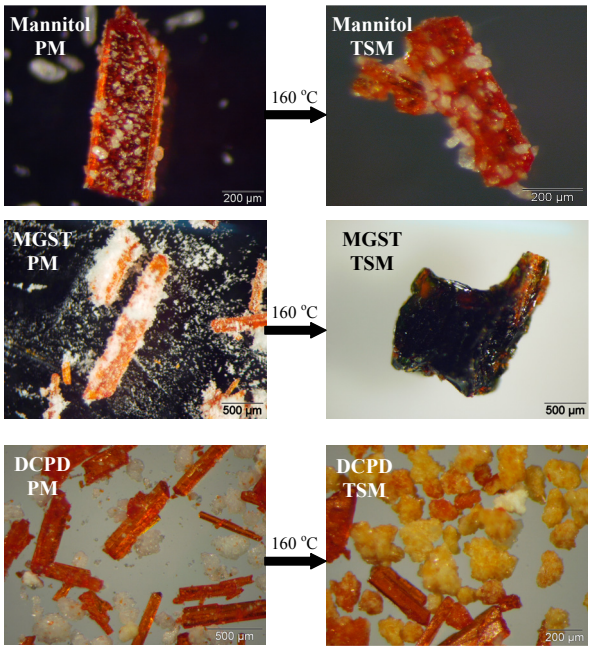

Fig. 7.8. OM micrographs of some of the mixtures indicated.

The same conclusion was achieved after additional research on RMβCD and HPβCD-βLAP samples. FTIR data (Fig. 7.9) and HC-DSC (Fig. 7.10) on HPβCD-βLAP and RMβCD-βLAP mixtures respectively do not show significant changes on the characteristic behaviour of the pure substances even after thermal stress (TSM) or after a melting-crystallization-melting cycle. Interactions between those CDs and the drug suggested by the preliminary DSC results (Table 7.1) should be interpreted in terms of the inclusion of βLAP into the CD cavity and the formation of inclusion complexes, thus being a beneficial interaction with profitable repercussion in the βLAP hydrosolubility [12].

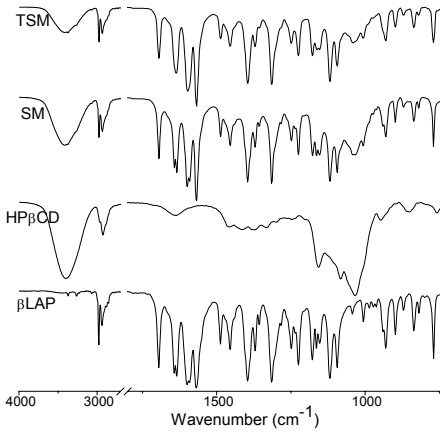

βLAP	HPβCD	SM	TSM
2977.9 (s)	-	2977.8 (m)	2977.8 (m)
2935.5 (m.b)	2927.6 (s.b)	2933.4 (m.b)	2935.3 (m.b)
1695.3 (s)	-	1695.2 (s)	1695.2 (s)
1643.2 (s)	-	1643.2 (s)	-
1635.5 (s)	1637.4 (m.b)	1635.5 (s)	1637.4 (s)
1598.9 (m)	-	1598.8 (m)	1596.9 (m)
1568.0 (m)	-	1568.0 (m)	1568.0 (m)
1487.0 (m)	-	1487.0 (w)	1487.0 (w)
1454.3 (m)	-	1454.2 (m)	1454.2 (m)
1396.4 (s)	-	1396.3 (s)	1396.3 (s)
1371.3 (s)	-	1371.2 (m)	1371.2 (m)
1315.4 (s)	-	1315.3 (s)	1315.3 (s)
1247.9 (m)	-	1247.8 (m)	1247.8 (m)
1153.4 (m)	1157.2 (m.b)	1155.3 (w.b)	1155.3 (w.b)
1118.6 (s)	-	1118.6 (s)	1118.6 (s)
1093.6 (s)	1081.9 (m.b)	1093.5 (m)	1093.5 (m)
-	1033.7 (s.b)	1033.7(w)	-

Fig. 7.9. FTIR spectra and data of βLAP, HPβCD and its mixtures SM and TSM. Bands are classified in function of its intensity as s (strong), m (medium), w (weak) and b (broad).

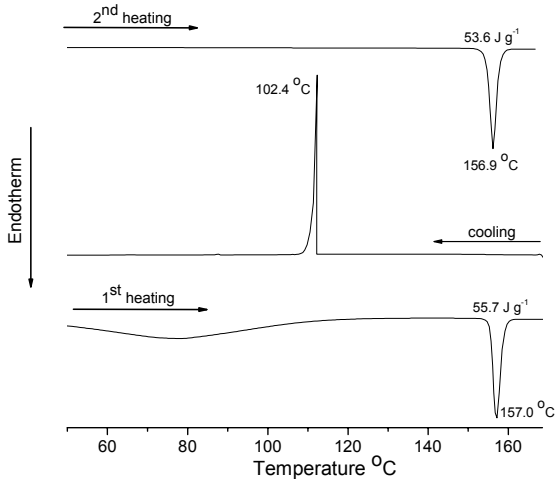

Fig. 7.10. HC-DSC of the βLAP-RMβCD PM binary system.

The DCPD-βLAP incompatibility was confirmed by FTIR data (Fig. 7.11). Accentuated changes were detected in the bands corresponding to the functional groups of the drug, especially in the TSM samples, which indicate chemical decomposition of βLAP. The OM results showed the intrinsic association between the compounds. The mixture (TSM) is composed by several βLAP crystals and also coloured excipient particles (Fig. 7.8).

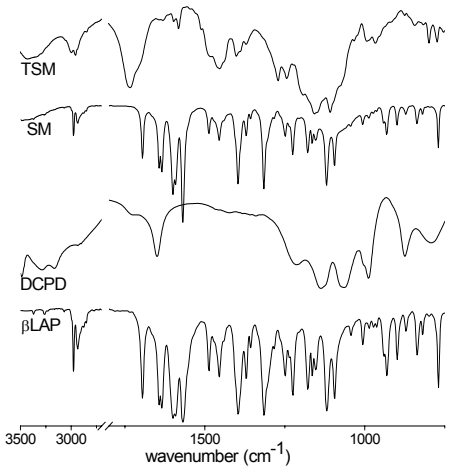

βLAP	DCPD	SM	TSM
2977.9 (s)	-	2977.8 (m)	2993.2 (w.b)
2935.5 (m.b)	-	2935.3 (w.b)	2952.7 (w.b)
1695.3 (s)	-	1695.3 (m)	1731.9 (s.b)
-	1649.0 (s.b)	-	-
1643.2 (s)	-	1643.2 (s)	-
1635.5 (s)	-	1633.5 (s)	-
1598.9 (m)	-	1600.7 (m)	1595.0 (w)
1568.0 (m)	-	1568.0 (s)	1579.5 (w)
1487.0 (m)	-	1487.0 (w)	1479.2 (w)
1454.3 (m)	-	1454.2 (w)	1450.3 (m.b)
1396.4 (s)	-	1396.3 (s)	1400.2 (w.b)
1371.3 (s)	-	1369.3 (s)	1369.3 (w.b)
1315.4 (s)	-	1315.3 (s)	-
1247.9 (m)	-	1247.8 (m)	1242.0 (w)
-	1211.2 (m.b)	-	-
1118.6 (s)	-	1118.6 (s)	-
-	1135.9 (s.b)	-	-
1093.6 (s)	-	1093.5 (m)	-
-	1064.6	-	-
-	987.4 (s.b)	-	-

Fig. 7.11. FTIR spectra and data of βLAP, DCPD and its mixtures SM and TSM. Bands are classified in function of its intensity as s (strong), m (medium), w (weak) and b (broad).

The Heating-Cooling DSC results suggest that βLAP promotes DCPD dehydration at lower temperature, at the same time as the melted drug (Fig. 7.12). The DCPD water hydration (20.9 % of the DCPD weight) partially dissolves the βLAP and the basic environment from this [28] could decompose the βLAP, which are especially sensitive to an alkaline pH. This was verified on the second heating, by a broad drug melting peak, shifting to lower temperature and with a slight associated enthalpy, thus a clear sign of drug degradation. The DCPD is one of the most common diluents for tablets but it has been described as an excipient susceptible to dehydration at low temperature in the presence of water vapour, which is clearly relevant to the choice of conditions for processing and storage of the dosage forms [20]. Our results suggest great

modifications in both βLAP and DCPD characteristics as a result of their incompatibility that would not recommend the use of DCPD in the development of βLAP solid dosage forms.

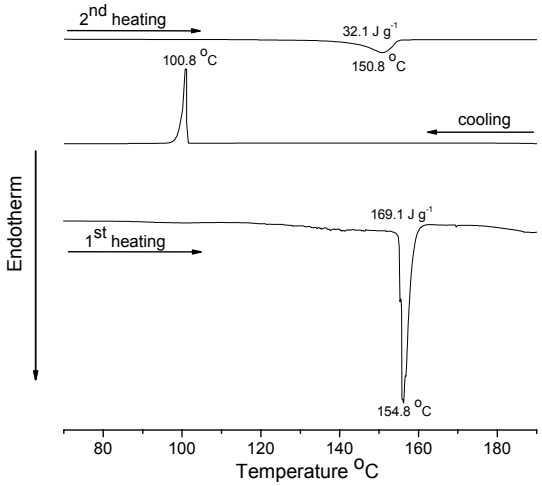

Fig. 7.12. HC-DSC of the βLAP-DCPD PM binary system.system.

The MGST-βLAP interactions have also been confirmed by FTIR data (Fig. 7.13). The disappearance of different MGST bands (1579.5 and 1465.7 cm^{-1}) from both, SM and TSM FTIR spectra, suggests the decomposition of the excipient. Additionally, some modifications in the βLAP bands (2978 and 1568 cm^{-1}) assigned to the aromatic region of the drug, C-H and C-C, respectively, take place. The HC-DSC experiments (Fig. 7.14) corroborate the hypothesis of MGST degradation as in the second heating only the melting peak of βLAP, at lower temperature and associated enthalpy, can be observed and none of the MGST events. Heating up 160 ºC does not promote changes in the morphology of βLAP or MGST single systems but when heated together (Fig. 7.8) the sample becomes black as a consequence of the degradation of MGST.

Lubricants are used in tablets at a ratio far lower than the one used in this study so, at the ratio 1:1 w/w greater MGST degradation would be expected on ageing. However, the interaction evidences between products suggest that MGST should be avoided in the βLAP formulations.

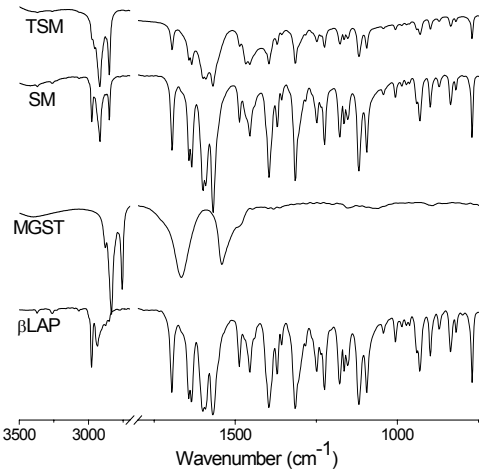

βLAP	MGST	SM	TSM
2977.9 (s)	-	2977.8 (s)	-
2935.5 (m.b)	-	-	-
-	2918.0 (s)	2918.0 (s.b)	2919.9 (s.b)
-	2850.5 (s)	2850.5 (m)	2850.5 (m)
1695.3 (s)	-	1695.3 (s)	1695.5 (m)
1643.2 (s)	-	1643.2 (s)	1643.2 (w)
1635.5 (s)	-	1633.5 (s)	1633.5 (w)
1598.9 (m)	-	1598.8 (m)	1598.8 (w)
-	1579.5 (s.b)	-	-
1568.0 (m)	-	1568.0 (s)	1569.9 (w)
1487.0 (m)	-	1487.0 (m)	1487.0 (w)
-	1465.7 (s.b)	-	-
1454.3 (m)	-	1454.2 (m)	1454.2 (w)
1396.4 (s)	-	1396.3 (s)	1396.3 (m)
1371.3 (s)	-	1371.2 (s)	1371.2 (w)
1315.4 (s)	-	1315.3 (s)	1315.3 (m)
1247.9 (m)	-	1247.8 (m)	1247.8 (w)
1118.6 (s)	-	1118.6 (s)	1118.6 (m)
1093.6 (s)	-	1093.5 (s)	1093.5 (m)

Fig. 7.13. FTIR spectra and data of βLAP, MGST and its mixtures SM and TSM. Bands are classified in function of its intensity as s (strong), m (medium), w (weak) and b (broad).

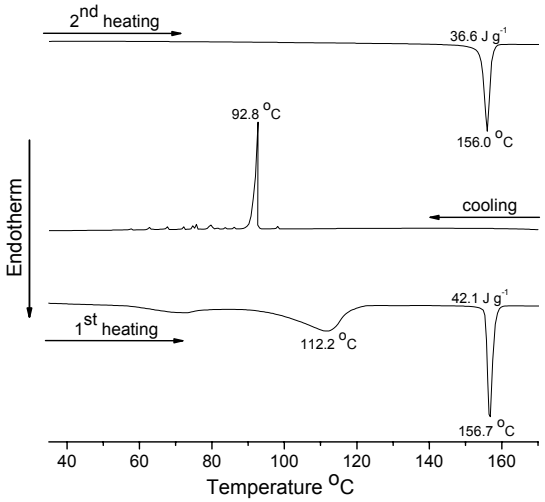

Fig. 7.14. HC-DSC of the βLAP-MGST PM binary system.

7.5. CONCLUSIONS

Six (magnesium stearate, PRUV, DCPD, mannitol, RMβCD and HPβCD) of the seventeen excipients studied presented thermal interactions with the βLAP. However, additional studies using FTIR, optical microscopy and Heating-Cooling DSC studies (HC-DSC) confirmed the incompatibility of βLAP with magnesium stearate and dicalcium phosphate dihydrate. Those excipients should be avoided in the development of solid dosage forms.

7.6. ACKNOWLEDGEMENTS

Authors thank LAFEPE/Brazil, and Professor Dr. Pedro Jose Rolim Neto, Federal University of Pernambuco, Brazil, for their kind gift of the βLAP. Janssen Pharmaceutica, Roquette Freres and CyDex are grateful for the generous donation of cyclodextrins. This work was supported by Xunta de Galicia (PGIDIT05BTF20301PR) and the Programme Alβan, the European Union Programme of High level Scholarships for Latin America, scholarship nº E04D043994BR.

7.7. REFERENCES

[1] A.R. Burnett, R.H. Thomson, J. Chem. Soc. C. 7 (1968) 850-853.

[2] S.C. Hooker, H.W. Shepard, J.G. Walsh Jr., G.H. Connitt, J. Am. Chem. Soc. 58 (1936) 90-1197.

[3] C. J. Li, C. Wang, A.B. Pardee, Cancer Res. 55 (1995) 3712-3715.

[4] M. Planchon, S. Wuerzberger, B. Frydman, D.T. Witiak, P. Hutson, D.R. Church, G. Wilding, D.A. Boothman, Cancer Res. 55 (1995) 3706-3711.

[5] M. Ough, A. Lewis, E.A. Bey, J. Gao, J.M. Ritchie, W. Bornmann, D.A. Boothman, L.W. Oberley, J.J. Cullen, Cancer. Biol. Ther. 4 (2005) 95-102.

[6] G. Damien, STP Pharma Pratiques. 14 (2004) 303-310.

[7] R.K. Verma, S. Garg, J. Pharm. Biomed. Anal. 38 (2005) 633-644.

[8] D. Kiss, R. Zelko, C. Novak, Z. Ehen, Therm. Anal. Calorim. 84 (2006) 447-451.

[9] P.C. Mora, M. Cirri, P. Mura, J. Pharm. Biomed. Anal. 42 (2006) 3-10.

[10] N. Nasongkla, A.F. Wiedmann, A. Bruening, M. Beman, D. Ray, W.G. Bornmann, D.A. Boothman, J. Gao, Pharm. Res. 20 (2003) 1626-1633.

[11] F. Wang, E. Blanco, H. Ai, D.A. Boothman, J. Gao, J. Pharm. Sci. 95 (2006) 2309-2319.

[12] M. Cunha-Filho, B. Dacunha-Marinho, J.J. Torres-Labandeira, R. Martínez-Pacheco, M. Landín, AAPS PharmSciTech. 8 (2007) Article 60.

[13] H. Nyqvist, Int. J. Pharm. Tech & Prod. 4 (1983) 47-48.

[14] D.E. Bugay, W.P. Findlay, Pharmaceuticasl Excipients: by IR, Raman, and NMR spectroscopy, Marcel Dekker, New York, 1999.

[15] J. Wells, Pharmaceutical preformulation, Ellis Horwood, Chichester, 1988.

[16] American Pharmaceutical Association, Handbook of Pharmaceutical Excipients, fourth ed., Pharmaceutical Press, London, 2006.

[17] J. Sawicka, Pharmazie. 46 (1991) 519-521.

[18] M.A. Hassan, J. Kaloustian, P. Prinderre, H. Ramsis, K.A. Khaled, T.H. El-Faham, S.S. Tous, L. Maury, J. Joachim, Pharmazie. 51 (1996) 400-403.

[19] M. Tomassetti, A. Catalani, V. Rossi, S. Vecchio, J. Pharm. Biomed. Anal. 37 (2005) 949-955.

[20] M. Landín, R. Martínez-Pacheco, J.L. Gómez-Amoza, C. Souto, A. Concheiro, R.C. Rowe, Int. J. Pharm. 103 (1994) 9-18.

[21] M. Landín, R.C. Rowe, P. York, Int. J. Pharm. 104 (1994) 271-275.

[22] G. Pyramides, J.W. Robinson, S.W. Zito, J. Pharm. Biomed. Anal. 13 (1995) 103-110.

[23] G.G. Oliveira, H.G. Ferraz, J.S.R. Matos, Therm. Anal. Calorim. 79 (2005) 267-270.

[24] A. Marini, V. Berbenni, S. Moioli, G. Bruni, P. Cofrancesco, C. Margheritis, M. Villa, Therm. Anal. Calorim. 73 (2003) 529-545.

[25] R.K. Verma, S. Garg, J. Pharm. Biomed. Anal. 35 (2004) 449-458.

[26] C.E. Malan, M.M. Villiers, A.P. Lotter, J. Pharm. Biomed. Anal. 15 (1997) 549-557.

[27] M.E. Davis, M.E. Brewster, Nat. Rev. Drug Discov. 12 (2004) 1023-1035.

[28] M. Landín, M.J. Fontao, R. Martinez-Pacheco, Drug Dev. Ind. Pharm. 31 (2005) 249-256s inclusion compounds. *Eur J Pharm Sci*. 2002;15:79-88.

Praza das Praterías, Santiago de Compostela

Capítulo 8

Enhancement dissolution rate of novel antineoplastic β-lapachone using precipitation hydrophilic surface procedure

Autores: Marcílio S. S. Cunha-Filho[1], Ramón Martínez-Pacheco[1] and Mariana Landín[1]

[1]Departamento de Farmacia y Tecnología Farmacéutica, Facultad de Farmacia, Universidad de Santiago de Compostela, Santiago de Compostela, Spain.

Manuscript in preparation

8.1. ABSTRACT

β-lapachone [βLAP] is a novel antitumoral drug, recently on clinical trials with promising preliminary results. It directly activates DNA damage response pathways resulting in selective apoptosis in a broad range of cancer cells. Low water solubility and large therapeutic doses constitute the main problems to overcome in the development of dosage forms of this drug. The purpose of the present research was to enhance the limited dissolution rate of βLAP by promoting the spontaneous, crystalline growth of βLAP at the surface of large excipient particles. Physicochemical characterization of the particles was carried out as well as the dissolution rate. The utility of the βLAP powder in the development of tablets obtained by direct compression has been also noted. Particles produced by natural crystalline growth of βLAP on MCC hydrophilic surface have a reduced size (mean diameters between 55-65μm) certainly influenced by the microcrystalline cellulose particle size (around 50 μm) and an excellent drug dissolution rate (90% drug dissolved at 50min). Neither physical nor chemical instability of the drug have been detected after the precipitation procedure. The compression process does not deteriorate the dissolution behaviour of the systems extensively when an adequate compression pressure is used. Therefore, this technique offers a simple way to produce βLAP powder and tablets with improved dissolution rate for oral administration.

Keywords: β-Lapachone; dissolution rate; precipitation; tablets, hydrophilic surface

8.2. INTRODUCTION

β-lapachone [βLAP] is a naphtoquinone obtained on a small scale from the South American tree named popularly as *Ipê roxo* (*Tabebuia avellanedae* Lor. (Gonçalves de Lima et al., 1956). On a large scale, it can be produced following the method developed by Hooker and co-workers through cyclization of lapachol in sulphuric acid by nucleophilic attack of oxygen of the isoprenyl side chain and purification by further recrystallizations (Hooker et al., 1936).

Over the years, βLAP has been reported to possess a wide range of pharmacological properties (Ferreira de Santana et al., 1968; Pinto et al.,1977; Docampo et al., 1977; Li et al., 1993) outstanding its chemotherapic potential in cancer treatment (Li et al., 2003: Ough et al., 2005). *In vitro* and *in vivo* studies have shown that βLAP inhibits conventional therapy-resistant tumours, particularly the proliferation of neoplasm of slow cell cycle like prostate, pancreatic, colon and some ovarian and breast cancer (Pardee et al., 2002; Suzuki et al., 2006). βLAP induces selective apoptosis in cancer cells by inducing a rapid and sustained increase of the pro-apoptotic protein E2F-1. Clinical trials of phase I and II have recently been launched on this molecule with encouraging results (Shapiro et al., 2005; Kawecki et al., 2007).

Despite of the therapeutic potential of βLAP, some problems have derived from its poor water solubility and large therapeutic doses represent some challenges for pharmaceutical technology researchers (Planchon et al., 1995; Shapiro et al., 2005).

The adsorption of drugs into the surface excipient has been used in the pharmaceutical industry with different purposes, such as achieving content uniformity for low-dose drugs or improving drug stability or dissolution rate (Wen and Qiu, 2006).

Different authors have been reported spontaneous precipitation techniques as a way of obtaining reductions in particle size with increasing drug dissolution rates (Rasenack and Miller, 2002; Steckel et al., 2003). The precipitation of drugs on excipients with large particle size and good flowability can help to avoid the formation of drug agglomerates, giving a product formed by adsorb individual small drug particles onto the surface of the excipient, the properties of which are mainly determined by the characteristics of the excipient.

This approach is advantageous against traditional milling techniques that produce agglomerates due to the high energetic surfaces and led to problems in the wettability of particles. Precipitation techniques allow homogeneous systems of small and non-cohesive particles of different poor water soluble drugs (Gassmann et al., 1994; Sarkari et al., 2002).

On this basis, the aim of this study was to prepare and characterize enhanced dissolution βLAP particles produced by precipitation on hydrophilic surface excipient. The utility of the βLAP precipitation particles in the development of fast dissolving tablets was also be carried out.

8.3. EXPERIMENTAL

Materials

β-lapachone [βLAP] (3,4-dihydro-2,2-dimethyl-2H-naphthol[1,2-b]pyran-5,6-dione; MW 242.3; bacth L503) was supplied by Laboratório Farmacêutico do Estado de Pernambuco/LAFEPE (Recife, Brazil). Purity estimated by DSC and HPLC is 99.9 %.

Microcrystalline cellulose PH 101 [MCC] (batch 9120562001) supplied by Guinama (Valencia, Spain) and sodium stearyl fumarate [PRUV] (batch 142-01) from Juliá- Parrera S.A. (Barcelona, Spain). All solvents were of analytical grade.

Precipitation on hydrophilic surface procedure [PHS]

βLAP ethanolic solution at 20 $mg \cdot mL^{-1}$, closed to saturation concentration, was mixed with MCC in the drug/excipient ratios of 1:4 [PHS1] and 1:2 [PHS2] (w/w). The ethanolic suspensions were dried in an oven at 70 ºC ± 2 ^{o}C for 1 hour.

Product characterization

Drug content

Ą UV spectrophotometric method was developed for quantitative βLAP determination using an UV-visible spectrophotometer Agilent 8453 (Agilent corp., Santa Clara, USA) with photodiode array detector at 257nm. Calibration curve in water/ethanol (1:1 v/v) was made using standard solutions in the range of 2 to 10 $\mu g \cdot mL^{-1}$. No effect of excipients

addition on the UV spectrum of βLAP solution was verified according to previous validation.

The chemical stability of βLAP was performed on a high performance liquid chromatograph, Waters M600, equipped with a C18 cartridge column (125 mm x 45 mm x 5 µm) (Waters, Milford, USA) using in the mobile phase a mixture of methanol/water 65 % (v/v). The isocratic flow rate was 1 $mL \cdot min^{-1}$ at room temperature. The injection volume was 20 µL. Chromatographic detection was set at 253 nm with a photodiode array detector. The mobile phase and samples were filtered using a 0.45 µm nylon membrane (Waters, Milford, USA) (Cunha-Filho et al., 2005).

Morphological Particle Characterization

Optical morphological characteristics of the particle systems were analysed using an Olympus SZ60 (Opelco, Tokyo, Japan) microscope connected to a videocamera Olympus DP12 (Opelco, Tokyo, Japan). The images were processed using Analysis® version 3.2 (Analysis Software, Müster, Germany). The particle size distribution was calculated by mean Feret diameter based on gradient colour particle.

X-ray powder diffractometry [XRPD]

The X-ray powder diffraction patterns were collected using Copper radiation (40 Kv, 30 mA), on a Philips PW 1729 diffractometer (Philips corp., Netherlands) with Bragg-Brentano geometry, in the $2<^{o}2\theta<60$ range with a step size of 0.02 $^{o}2\theta$ and counting time of 2 s per step.

Differential Scanning Calorimetry [DSC]

Samples weighing 2-3 mg were placed in open aluminium pans and heated from 30 to 250 ºC at a rate of 10 $^{o}C \cdot min^{-1}$ using a temperature modulated DSC Q100 calorimeter (TA Instruments, New Castle, USA).

Nitrogen was used as purge gas at a flux rate of 50 $mL \cdot min^{-1}$. Calibration of temperature and heat flow was performed with standard indium samples. All measurements were carried out in duplicate.

Tablets manufacture

The PHS2 particles were blended with 1% of PRUV in a Turbula T2C mixer for 15 min at 30 rpm. Tablets of 100 mg containing approximately 50 mg βLAP were produced by direct compression using an instrumentalized Bonals modelo B tipo MT (Barcelona, Spain) eccentric press fitted with 6 mm flat punches at compression forces of 700 and 2000 N.

Characterisation of tablets

Tablets were subjected to the following tests:

Dimensions: The thickness and diameter of six tablets were determined with a digital calibrator (Mitutoyo 0-25 mm range; 0.001 mm sensibility).

Weight: The weight of 20 tablets were determined individually and the mean weight and coefficient of weight variation were calculated.

Tensile strength [*TS*]: The crushing strengths of six tablets were obtained using an Erweka TB2A apparatus (Heusenstamm, Germany) and the tensile strength was determined from the equation (Fell and Newton, 1970):

$TS = 2CS/\pi \cdot D \cdot E$ (1)

where *CS* is the crushing strength, *D* denotes the diameter and *E* is its thickness.

Friability: Weight loss through friability was determined for 10 tablets after 100 rev in an Erweka TAP (Erweka corp.,) apparatus at 25rpm.

Disintegration time: The disintegration times of six tablets were measured individually in water in an apparatus Turu Grau DT-1 (Barcelona, Spain) fulfilling the USP specifications.

Powder and tablets dissolution testing

Dissolution studies were carried out following FDA specifications for poor soluble drugs using a USP dissolution apparatus 2 (paddle) (Turu Grau DT-6, Barcelona, Spain) at 75 rpm and 37ºC ± 0.5 ºC. In order to ensure sink conditions and increase the ability of the dissolution test to distinguish between formulations, the solubility of βLAP in water containing surfactants was tested. An aqueous solution volume of 900 mL containing sodium lauryl sulphate at a concentration of 0.5 % was selected as dissolution medium.

βLAP samples of 50 milligrams or equivalent amounts of each system (powder microparticles or tablets) were tested in triplicate. Microparticles samples were submerged rapidly in the medium. At required time intervals samples were collected, filtered through cellulose filters and the concentration of drug dissolved determined spectrophotometrically. The dissolution profiles were evaluated and compared using the dissolution efficiency at 15 and 30 min parameters (Khan and Rhodes, 1972).

8.4. RESULTS AND DISCUSSION

PHS technique represents a simple process of reducing particle size with high yields. Figure 8.1 show images from optical microscopy of physical mixture between βLAP and MCC and the two batches of precipitated particles obtained by PHS. As it can be seen for the PHS systems a crystallization of βLAP take place on the surface of cellulose fibbers. An orange drug cover around the MCC can be also appreciated.

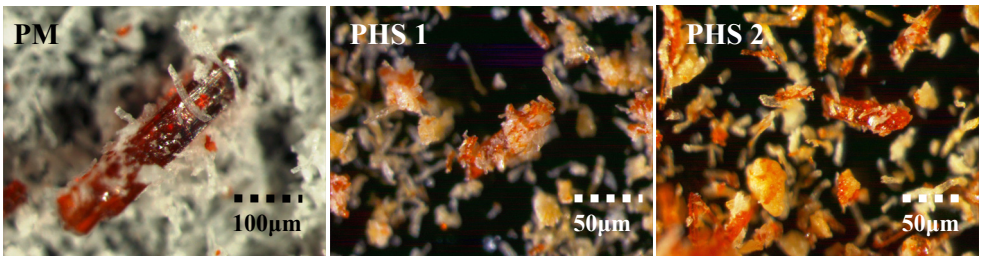

Figure 8.1. Photomicrographs from OM of physical mixture of βLAP-CCM [PM] and precipitated systems PHS1 and PHS2.

The particle size distribution of βLAP as supplied and the PHS systems are plotted in Figure 8.2. Samples fit normal logarithm particle size distributions with mean Feret diameters of 56.3 µm ± 1.6 for PHS1 and 63.6 µm ± 1.87 for PHS2, certainly influenced by the microcrystalline cellulose particle size (around 50 µm) (American Pharmaceutical Association, 2006).

The important reduction on drug particle size compared with original drug particles (106.8 μm ± 2.32) and the intrinsic interaction with hydrophilic surface of MCC would have consequences for the drug dissolution behaviour.

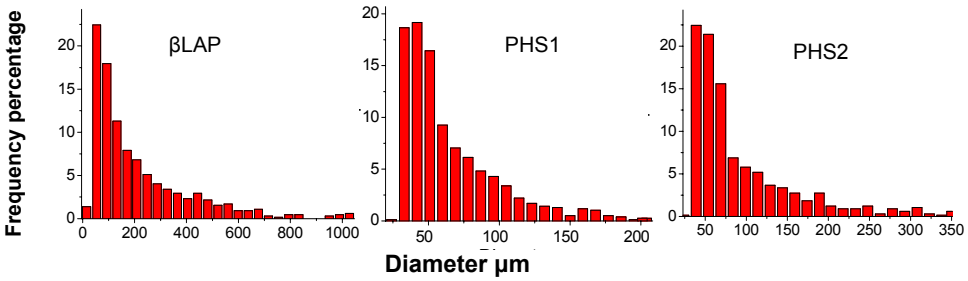

Figure 8.2. Particle size distribution of βLAP and PHS systems by OM (mean Feret diameter).

XRPD and DSC profiles of individual compounds and the PHS formulations are presented in Figures 8.3 and 8.4. No changes in peak positions can be observed in X ray diffraction patterns as a consequence of the precipitation process. The XRDP patterns of PHS formulations correspond to the superposition of individual compound patterns (Cunha-Filho et al., 2006) (Figure 8.3). DSC profiles (Figure 8.4) do not show changes in the melting peak of βLAP (157.4 ^{o}C), indicating no interaction between the components. The thermal behaviour corroborates the XRPD and OM data suggesting the maintenance of the original βLAP crystal habit. After the PHS process, the chemical stability of βLAP is maintained since no evidence of decomposition was observed by the HPLC.

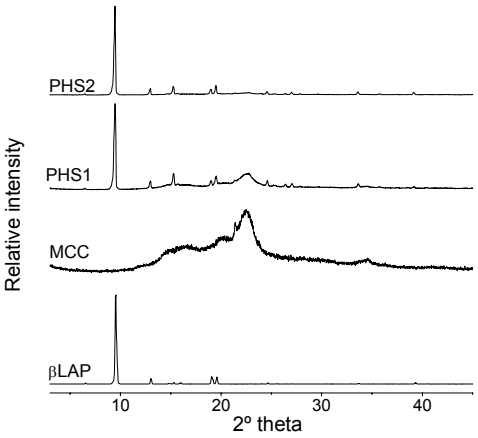

Figure 8.3. XRPD of βLAP, MCC and PHS systems.

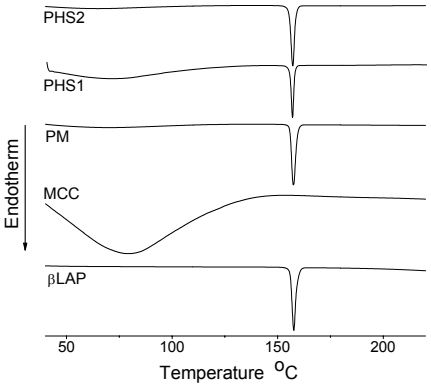

Figure 8.4. DSC of βLAP, MCC, equimass physical mixture of βLAP-celulosa and PHS systems.

Tablets elaborated at a high compression force (2000 N) have a bright orange colour with some heterogeneities and do not disintegrate (Figure 8.5). Those facts probably are due to the strong interaction between drug particles by the excessive pressure. Compression at a lower pressure (700 N) produces tablets where βLAP is homogeneously distributed. Mechanical and physical properties of those tablets are suitable. Their friability is 0 %, they have an adequate tensile strength (0.54 MPa) and the disintegration time is lower than 1 min.

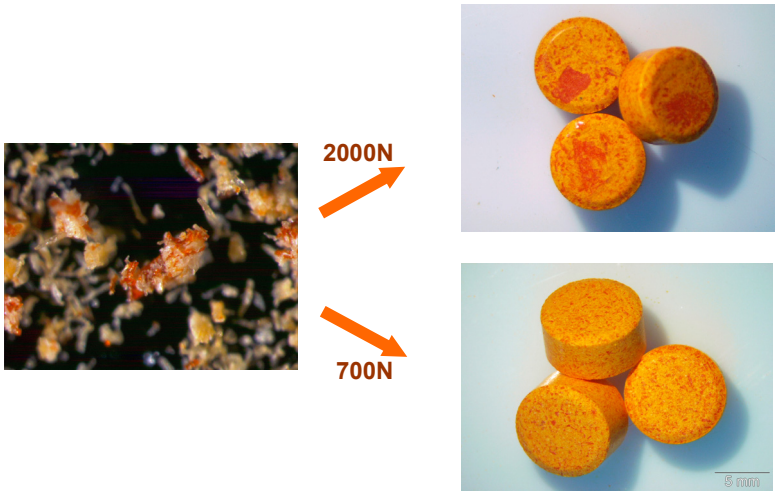

Figure 8.5. The compression force effect on tablets of PHS samples by optical microscopy.

Both, PHS βLAP powders and tablets made in this way show an enhancement in dissolution rate (Figure 8.6, Table 8.1) compared to the drug as supplied and with its physical mixture with MCC [PM]. A 90 % percentage of the drug dissolved is achieved after 50min for PHS systems while the original crystalline drug or the PM the dissolution process takes more than 3h. The reduction of the drug particle size by growing the crystals on the MCC increases the βLAP surface area and the hydrophilic nature of the cellulose provides a highly wettable environment that contributes to improve dissolution process.

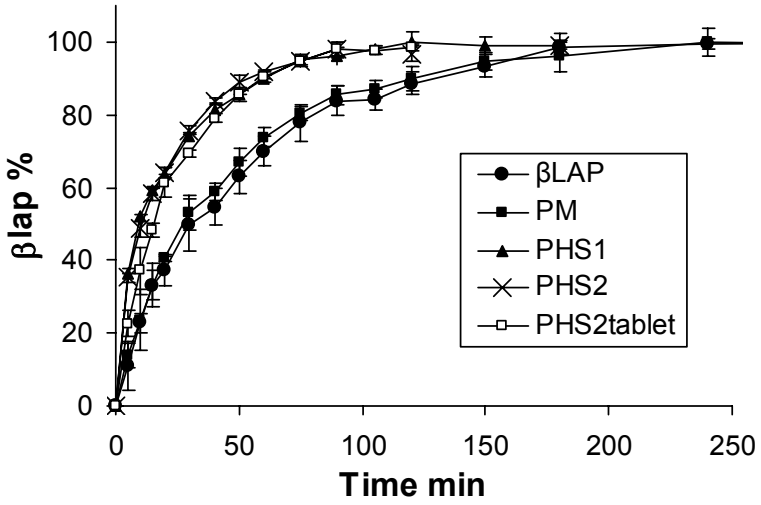

Figure 8.6. Dissolution profiles of βLAP as supplied, physical mixture of βLAP-MCC and PHS systems in Sink conditions

No significant differences can be observed between the PHS formulations when dissolution efficiencies at 15min or 30min are compared. As βLAP pre-clinical and clinical trials (Li et al., 1999; Shapiro et al., 2005) have pointed out, high therapeutic doses (800mg-1g) for the drug are needed, PHS2 powder with a high proportion of drug (50 %) was selected to produce the βLAP tablets. As it can be see (Table 8.1) the compression process does not deteriorate, to any great extent the dissolution behaviour of PHS powder when a low compression force is used.

Table 8.1. Mean values of the dissolution efficiency for 15 and 30 min. Standard deviation in parenthesis.

Samples	Dissolution efficiency %	
	15min	30min
βlap	16,7 (0,2)	28,5 (0,9)
PM	18,8 (0,9)	31,2 (0,9)
PHS1	38,2 (1,1)	56,4 (0,8)
PHS2	37,6 (0,8)	52,3 (0,9)
$PHS2_{tablet}$	28,0 (3,3)	44,9 (1,8)

8.5. CONCLUSIONS

Particles produced by natural crystalline growth of βLAP on MCC hydrophilic surface can be produced at a reduced size, thus avoiding the critical effects resulting from traditional milling processes, such as instability, agglomeration or electrostatic behaviour. The microcrystalline cellulose as hydrophilic support also presents the advantage of being an excipient suitable for direct compression tabletting which is important from an industrial point of view.

Significant improvements on the dissolution rate of βLAP were achieved with the powder formulations, which are maintained when tablets are produced. The compression pressure is a critical parameter which must be controlled in order to maintain the excellent dissolution properties of βLAP.

This technique offers a simple way to produce βLAP powder and tablets with adequate dissolution rate for oral administration.

8.6. ACKNOWLEDGEMENTS

Authors thank LAFEPE, Brazil, and Professor Dr Pedro Jose Rolim Neto, Federal University of Pernambuco, Brazil, for their kind gift of the βLAP. This work was supported by Xunta de Galicia (PGIDIT04BTF203011PR) and the Programme Alβan, the European Union Programme of High level Scholarships for Latin America, scholarship nº E04D043994BR.

8.7. REFERENCES

American Pharmaceutical Association, Handbook of Pharmaceutical Excipients, Pharmaceutical Press, London, 2006.

Cunha Filho M, Alves FC, Alves GMC, Monteiro DB, Morais de Medeiros F, Rolim Neto PJ. Beta-lapachone: development and validation of analytical method for the new therapeutic antineoplastic alternative. Rev. Bras. Farm. 2005;86(1):39-43.

Cunha-Filho MS, Landin M, Martinez-Pacheco R, Dacunha-Marinho B. beta-Lapachone, Acta Crystallogr. C. 62 (2006) o473-475.

Docampo R, Lopes JN, Cruz FS, Souza W. Trypanosoma cruzi: ultrastructural and metabolic alterations of epimastigotes by beta-lapachone. Exp. Parasitol. 1977;42(1):142-149.

Fell JT, Newton JM. The prediction of the tensile strength of tablets, J. Pharm. Pharmacol. 1970;22:247-248.

Ferreira de Santana C, Gonçalves de Lima O, D'Albuquerque IL, Lacerda AL, Martins DG. Antitumor and toxicological properties of an extract of wood from the trumpet bush, Tabebuia avellanedae. Rev. Inst. Antibiot. 1968;8(1-2):89-94.

Gassmann P, List M, Schweitzer A, Sucker H. Hidrosols – alternatives for the parenteral application of poorly water soluble drugs. Eur. J. Pharm. Biopharm. 1994;40;64-72.

Gonçalves de Lima O, D`Albuquerque IL, Machado MP, Silva E, Pinto GP. Primeiras observações sobre a ação antimicrobiana do lapacho. An. Soc. Biol. Pe. 1956;14:129-135.

Hooker SC, Jr, Shepard HW, Jr, Walsh JG, Jr, Connitt GH. Constitution of lapachol and its derivatives. *J Am Chem Soc.* 1936;58:1190-1197.

Kawecki A, Adkins DR, Cunningham CC, Vokes E, Yagovane DM, Dombal G, et al. A phase II study of ARQ 501 in patients with advanced squamous cell carcinoma of the head and neck. Proceedings of 2007 ASCO Annual Meeting; Chicago, USA. June 1-5, 2007: 16509.

Khan KA, Rhodes CT. Effect of compaction pressure on the dissolution efficiency of some direct compression systems. Pharm. Acta. Helv. 1972;47:594-607.

Li CJ, Zhang LJ, Dezube BJ, Crumpacker CS, Pardee AB. Three inhibitors of type 1 human immunodeficiency virus long terminal repeat-directed gene expression and virus replication. Proc. Natl. Acad. Sci. U.S.A. 1993;90(5):1839-1842.

Li CJ, Li Y, Pinto AV, Pardee AB. Potent inhibition of tumor survival in vivo by β-lapachone plus taxol: combining drugs imposes different artificial checkpoints. Proc. Natl. Acad. Sci. U.S.A. 1999;96(23):13369-13374.

Li Y, Sun X, LaMont JT, Pardee AB, Li CJ. Selective killing of cancer cells by β-lapachone: Direct checkpoint activation as a strategy against cancer. Proc. Natl. Acad. Sci. U.S.A. 2003;100(5):2674-2678.

Ough M, Lewis A, Bey EA, Gao J, Ritchie JM, Bornmann W, et al. Efficacy of beta-lapachone in pancreatic cancer treatment: exploiting the novel, therapeutic target NQO1. Cancer.Biol.Ther. 2005;4(1):95-102.

Pardee AB, Li YZ, Li CJ. Cancer therapy with β-lapachone. Curr. Cancer. Drug Targets 2002;2(3):227-242.

Planchon SM, Wuerzberger S, Frydman B, Witiak DT, Hutson P, Church DR, et al. Beta-lapachone-mediated apoptosis in human promyelocytic leukemia (HL-60) and human prostate cancer cells: a p53-independent response. Cancer Res. 1995;55:3706-3711.

Pinto AV, Pinto MdCR, Gilbert B, Pellegrino J, Mello RT. Schistosoma mansoni: blockage of cercarial skin penetration by chemical agents. I. Naphthoquinones and derivatives. Trans. R. Soc. Trop. Med. Hyg. 1977;71(2):133-135.

Rasenack N, Muller BW. Dissolution rate enhancement by in situ micronization of poorly water-soluble drugs. Pharm. Res. 2002;19:1894-1900.

Sarkari M, Brown J, Chen X, Swinnea S, Williams RO, Johnston KP. Enhanced drug dissolution using evaporative precipitation into aqueous solution, Int. J. Pharm. 2002 ;243:17-31.

Shapiro G, Supko JG, Ryan DP, Appelman L, Berkenblit A, Craig AR, et al. Eder Phase I trial of ARQ 501, an Activated Checkpoint Therapy (ACT) agent, in patients with advanced solid tumors. Proceedings of 2005 ASCO Annual Meeting; Orlando, USA. 13-17 May, 2005: 3042.

Steckel H, Rasenack N, Muller BW. In-situ-micronization of disodium cromoglycate for pulmonary delivery. Eur. J. Pharm. Biopharm. 2003;55: 173-180.

Suzuki M, Amano M, Choi J, Park HJ, Williams BW, Ono K, Song CW. Synergistic effects of radiation and beta-lapachone in DU-145 human prostate cancer cells in vitro. Radiat. Res. 2006;165:525-531.

Wen H, Qiu Y. Adsorption of small drug particles at the surface of large excipients. Pharm. Tech. Eur. 2006: 39-44.

Capítulo 9

Enhancement of the novel antitumoral β-lapachone dissolution rate using phase change drug micronization

Autores: Marcílio S. S. Cunha-Filho[1], Ramón Martínez-Pacheco[1] and Mariana Landín[1]

[1]Departamento de Farmacia y Tecnología Farmacéutica, Facultad de Farmacia, Universidad de Santiago de Compostela, Santiago de Compostela, Spain

Manuscript submitted to Eur. J. Pharm. Biopharm.

Praza Roxa, Santiago de Compostela

9.1. ABSTRACT

β-lapachone [βLAP] is a novel antitumour drug, recently on clinical trials with promising preliminary results. Problems derived from its low water solubility, its instability in solution and its high therapeutic dose constitute some challenges for pharmaceutical researchers. The purpose of the present work was to enhance the limited dissolution rate of βLAP by the design of particles using a phase change micronization process. The procedure induces the spontaneous crystalline growth of the βLAP in the presence of a stabilizing polymer (Hidroxypropilmethylcellulose) that limits the size of the particles generated. Physicochemical characterization of microparticles and the βLAP dissolution rate was carried out. The utility of the βLAP microcrystals in the development of tablets with adequate dissolution properties was also stated. The procedure was optimized in order to obtain stable and homogeneous particles with a small mean particle size (~ 3 μm) and a narrow particle size distribution. There were no differences between the drying methods evaluated (in an oven and freeze-drying) with regard to particle morphology or dissolution behaviour, which is almost instantaneous. Tablets having suitable mechanical properties were produced by compression previous dry granulation. The compression process did not compromise βLAP dissolution characteristics.

Keywords: β-Lapachone, phase change micronization, stabilizing agent, dissolution rate, tablets.

9.2. INTRODUCTION

β-lapachone [βLAP] is a novel drug with promising biological activity against several diseases, outstanding its antineoplastic potential [1]. This molecule acts by an innovator mechanism based on DNA checkpoint activation inducing selectively apoptosis in a broad range of cancer cells without causing the death of normal cells [2]. Currently, βLAP clinical trials are being carried out with encouraging preliminary results [3-5] especially those corresponding to the combinations with other antitumoral drugs as taxol [6] or gemcitabine [7].

Despite of the potential of βLAP as anticancer drug, some problems have been derived from its poor water solubility, instability in solution and large therapeutic doses represent some challenges for pharmaceutical technology researchers [3,8]. Different approaches to the formation of inclusion complexes of βLAP with cyclodextrins have been tested in order to mitigate the problem associated to its low solubility (0.03 $mg \cdot mL^{-1}$) [9,10] that would also have an effect on its bioavailability. However, the use of cyclodextrins means a high load excipient which is not the best approach when oral dosage forms including high doses are required (higher than 800 mg of βLAP were used for the clinical trials) [3,4]. Thus, research on βLAP particle design in order to improve drug dissolution rate is of a great interest.

Different authors have reported techniques of obtaining microcrystals [11,12] or submicro size particles or even amorphous particles [13,14] using phase change precipitation in the presence of a stabilizing agent as a way of increasing drug dissolution rate. This

approach is advantageous against the traditional milling techniques. Jet-milling, milling in a pearl-ball mill or high-pressure homogenization frequently produce agglomerates due to the high energetic surfaces creating materials with poor wettability properties. Microcrystallization by precipitation permits homogeneous systems of small and non-cohesive particles of different poor water soluble drugs with enhanced dissolution properties to be obtained, such as carbamazepine [14], ibuprofen, ketoconazol or itraconazol [11,15,16].

On this basis, the aim of this study was to prepare and characterize enhanced dissolution βLAP particles by Phase Change micronization technique [PC]. An optimization of phase change micronization process with regard to solvent ratio and stabilizing agent concentration has been previously carried out. The utility of the βLAP microcrystals in the development of fast dissolving tablets will also be carried out.

9.3. EXPERIMENTAL

Materials

β-lapachone [βLAP] (3,4-dihydro-2,2-dimethyl-2H-naphthol[1,2-b]pyran-5,6-dione; MW 242.3; batch L503) was supplied by Laboratório Farmacêutico do Estado de Pernambuco/LAFEPE (Recife, Brazil). Purity estimated by DSC and HPLC is 99.9 %.

Hydroxypropilmethylcellulose 100 LV Methocel Premium [HPMC] (batch NE04012N22), furnished by Colorcon (Kent, UK), Microcrystalline cellulose PH 101 [MCC] (batch 9120562001) supplied by Guinama

(Valencia, Spain), and sodium stearyl fumarate [PRUV] (batch 142-01) from Juliá- Parrera S.A. (Barcelona, Spain). All solvents were of analytical grade.

Optimization of phase change micronization procedure [PC]:

The phase change micronization was conducted using the solvent change method by instantaneously mixing two liquids in the presence of a stabilizing agent as described by Gabmann and coworkers [13]. The organic phase was a βLAP ethanolic solution at 20 $mg \cdot mL^{-1}$, close to saturation concentration. For the aqueous phase, a low viscosity HPMC was selected as stabilizing agent based on Rasenack and coworkers previous results [11].

The nonsolvent (water) was poured rapidly from a beaker into the drug solution under stirring conditions using a magnetic stirrer. The process was carried out at room temperature. Four different solvent ratios (organic: water) were tested, 1:2, 1:4, 1:9 and 1:19 in order to select the most appropriate to simultaneously achieve the smallest particles and the maximum yield of the process. For this experiment a high concentration of HPMC 0.5 % was selected in order to avoid the stabilizing agent concentration being a limiting factor. A second experiment was carried out using the selected solvent ratio and five different HPMC concentrations (0, 0.01, 0.05, 0.1 and 0.5 %) in order to estimate the minimum concentration of HPMC necessary to obtain the smallest stable drug particle size.

Crystallization Procedure

βLAP crystals were obtained by pouring an aqueous solution of HPMC (0.05 %) into a βLAP ethanolic solution (20 $mg \cdot mL^{-1}$) under stirring conditions at room temperature for approximately 2 minutes.

The aqueous microsuspension of βLAP was dried using two different methods. Freeze-drying in an apparatus Labconco (Labconco corp., Kansas City, USA) by previous frozen microsuspension in liquid nitrogen and freeze dried for 48 hours [PCL] and drying in an oven at 40ºC ± 2 ^{o}C for 2 hours previous filtration through a nylon membrane (0.22 µm) [PCE].

Product characterization

Drug content

Ą UV spectrophotometric method was developed for quantitative βLAP determination using an UV-visible spectrophotometer Agilent 8453 (Agilent corp., Santa Clara, USA) with photodiode array detector at 257 nm. Calibration curve in water/ethanol (1:1 v/v) was made using standard solutions in the range of 2 to 10 $\mu g \cdot mL^{-1}$. No effect of HPMC addition on the UV spectrum of βLAP solution was verified.

The chemical stability of βLAP was performed on a high performance liquid chromatograph, Waters M600, equipped with a C18 cartridge column (125 mm x 45 mm x 5 µm) (Waters, Milford, USA) using in the mobile phase a mixture of methanol/water 65 % (v/v). The isocratic flow rate was 1 $mL \cdot min^{-1}$ at room temperature. The injection volume was 20 µL. Chromatographic detection was set at 253 nm with a photodiode

array detector. The mobile phase and samples were filtered using a 0.45 µm nylon membrane (Waters, Milford, USA) [17].

Particle morphology

Optical morphological characteristics of samples were analysed using an Olympus SZ60 (Opelco, Tokyo, Japan) microscope connected to a videocamera Olympus DP12 (Opelco, Tokyo, Japan). Particle surface morphologies were also examined using Scanning Electron Microscopy [SEM] LEO-435VP (Leica Microsystems, Cambridge, UK) fixed on a brass stub using double-sided tape and gold coated in vacuum.

Particle size

Particle size distribution of microsuspensions was analysed using equipment Coulter Counter Multisizer II (Beckman Coulter, High Wycombe, UK) using Isoton II® and fitted with tube analysis of aperture size of 30 µm. The mean equivalent diameter and standard deviation of the reference particle size distributions were estimated by probit transformation.

X-Ray Powder Diffractometry [XRPD]

The X-ray powder diffraction patterns were collected using Copper radiation (40 Kv, 30 mA), on a Philips PW 1729 diffractometer (Philips corp., Netherlands) with Bragg-Brentano geometry, in the $2<2\theta<60$ range with a step size of 0.02º and counting time of 2 s per step. Indexation was carried out using LeBail fit [18] by the program Riatica® (IUCR Powder Diffraction 22,21/1997) which permits the calculation of the crystal data; cell parameters (a, b and c), cell angles (α, β and γ) and cell volume and the theoretical density.

Differential Scanning Calorimetry [DSC]

Samples weighing 2-3 mg were placed in open aluminium pans and heated from 30 to 250 ºC at a rate of 10 ºC·min^{-1} using a temperature modulated DSC Q100 calorimeter (TA Instruments, New Castle, USA). Nitrogen was used as purge gas at a flux rate of 50 mL·min^{-1}. Calibration of temperature and heat flow was performed with standard indium samples. All measurements were carried out in duplicate.

Tablets manufacture

Mixtures of 52 % of PCE (aprox. 50 mg βLAP), 47 % of MCC and 1 % of PRUV were blended in a Turbula T2C mixer for 15 min at 30 rpm. Tablets of 100 mg were produced by compression previous dry granulation. The slugs (300 mg) were elaborated using an instrumentalized Bonals modelo B tipo MT (Barcelona, Spain) eccentric press fitted with 12 mm diameter flat Teflon® punches at compaction force of 700 N. Slugs were broken in a mortar, sieved through 450 µm and compressed in the tablet machine fitted with 6 mm flat punches at a compression force of 1500 N.

Characterisation of tablets

Formulation samples were subjected to the following tests:

Dimensions: The thickness and diameter of six tablets were determined with a digital calibrator (Mitutoyo 0-25 mm range; 0.001 mm sensibility).

Weight: The weights of 20 tablets were determined individually and the mean weight and coefficient of weight variation were calculated.

Tensile strength [*TS*]: The crushing strengths of six tablets were obtained using an Erweka TB2A apparatus (Heusenstamm, Germany) and the tensile strength was determined from the equation [19]:

$TS = 2CS/\pi \cdot D \cdot E$ (1)

where *CS* is the crushing strength, *D* denotes the diameter and *E* is its thickness.

Friability: Weight loss through friability was determined for 10 tablets after 100 rev in an Erweka TAP (Erweka, Heusenstamm, Germany) apparatus at 25 rpm.

Disintegration time: The disintegration times of six tablets were measured individually in water in an apparatus Turu Grau DT-1 (Barcelona, Spain) fulfilling the USP specifications.

Powder and tablets dissolution testing

Dissolution studies were carried out following FDA specifications for poor soluble drugs using a USP dissolution apparatus 2 (paddle) (Turu Grau DT-6, Barcelona, Spain) at 75 rpm and 37 ºC ± 0.5 ºC. In order to ensure sink conditions and increase the ability of the dissolution test to distinguish between formulations, the solubility of βLAP in water containing surfactants was tested. An aqueous solution volume of 900 mL containing sodium lauryl sulphate at a concentration of 0.5 % was selected as dissolution medium.

βLAP samples of 50 milligrams or equivalent amounts of each system (powder microparticles or tablets) were tested in triplicate. Microparticles samples were submerged rapidly in the medium. At required time intervals samples were collected, filtered through cellulose filters and the concentration of drug dissolved determined spectrophotometrically. The dissolution profiles were evaluated and compared using the dissolution efficiency at 15 and 30 min parameter [20].

9.4. RESULTS AND DISCUSSION

Table 9.1 shows mean particle diameters of approximately 3 μm and below when precipitated in the presence of HPMC stabilizing agent. A normal and narrow drug particle size distribution was obtained for the different ethanol:water ratios tested with all particles lower than 6 μm. This means a dramatic reduction in the particle size when compared with the mean geometric particle diameters of βLAP as supplied which presents 122.1 μm and geometric standard deviation of 2.16. There are no significant differences between the 0h and 24h after precipitation, meaning that HPMC is able to protect βLAP microparticles from growth.

As no important disparity was achieved in particle size values, the selection of optimum ethanol/water ratio was based on the differences in the percentage of drug precipitated, the maximum process yield being at a solvent ratio 1:4 (Table 9.1). An ethanol/water ratio of 1:2 entails a little efficient polarity change whereas a 1:9 ratio means the use of a high aqueous phase volume that solubilizes a βLAP fraction.

Table 9.1
Mean particle size of micronized βLAP prepared using different etanol/water ratios and the percentage of drug lost in the process. Standard deviations in parentheses

EtOH/ water ratio v/v	Mean particle diameter µm		Drug loss %
	T = 0h	T = 24h	
1:2	2.34 (1.24)	2.48 (1.86)	6.87 (1.21)
1:4	**2.55 (1.76)**	**2.99 (1.60)**	**3.55 (0.20)**
1:9	2.70 (1.80)	2.75 (2.02)	3.84 (0.17)
1:19	2.87 (2.03)	2.47 (2.18)	6.01 (0.23)

The importance of using HPMC as a stabilizer can be derived from Table 9.2 that presents the mean diameter of βLAP particles precipitated using different concentrations of stabilizing agent after 24h phase change. The minimum necessary HPMC concentration to obtain small and stable size particles of βLAP was 0.05 %, below this concentration, the particle growth occurs.

Table 9.2
Mean particle size of micronized βLAP prepared using different HPMC concentrations. Standard deviations in parentheses.

HPMC %	Mean diameter µm after 24h
0	8.77 (12.1)
0.01	4.53 (3.6)
0.05	**2.22 (2.6)**
0.01	**2.90 (1.6)**
0.5	**2.20 (2.1)**

βLAP particles produced by micronization without HPMC have a bigger size and broader particle size distribution which increases in size during the first 24 hours after precipitation (Fig. 9.1) whereas the system with the stabilizer HPMC stops the molecular association and the crystal growth instantaneously at the moment of phase change, which in agreement with other authors' reports [15,16].

HPMC is a cellulose ether which is water soluble. It has been shown that cellulose ethers show surface activity especially derivatives with methoxyl and hydroxypropyl groups making it suitable to be adsorbed onto hydrophobic solid surfaces as the newly created βLAP ones [21]. The interaction in the solid-liquid interface produces stable βLAP particles with narrow particle size distributions. The concentration of the stabilizing agent has a great effect on the resulting particle size, probably as a consequence of the variations in the viscosity of the precipitating liquid as it has been pointed out previously [15].

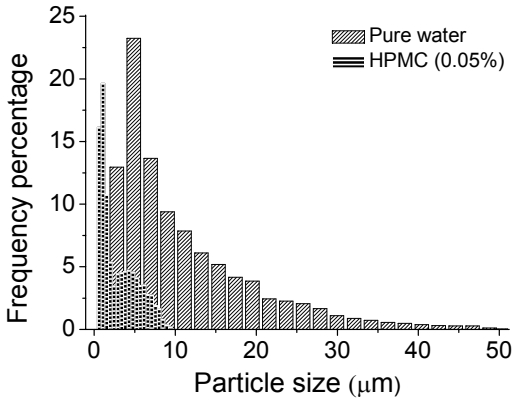

Fig. 9.1. Particle size distribution of βLAP 24h after precipitation with and without 0.05 % HPMC.

Crystallization was carried out employing the solvent change method using HPMC at 0.05 % as the stabilizing agent and a solvent ethanol/water ratio 1:4. Fluffy powders were obtained by the two drying methods used, drying in an oven (PCE) and freeze-drying the microsuspension system (PCL). SEM photographs (Fig. 9.2) show homogeneous acicular crystals similar to the original βLAP particles in shape but smaller in size and thickness for both PC samples. No important differences in the PC crystals were observed between the drying methods.

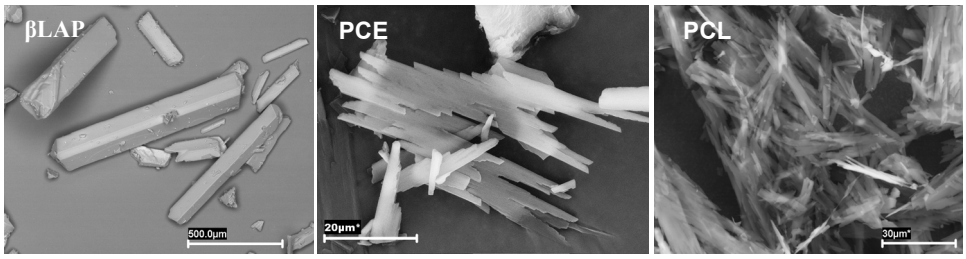

Fig. 9.2. SEM photographs of βLAP as supplied and PC samples.

This technique allowed micronized βLAP particles with a minimum amount of excipient to be produced. The resulting drug load in the dried powder was 95 % and 85 % for the PCE and PCL, respectively, which is special advantageous in order to produce solid dosage forms containing βLAP, that require a large therapeutic dose.

Fig. 9.3 shows XRPD patterns of βLAP, that exhibit a main sharp peak at 9.5 º2θ and other secondary peaks at 13.05, 19.05, 19.59, 24.67 and 39.31 º2θ,. HPMC with an amorphous pattern, and PC samples. Apparently, some marked changes can be appreciated in PC samples compared with their individual components. New peaks and changes in the relative intensity of some peaks are observed. This fact, together with

a slight shift in the drug melting peak observed by DSC thermograms from 157.4 ^{o}C to 156.5 ^{o}C (Fig. 9.4), suggests a change in the crystalline phase of the drug.

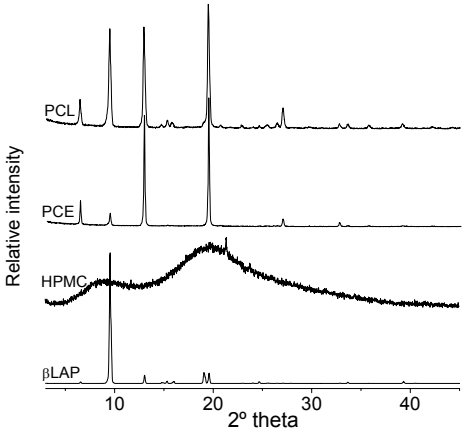

Fig. 9.3. XRPD of βLAP, HPMC and PC samples.

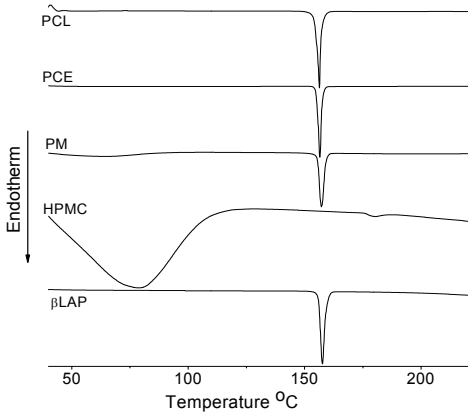

Fig. 9.4. DSC of βLAP, HPMC, 1:1 physical mixture (PM) and PC samples.

A deeper analysis of PC samples crystallinity was carried out by indexation XRPD dates compared with βLAP single crystal data [22]. These results (Table 9.3) allow us to state that both PCE and PCL crystals are not new crystalline entities or polymorphs, but keep the same orthorhombic crystallinity phase of original βLAP. The chemical stability of βLAP was also evaluated by HPLC. No evidence of decomposition was observed after the PC process.

Table 9.3
Indexation data from XRPD results.

		βLAP as supplied	**PCE**	**PCL**
Crystal data		Orthorombic	Orthorombic	Orthorombic
Cell parameters (Å)	**a**	12.80	12.77	12.76
	b	7.04	7.06	7.04
	c	27.27	27.32	27.29
Cell angles (º)	**α**	90	90	90
	β	90	90	90
	γ	90	90	90
Z		8	8	8
Cell volume ($Å^3$)		2458.1	2462.3	2449.3
Density ($g \cdot mL^{-1}$)		1.31	1.31	1.31

The phase change micronized βLAP powders show a dramatic enhancement in dissolution rate as illustrated in Fig. 9.5 the dissolution process being completed within the first 5min, compared to the drug as supplied and the granulometric fraction selected (50-100 μm). This effect can be explained by the dramatic reduction in the particle size and as a consequence the increment in the surface area, which is additionally hydrophilized by the adsorbed hydrophilic polymer. Moreover, the natural crystalline growth creates particles with no electrostatic charge and with better wettability properties [11].

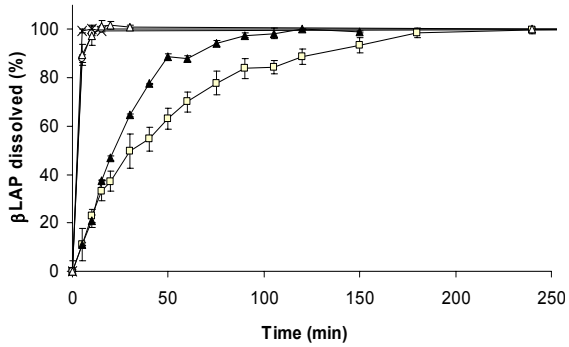

Samples	Dissolution efficiency [%]	
	15min	30min
$\beta lap_{\text{as supplied}}$	16.7 (0.2)	28.5 (0.9)
$\beta lap_{\text{micronized}}$	16.9 (0.1)	34.1 (0.2)
PCE	84.0 (0.6)	92.0 (0.4)
PCL	78.0 (1.9)	89.6 (1.0)
PCE_{tablet}	79.2 (1.5)	90.8 (0.9)

Fig. 9.5. Dissolution profiles of βLAP (□) as supplied and (▲) mechanical micronized (50-100 μm); (○) PCL powder and PCE (x) powder and (Δ) tablet, in Sink conditions, together with the corresponding mean values of the dissolution efficiency for 15 and 30 min. Standard deviation in parenthesis.

No differences among drying methods were found with regard to the dissolution profiles; therefore, the PCE was selected to develop solid dosage forms. Filtering and drying in an oven a 40 ºC is simpler and cheaper than other proposed methods such as freeze drying or spray drying [11, 14].

The compression behaviour of this kind of microparticles was evaluated for the first time. The low densities of blends obtained by PC technique, together with their deficient flow properties made the direct volumetric filling of the dies to obtain 100 mg tablets impossible. Dry granulation using low pressure to produce the slugs helps in increasing particle size and density of the mixture and improves flow properties [23] (Fig. 9.6). The tablets produced have a glossy surface (Fig. 9.6), no friability (0 %), adequate tensile strength (1.96 MPa) and a disintegration time lower than 1 min. Regarding the drug dissolution profiles (Fig. 9.5), no statistical significant differences were found between the

microcrystalline powders (PCE, PCL) and the tablets as it can be derived from the their dissolution efficiency values at 15 and 30 min. The compression process does not deteriorate the excellent dissolution behaviour of βLAP particles obtained by the PC technique, demonstrated by the high values in dissolution efficiency for the tablet formulation at 30 min.

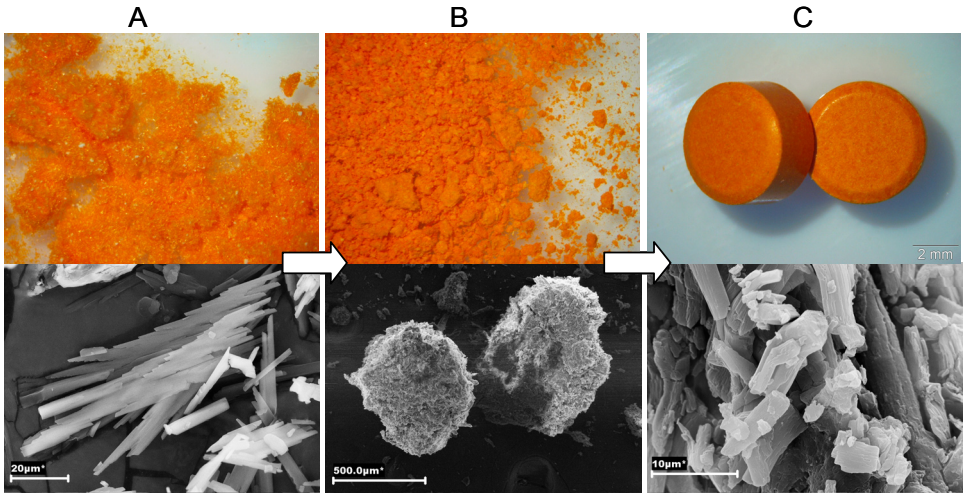

Fig. 9.6. SEM and Optical micrographs of PCE βLAP microcrystals (A), granules by dry granulation (B) and tablets (C).

9.5. CONCLUSIONS

By the method used in this study, small βLAP particles have been prepared by controlled crystallization of the original molecular dispersed drug, avoiding the critical effects resulting from milling processes, such as instability, agglomeration or electrostatic behaviour. As the production

process can be carried out continuously, a scale-up could be performed easily. From our experiments, the optimal conditions for producing βLAP particles by phase change micronization process includes a solvent ratio (ethanol/water) 1:4 and a minimum concentration of HPMC equal to 0.05 %. No differences between microcrystal characteristics have been found with regard to the drying methods studied, the use of the oven being a cheaper and easier to scale-up process.

PC βLAP microparticles are crystalline with a narrow particle size distribution, small mean particle size and an enhanced drug dissolution rate. Compared to other technological approaches to increase βLAP solubility as cyclodextrin inclusion complex, the amount of drug in the preparation is much higher (~90 %) and as a consequence the PC technique is more suitable in developing oral solid dosage forms. The high wettability of βLAP microcrystals enhances drug dissolution, which is maintained when the powder is used in tablet form.

9.6. ACKNOWLEDGEMENTS

Authors thank LAFEPE, Brazil, and Professor Dr Pedro Jose Rolim Neto, *Universidade Federal de Pernambuco*, Brazil, for their kind gift of the βLAP. This work was supported by Xunta de Galicia (PGIDIT04BTF203011PR) and the Programme Alβan, the European Union Programme of High level Scholarships for Latin America, scholarship nº E04D043994BR.

9.7. REFERENCES

[1] A.B. Pardee, Y.Z. Li, C.J. Li, Cancer therapy with beta-lapachone, Curr. Cancer. Drug Targets. 2 (2002) 227-242.

[2] Y. Li, X. Sun, J.T. LaMont, A.B. Pardee, C.J. Li, Selective killing of cancer cells by β-lapachone: Direct checkpoint activation as a strategy against cancer, Proc. Natl. Acad. Sci. U.S.A. 100 (2003) 2674-2678.

[3] G. Shapiro, J.G. Supko, D.P. Ryan, L. Appelman, A. Berkenblit, A.R. Craig, et al., Eder Phase I trial of ARQ 501, an Activated Checkpoint Therapy (ACT) agent, in patients with advanced solid tumors, Proceedings of 2005 ASCO Annual Meeting. Orlando, USA. May 13-17 (2005) 3042.

[4] L.P. Hartner, L. Rosen, M. Hensley, D. Mendelson, A.P. Staddon, W. Chow, et al., Phase 2 dose multi-center, open-label study of ARQ 501, a checkpoint activator, in adult patients with persistent, recurrent or metastatic leiomyosarcoma (LMS), Proceedings of 2007 ASCO Annual Meeting. Chicago, USA. June 1-5 (2007) 20521.

[5] A. Kawecki, D.R. Adkins, C.C. Cunningham, E. Vokes, D.M. Yagovane, G. Dombal, et al., A phase II study of ARQ 501 in patients with advanced squamous cell carcinoma of the head and neck, Proceedings of 2007 ASCO Annual Meeting. Chicago, USA. June 1-5, (2007) 16509.

[6] C. Li, J. Nemunaitis, N. Senzer, G. Edelman, S. Glasner, G. Dombal, et al., A phase Ib trial of ARQ 501, a selective checkpoint activator, in

combination with docetaxel in patients with advanced solid tumors, Proceedings of 2006 ASCO Annual Meeting. Atlanta, USA. June 2-6, (2006) 13053.

[7] H.T. Khong, L. Dreisbach, H.L. Kindler, D.F. Trent, K.G. Jeziorski, I. Bonderenko, et al., A phase 2 study of ARQ 501 in combination with gemcitabine in adult patients with treatment naïve, unresectable pancreatic adenocarcinoma, Proceedings of 2007 ASCO Annual Meeting, Chicago, USA. June 1-5 (2007) 15017.

[8] S.M. Planchon, S. Wuerzberger, B. Frydman, D.T. Witiak, P. Hutson, D.R. Church, et al., Beta-lapachone-mediated apoptosis in human promyelocytic leukemia (HL-60) and human prostate cancer cells: a p53-independent response, Cancer Res. 55 (1995) 3706-3711.

[9] N. Nasongkla, A.F. Wiedmann, A. Bruening, M. Beman, D. Ray, W.G. Bornmann, et al., Enhancement of solubility and bioavailability of beta-lapachone using cyclodextrin inclusion complexes, Pharm. Res. 20 (2003) 1626-1633.

[10] M.S. Cunha-Filho, B. Dacunha-Marinho, J.J. Torres-Labandeira, R. Martínez-Pacheco, M. Landín, Characterization of β-Lapachone and Methylated β-Cyclodextrin Solid-state Systems, AAPS PharmSciTech 8 (2007) Article 60.

[11] N. Rasenack, B.W. Muller, Dissolution rate enhancement by in situ micronization of poorly water-soluble drugs, Pharm. Res. 19 (2002) 1894-1900.

[12] H. Steckel, N. Rasenack, B.W. Muller, In-situ-micronization of disodium cromoglycate for pulmonary delivery, Eur. J. Pharm. Biopharm. 55 (2003) 173-180.

[13] P. Gassmann, M. List, A. Schweitzer, H. Sucker, Hidrosols – alternatives for the parenteral application of poorly water soluble drugs, Eur. J. Pharm. Biopharm. 40 (1994) 64-72.

[14] M. Sarkari, J. Brown, X. Chen, S. Swinnea, R.O. Williams, K.P. Johnston, Enhanced drug dissolution using evaporative precipitation into aqueous solution, Int. J. Pharm. 243 (2002) 17-31.

[15] N. Rasenack, H. Hartenhauer, B.W. Muller, Microcrystals for dissolution rate enhancement of poorly water-soluble drugs, Int. J. Pharm. 254 (2003) 137-145.

[16] N. Rasenack, B.W. Mueller, Micron-Size Drug Particles: Common and Novel Micronization Techniques, Pharm. Dev. Tech. 9 (2004) 1-13.

[17] M.S. Cunha Filho, F.C. Alves, G.M.C. Alves, D.B. Monteiro, F.P. Morais de Medeiros, P.J. Rolim Neto, Beta-lapachone: Development and validation of analytical method for the new therapeutic antineoplastic alternative, Rev. Bras. Farm. 86 (2005) 39-43.

[18] A. Le Bail, H. Duroy, J.L. Fourquet, Abinitio structure determination of Lisbwo6 by X-ray powder diffraction, Mater. Res. Bull. 23 (1988) 447-452.

[19] J.T. Fell, J.M. Newton, The prediction of the tensile strength of tablets, J. Pharm. Pharmacol. 22 (1970) 247-248.

[20] K.A. Khan, C.T. Rhodes, Effect of compaction pressure on the dissolution efficiency of some direct compression systems, Pharm. Acta. Helv. 47 (1972) 594-607.

[21] American Pharmaceutical Association, Handbook of Pharmaceutical Excipients, Pharmaceutical Press, London, UK, 2003, pp. 108-09.

[22] M.S. Cunha-Filho, M. Landin, R. Martinez-Pacheco, B. Dacunha-Marinho, beta-Lapachone, Acta Crystallogr. C. 62 (2006) o473-475.

[23] M.E. Aulton, Pharmaceutics: the science of dosage form design, Churchill Livingstone, Edinburgh, UK, 2002, pp 679.

Parque das Galeras, Santiago de Compostela

Capítulo 10

Characterization of β-lapachone and Methylated β-cyclodextrin Solid-State Systems

Autores: Marcílio S. S. Cunha-Filho[1], Bruno Dacunha-Marinho[2], Juan J. Torres-Labandeira[1], Ramón Martínez-Pacheco[1] and Mariana Landín[1]

[1]Departamento de Farmacia y Tecnología Farmacéutica, Facultad de Farmacia, Universidad de Santiago de Compostela, Santiago de Compostela, Spain
[2]ED. CACTUS, Unidade de Raios X, Universidad de Santiago de Compostela, Santiago de Compostela, Spain

Revista: AAPS PharmSciTech. 2007. 8(3). Article 60

10.1. ABSTRACT

The purpose of this research was to explore the utility of β-cyclodextrin [βCD] and β cyclodextrin derivatives (hydroxypropyl-β-cyclodextrin [HPβCD], sulfobutylether-β-CD [SBβCD] and a randomly methylated-β-CD [RMβCD]) to form inclusion complexes with the antitumoral drug, β-lapachone [βLAP], in order to overcome the problem of its poor water solubility. RMβCD presented the highest efficiency for βLAP solubilization and was selected to develop solid-state binary systems. Differential scanning calorimetry [DSC], X-ray powder diffraction [XRPD], Fourier transform infrared [FTIR] and optical and scanning electron microscopy results suggest the formation of inclusion complexes by both freeze-drying and kneading techniques with a dramatic improvement in drug dissolution efficiency at 20-minute dissolution efficiency (DE_{20} 67.15 % and 88.22 %, respectively) against the drug (DE_{20} 27.11 %) or the βCD/drug physical mixture (DE_{20} 27.22 %). However, the kneading method gives a highly crystalline material that together with the adequate drug dissolution profile make it the best procedure in obtaining inclusion complexes of RMβCD/βLAP convenient for different applications of βLAP.

Keywords: β-lapachone; antitumoral, cyclodextrin; inclusion complex, crystallinity, dissolution rate.

10.2. INTRODUCTION

β-lapachone [βLAP] is a naphtoquinone obtained on a small scale from South American trees of the families Bigoniaceae and Verbenaceae (Figure 10.1).[1] On a larger scale it can be produced following the method developed by Hooker and co-workers through cyclization of lapachol in sulphuric acid by nucleophilic attack of oxygen of the isoprenyl side chain and purification by further recrystallizations.[2]

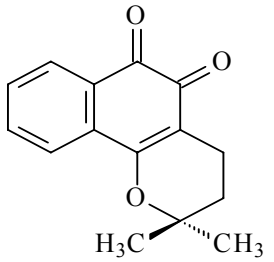

Figure 10.1. Chemical structure of βLAP.

Over the last few years β-lapachone has been reported to possess a wide range of pharmacological properties. It has antifungal, antiviral, antibacterial, anti-psoriatic, anti-inflammatory activities and also is an active agent against parasites as *Trypanosoma cruzi*, the etiologic agent of Chagas disease.[3-8] However, its antineoplasic activity has certainly generated the greatest expectations on the molecule. *In vitro* and *in vivo* studies have shown that β-lapachone inhibits conventional therapy-resistant tumors, particularly the proliferation of neoplasms of slow cell cycle as prostate, pancreatic, colon and some ovarian and breast cancers. [9-12]

The low water solubility of β-lapachone, 0.038 $mg \cdot mL^{-1}$, probably the cause of a low and erratic bioavailability, is the first problem to overcome in the development of dosage forms including the drug.[13]

Cyclodextrins [CDs] are cyclic oligosaccharides with lipophilic inner cavities and hydrophilic outer surfaces capable of interacting with a large variety of drugs giving noncovalent inclusion complexes that have been used extensively to improve solubility, dissolution rate, bioavailability and stability.[14] Drugs such β-lapachone, having aqueous solubility in micromole/liter range are good candidates for solubility enhancement through cyclodextrin complexation.[15] Cyclodextrins have been shown to increase the solubility of β-lapachone as studied by Nasongkla and co-workers but the available information on this subject is extremely limited, particularly on solid systems.[16] The use of α, β, HPβ and γ cyclodextrins has been explored, concluding that βCD and, specially HPβCD, are useful in achieving an increase of water solubility up to 400-fold and overcoming the problem of parenteral administration.[16,17] However, with a view to use the oral route the difficulty is maintained.

A limiting factor in selecting the appropriate CD for a formulation is the amount of complex to be administered. A dosage form for the oral route, a tablet for example, should not exceed 500 mg to 1 g. Since βLAP has a molecular weight of 242.3 and HPβCD of 1390, 100 mg of a complex βLAP/HPβCD 1:1 contains about 14.8 mg of βLAP. It would be useful to find a CD derivative with a higher capacity of increasing βLAP solubility.[18]

On this basis, the main purpose of this research was to explore and compare, using solubility diagram method, the utility of βCD

derivatives to form inclusion complexes with βLAP in order to improve the capacity of increasing βLAP solubility. Four cyclodextrins have been selected: β-cyclodextrin [βCD] and hydroxipropyl-β-cyclodextrin [HPβCD], previously reported by Nasongkla and coworkers and two additional βCD derivatives, sulfobutylether-β-cyclodextrin [SBβCD] and a randomly methylated-β-cyclodextrin [RMβCD].[19]

Solid drug-RMβCD binary systems were prepared according to different techniques (physical mixing, kneading and freeze-drying) and characterized by DSC, X-ray powder diffractometry, FTIR, optical and scanning electron microscopy in order to achieve an improvement on βLAP dissolution properties useful for different applications.

10.3. MATERIALS AND METHODS

Materials

β-lapachone (3,4-dihydro-2,2-dimethyl-2H-naphthol[1,2-b]pyran-5,6-dione; $C_{15}H_{14}O_3$; MW 242.3) was supplied by Laboratorio Farmacêutico do Estado de Pernambuco/LAFEPE (Recife, Brazil). Purity estimated by DSC and HPLC is 99.9 %. βCD and RMβCD (degree of molar substitution 0.57) were kindly donated by Roquette (Barcelona, Spain); HPβCD (degree of molar substitution 2.7) was a Janssen Pharmaceutica (Beerse, Belgium) gift and SBβCD (degree of molar substitution 1.0) was a CyDex (Lenexa, KS) gift. All the βCD derivatives have an aqueous solubility higher than 20 % (wt/vol). All other materials were of analytical grade. The solutions were prepared using distilled

water and filtered through 0.22-µm Millipore filters (Millipore Corp., Billerica, MA).

Analytical Methods

Ą UV spectrophotometric method was developed for quantitative βLAP determination using an UV-visible spectrophotometer Agilent 8453 (Agilent Corp., Santa Clara, CA) with photodiode array detector at 257 nm. Calibration curve in water/ethanol (1:1 vol/vol) was made using standard solutions in the range of 2 to 10 $\mu g \cdot mL^{-1}$. The molar extinction coefficient found was $2.452 \cdot 10^4$ absorbance units. No effect of cyclodextrins addition on the UV spectrum of βLAP solution was verified by comparison of βLAP and CDs/βLAP spectra for any of the CDs studied.

Drug chemical integrity on the liquid and solid systems was evaluated by HPLC analysis using a Waters M600 apparatus with photodiode array detector (Waters Corp., Milford, MA) equipped with a 5 µm C18 cartridge (125 x 4 mm) according to a previously reported method.[20]

Phase Solubility Studies

Phase solubility studies were performed according to the method reported by Higuchi and Connors.[21] Excess amounts of βLAP (~ 15 mg) were added to 3 mL of aqueous solutions containing increasing concentrations of CDs, in the range of 0 % to 1 % (wt/vol) for βCD; 0 % to 2 % (wt/vol) for HPβCD; 0 % to 3 % (wt/vol) for RMβCD; and 0 % to 4 % (wt/vol) for SBβCD. Suspensions were introduced into an ultrasound bath

for 15 min and shaken in an oscillating water bath thermostatically controlled at 25 ºC for 7 days, enough time to guarantee the equilibrium, according to previous studies. Samples were filtered and appropriated diluted. βLAP concentration was determined spectrophotometrically.

Experiments were performed in triplicate. The drug-CD association constants [$K_{1:1}$] were calculated, from the linear portion of the phase solubility diagrams assuming a 1:1 stoichiometry, using the following equation:

$$K_{1:1} = \frac{Slope}{S_0 \times (1 - Slope)} \quad (1)$$

where S_0 is βLAP water solubility in the absence of CD.

Preparation of Solid βLAP-RMβCD Systems

Preparation of Physical Mixture [PM]

A physical mixture of previous sieved granulometric fractions (100-250 μm) of βLAP and RMβCD in 1:1 molar ratio was obtained by mixing in a mixer Turbula WAB T2C (Willy A. Bachofen Corp., Basel, Switzerland) for 30 minutes.

Preparation of Kneaded Systems [KN]

The KN was prepared from physical mixture in a mortar by slowly adding ethanol/water (1:1 vol/vol), in an amount of 20 % wt/wt, and mixing until the homogeneous system was obtained.[22] Samples were dried in an oven at 40 ºC for 24 h and powdered. A granulometric fraction (100-250 μm) was selected and characterized.

Preparation of Freeze-dried Systems [FD]

The physical mixture was dissolved in ethanol:water (1:1 vol/vol). The solution was frozen by immersion in liquid nitrogen and freeze dried in an apparatus Labconco (Labconco Corp., Kansas City, MO). A 100-250 μm sieve granulometric fraction was collected for further characterization.

Solid βLAP-RMβCD System Characterization

X-ray Powder Diffraction [XRPD]

The X-ray powder diffraction patterns were collected using copper radiation (40 Kv, 30 mA), on a Philips PW 1729 diffractometer (Philips Corp., Netherlands) with Bragg-Brentano geometry, in the $2<2\theta<60$ range with a step size of 0.02º and counting time of 2 seconds per step. The microstructure study of the measured samples was determined through line profile analysis [LPA], which included a profile fitting stage to extract profile information from the powder diffraction peaks.

In order to compare the relative crystallinity of β-lapachone in the analysed samples, the microstructural factor crystallite size was obtained using the analysis of the profile information by inverting the Warren-Averbach procedure.[23,24] A Winplotr software that implements the LPA method was used.[25] On this basis it is possible to obtain:

$$Dv= \lambda/(Beta\_G(corrected)*\cos\theta) \quad (2)$$

where Dv is the volume-weighted domain size, Beta_G (corrected) is the Gaussian contribution to the integral breath after the instrumental broadening correction, λ represents the wavelength and θ the peak Bragg angle.

The instrumental profile component was determined experimentally by means of suitable profile standards.[26] As a further general assumption, we consider that our best polycrystalline analysed sample with coherent diffraction crystallites is sufficiently small to provide an appropriate standard for the correction of the instrumental broadening.

Differential Scanning Calorimetry [DSC]

Samples weighing 2 to 3 mg were placed in open aluminium pans and heated from 30 ºC to 250 ºC at a rate of 10 ºC·min^{-1} using a temperature modulated DSC Q100 calorimeter (TA Instruments, New Castle, DE). Nitrogen was used as purge gas at a flux rate of 50 mL·min^{-1}. Calibration of temperature and heat flow was performed with standard indium samples. All measurements were performed in triplicate. The percentage of βLAP in the original crystalline form (OCF) in the binary systems was calculated by the following equation[27]:

$$OCF = 100\frac{\Delta H_{BS}}{\Delta H_{PD}} \quad (3)$$

where ΔH_{BS} is the fusion enthalpy of β-lapachone in the binary system and ΔH_{PD} is the fusion enthalpy of pure βLAP.

Fourier Transformation-Infrared Spectroscopy [FTIR]

Infrared spectra were obtained using a Bruker IFS-66V spectrometer (Bruker Daltonics Inc., Bremen, Germany). Samples were ground, mixed thoroughly with potassium bromide, and compressed in a hydraulic press. Thirty-two scans were obtained at a resolution 4 cm^{-1}.

Optical [OM] and Scanning Electron [SEM] Microscopy

Optical morphological characteristics of the βLAP-CD systems were analysed using an Olympus SZ60 (Opelco, Tokyo, Japan) microscope connected to a videocamera Olympus DP12 (Opelco, Tokyo, Japan). The images were processed using Analysis® version 3.2 (Analysis Software, Müster, Germany). Samples surface morphologies were examined using a LEO-435VP scanning electron microscopy (Leica Microsystems, Cambridge, UK). Particles were fixed on a brass stub using double-sided tape and gold coated in vacuum.

Dissolution Studies

In vitro dissolution studies were performed following FDA specifications for poor soluble drugs using a USP dissolution apparatus 2 (paddle) (Turu Grau DT-6, Barcelona, Spain) at 75 rpm and 37 ºC ± 0.5 ºC.[28]

In order to ensure sink conditions and increase the ability of the dissolution test to distinguish between formulations, the solubility of βLAP in water containing surfactants were tested. A volume of 900 mL of aqueous solution of sodium lauryl sulphate at a concentration of 0.5 % was selected as dissolution medium (solubility of βLAP in the dissolution medium selected was 0.163 $mg \cdot mL^{-1}$).[18]

Powdered samples of 50 mg of βLAP or equivalent amounts of each βLAP/CD system (particle size 100-250 μm) were tested. Powdered samples were submerged rapidly in the medium. At certain time intervals samples were collected, filtered through cellulose filters and the concentration of drug dissolved determined by spectroscopy at 257 nm.

For each binary system three replicates were tested. The dissolution profiles were evaluated and compared using the dissolution efficiency at 20min [DE_{20}] parameter.[29] The statistical analysis of the DE_{20} was performed by the one-way analysis of variance [ANOVA] followed by least significant difference test using Statgraphics® plus version.[30]

10.4. RESULTS AND DISCUSSION

Phase Solubility Diagrams

The effect of selected CDs on the aqueous solubility of βLAP (0.1264 mM) was evaluated using the phase solubility diagrams (Figure 10.2). The enhancement of βLAP solubility was highly dependent on the type of βCD. In all cases, the solubility of βLAP increased linearly as a function of cyclodextrin concentration over the studied concentration range with slopes lower than one (Table 10.1). Diagrams can be classified as A_L type and suggest a 1:1 mol:mol βLAP-CD stoichiometry, according to Higuchi and Connors.[21]

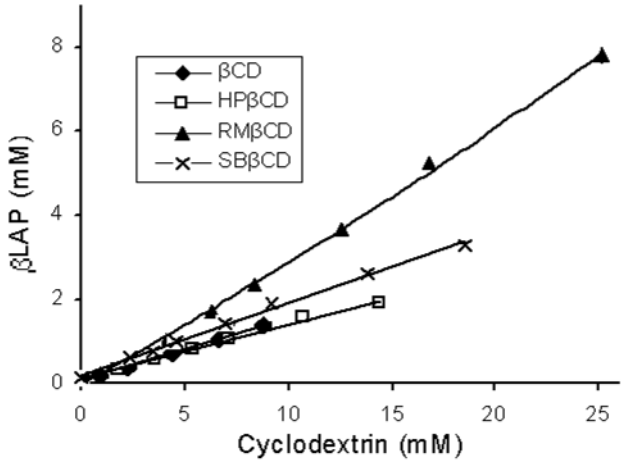

Figure 10.2. Phase solubility diagrams of βLAP as a function of cyclodextrin concentrations at 25 ºC in water.

Table 10.1. Association constants [$K_{1:1}$], slopes and correlation coefficients [r^2] obtained from the phase solubility diagrams (n=3). Standard deviations in parentheses.

CD	Slope	r^2	$K_{1:1}$ x10^3 M^{-1}
βCD	0.1484	0.9977	0.996 (0.020)
HPβCD	0.1270	0.9976	0.876 (0.026)
SBβCD	0.1712	0.9965	1.122 (0.027)
RMβCD	0.3127	0.9963	1.700 (0.024)

Association constants estimated for βLAP-βCD and βLAP-HPβCD were in agreement with previous data reported by Nasongkla and co-workers ($1.23 \cdot 10^3$ M^{-1} for βCD and $0.94 \cdot 10^3$ M^{-1} for HPβCD).[16] The SBβCD and RMβCD, not yet evaluated in previous studies, had higher solubilizing effect on the drug than βCD and HPβCD. The association constant ($K_{1:1}$) obtained with RMβCD was almost two times higher than with the other βCD derivatives. The solubilization performance of RMβCD could be derived from the presence of the methyl groups, which can extend the hydrophobic region of the cyclodextrin cavity favouring and stabilizing the inclusion complexation of the βLAP molecule.[31] A similar effect occurs also with the hydroxypropyl or the sulfobutil ether groups but results suggest more favourable molecular interaction within the methyl groups.

As it was indicated earlier, for a solid oral formulation it would be useful to select the CD derivative with the highest capacity of increasing βLAP solubility. Therefore, the general characteristics of methylated βCD, specially its high aqueous solubility and low toxicity together with its higher efficiency for βLAP solubilization made RMβCD the candidate for inclusion in an oral solid dosage form.[32]

Preparation and Characterization of βLAP-RMβCD Systems

When a cyclodextrin and a potential guest are subjected to a treatment, there is not guarantee that a real inclusion complex will be produced. It has been reported that the product can be a mixture of complex, uncomplexed guest, empty cyclodextrin and also different kinds of drug-CD interaction. As a consequence, a cautious physical-chemical analysis has to be performed to clarify the interactions between the components and its effects on the properties of interest.[22]

The chemical stability of the drug in the solid systems was evaluated by HPLC finding neither chemical incompatibilities between components nor changes due to the stress of the process.

X-ray Powder Diffraction [XRPD]

The possible XRPD patterns of βLAP are shown in Figure 10.3. βLAP presents a typical polycrystalline diffraction pattern, exhibiting a main sharp peak at 9.5 º2θ and secondary peaks at 13.05, 19.05, 19.59, 24.67 and 39.31 º2θ. The profile slightly changes in the βLAP powdered sample (100-250 μm). The preferred orientation variation on the analysed crystallites could explain these differences because the relative intensity of the peaks showed changes. An ideal distribution of the crystallites can be seen at βLAP simulated pattern obtained from the single crystal data, where there is not preferred orientation at all.[33]

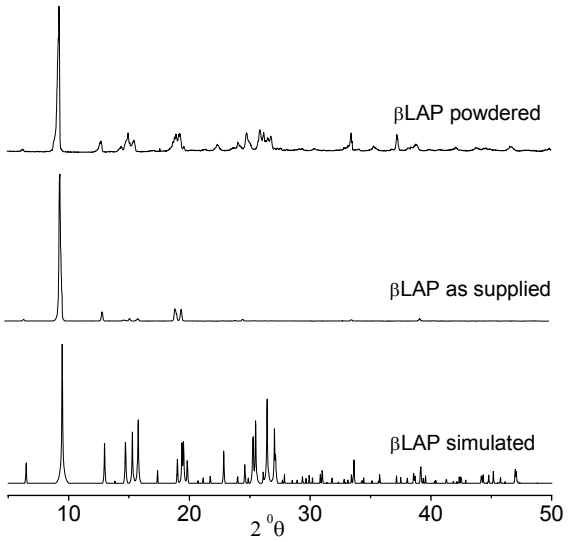

Figure 10.3. X-ray diffraction patterns of βLAP simulated; βLAP experimental as supplied and powdered.

The XRPD pattern of RMβCD as supplied shows a diffuse pattern typical of an amorphous product. As can be seen in Figure 10.4, the pattern of the PM of βLAP-RMβCD can be obtained by the superimposition of pure components patterns. However, the kneading βLAP-RMβCD system XRPD profile presents a great change, involving new peaks, compared with the PM, which could be explained by crystallographic modifications performed during the formulation process.

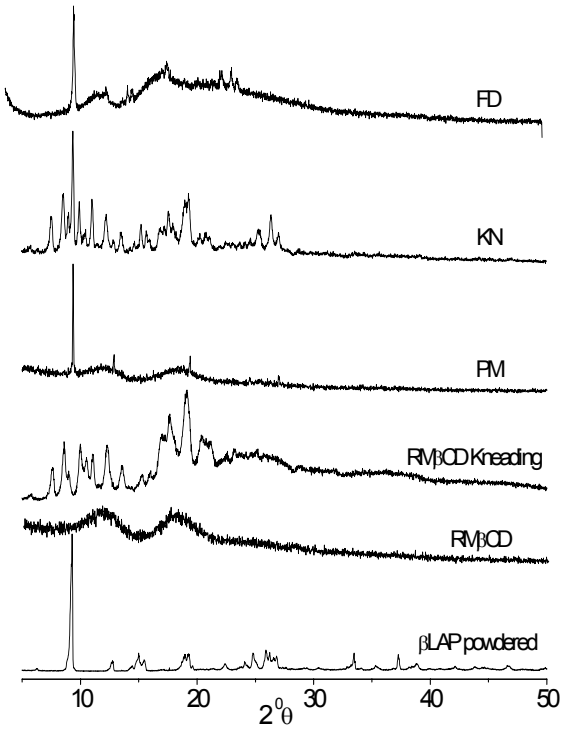

Figure 10.4. X-ray diffraction patterns of βLAP powdered; RMβCD as supplied and kneading; and equimolar βLAP-RMβCD physical mixture [PM], kneading [KN] and freeze-dried [FD] systems.

In order to understand such changes, RMβCD without drug was subjected to a kneading process under the same conditions. The product obtained ($RM\beta CD_{Kneading}$; Figure 10.4) and RMβCD, as supplied, show completely different X-ray diffraction patterns, peak relative intensities and shape, suggesting that the kneading process promotes the cyclodextrin crystallization. RMβCD has a random distribution of a few

sterically small methyl groups which do not completely block the ability to form crystals on the contrary to other βCD derivatives.

Finally, the FD system seems to have the greatest pattern difference. The differences cannot be explained by the simple addition of the components, suggesting a clear interaction between the compounds.

In order to obtain the βLAP relative crystallinity from the analysed samples, LPA was focused on the βLAP main peak. Figure 10.5 show the normalized main peaks for the βLAP pure component and for the binary samples. Changes on the peak profile depending on the treatment can be seen. This confirms different microstructure properties. Assuming that the βLAP main peak was small enough to provide an appropriate standard for the correction of the instrumental broadening, it is possible to state that the FD system presents the lowest crystallinity with a Dv of 538.2 $Å^3$. The KN system shows a relative crystallinity of 987.7 $Å^3$, higher than the PM system with a Dv of 676.9 $Å^3$. This could be explained by the appearance of another kind of crystalline form for the KN system, which is different from the original and that makes this system more crystalline than the physical mixture.

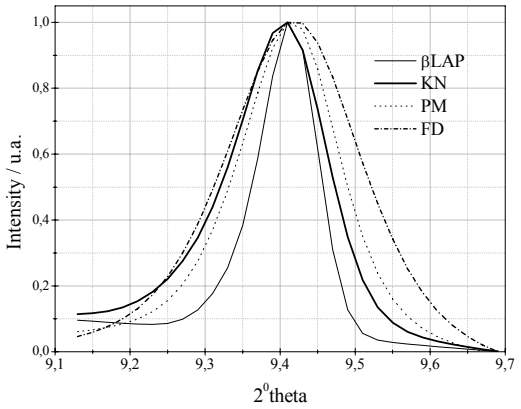

Figure 10.5. Normalized Bragg main peak for βLAP and for equimolar βLAP-RMβCD physical mixture [PM]; kneading [KN] and freeze-dried [FD] systems.

Differential Scanning Calorimetry [DSC] Analysis

DSC analyses of raw materials and binary systems studied are shown in Figure 10.6 and Table 10.2. It can be seen that βLAP DSC curve displays a sharp endotherm at 157.3 ºC, which is due to drug melting, characteristic of an anhydrous crystalline substance. RMβCD exhibits a broad endothermic effect ranging between 30 and 149 ºC associated with water loss from inside the cavity.

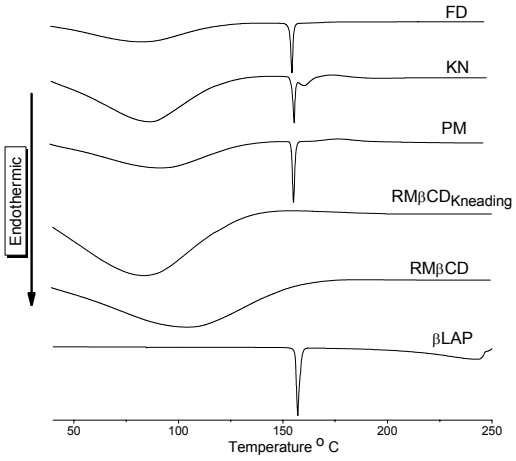

Figure 10.6. DSC thermograms of βLAP; RMβCD as supplied and kneading; and equimolar βLAP-RMβCD physical mixture [PM]; kneading [KN] and freeze-dried [FD] systems.

Disappearance of the fusion peak of the drug is often interpreted as evidence of an inclusion complex formation. In the present study, the thermal profiles of all the binary systems showed the drug melting peak of βLAP, indicating the presence of unchanged drug in all the preparations, which is in agreement with XRPD data. The βLAP pattern in the PM was substantially unaffected in its shape and peak temperature, but a new

small exothermic event was detected at 178.6 ºC (Table 10.2). This finding could be associated to a strong interaction between the CD and the melted drug and subsequent βLAP entrance into the empty CD cavity in an energetic favoured process that decreased the energy of the system.[34] The phenomenon is still detectable and reproducible for the KN sample but not for the FD sample.

The DSC curves for KN and FD systems presented a slight shift in the melting peak of βLAP and an important reduction in the values of the associated enthalpy (Table 10.2). In addition, the KN system thermogram shows an extra endothermic event possibly associated to a new crystalline form of the drug-CD complex as suggested by XRPD results.

Table 10.2. Thermal data from DSC of βLAP; RMβCD as supplied and kneading; and equimolar βLAP-RMβCD physical mixture [PM]; kneading [KN] and freeze-dried [FD] systems. Standard deviations in parentheses.

Samples	Dehydration			Melting			Exothermic peak			OCF (%)
	Range (ºC)	Peak (ºC)	Enthalpy (J g^{-1})*	Range (ºC)	Peak (ºC)	Enthalpy (J g^{-1})†	Range (ºC)	Peak (ºC)	Enthalpy (J g^{-1})	
βLAP	-	-	-	151-162	157.3 (0.1)	103.2 (1.4)	-	-	-	100
RMβCD	30-149	91.0 (4.0)	376.3 (8.8)	-	-	-	-	-	-	-
RMβCD_{KN}	30-149	90.6 (5.2)	233.9 (17.4)	-	-	-	-	-	-	-
PM	30-140	86.7 (1.5)	353.6 (11.5)	153-160	156.6 (0.1)	91.9 (0.1)	167-197	178.6 (0.4)	8.0 (0.4)	89.1 (0.1)
KN	30-138	83.9 (3.0)	368.1 (21.1)	152-157 157-167	155.7 (0.1) 160.5 (0.2)	53.3 (1.2) 38.6 (2.8)	166-188	174.1 (0.3)	4.0 (0.5)	51.6 (2.3)
FD	30-137	84.0 (0.7)	266.1 (20.8)	150-160	155.5 (0.1)	78.3 (0.7)	-	-	-	75.3 (0.7)

*per gram of RMβCD; †per gram of βLAP

An enthalpy reduction of the dehydration peak of $RM\beta CD_{Kneading}$ with respect to the RMβCD as supplied can be seen (Figure 10.6), which could be attributed to the crystallization of the CD in a less hydrated form during the process of kneading (confirmed by XRPD and microscopy

analysis).[27] A large reduction in the dehydration enthalpy takes place in the FD system and could be explained by the replacement of water molecules inside the CD for drug molecules during the freeze-drying process.

The OCF parameter (Table 10.2) shows important reductions for FD (25 %) and KN (49 %) systems, indicating that residual original drug crystallinity is higher in the FD formulation than in the KN system. The combination of XRPD data and DSC suggests that the FD system presents a higher percentage of uncomplexed βLAP with a lower crystallinity degree. On the contrary, the KN system presents a lower percentage of uncomplexed drug but probably the procedure promotes the generation of new crystal phases with an additional associated endotherm at 160.3 ºC (Table 10.2).[35]

Fourier Transformation-Infrared Spectroscopy [FTIR]

The FTIR analysis is a useful technique to assess the interaction and the complex formation between drug molecules and cyclodextrins in the solid state. Shifts or intensity changes in the characteristic bands of pure substance are considered as evidence of the complex existence.[36] However some changes are very subtle, requiring careful interpretation of the spectra.[22]

Infrared spectra of βLAP, RMβCD and the binary systems PM, KN and FD are presented in Figure 10.7 and in Table 10.3. The KN system shows a reduction in the band at 2978 cm^{-1}corresponding to C-H links of βLAP aromatic region compared with PM (Figure 10.7, Line 1), while the FD system shows the almost complete disappearance of this band.

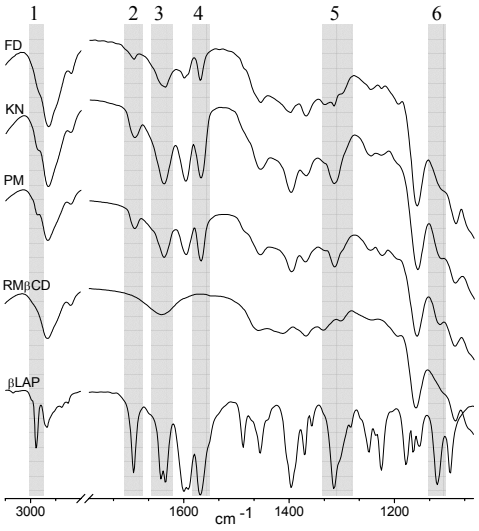

Figure 10.7. FTIR spectra of βLAP; RMβCD; and equimolar βLAP-RMβCD physical mixture [PM]; kneading [KN] and freeze-dried [FD] systems.

Table 10.3. FTIR data of βLAP and equimolar βLAP-RMβCD physical mixture [PM]; kneading [KN] and freeze-dried [FD] systems.

Line	Band	βLAP	PM	KN	FD
1	C-H_{ar}	2978	2978	-	-
2	C=O	1695	1694	1695	1695
4	C-C_{ar}	1600	1597	1597	1599
		1592			
		1569	1568	1568	1570
5	C-O-C	1315	1313	1315	-
6	C-O-C	1119	1115	-	-

In the region of 1700-1000 cm^{-1}, where RMβCD shows a broad band and βLAP did not overlap in the physical mixture, the band corresponding to C=O group (Figure 10.7, Line 2) at 1695 cm^{-1} was clearly reduced in the FD system. Even for this preparation, bands corresponding to C-C links of aromatic region (Table 10.3, Line 4) presented a marked reduction in intensity and a shift to higher frequencies. In the region of C-O-C link (Table 10.3 and Figure 10.7, Line 5 and 6), both KN and FD systems were affected by variations of the corresponding peak.

The results suggest that the inclusion of the drug inside the RMβCD cavity should take place by the aromatic group side (Figure 10.1). Although, the overlapping of drug-CD peaks in the methyl region of

the molecule, does not permit the rejection of the hypothesis of complexation on this side of the molecule. Line 3 (Figure 10.7) represents the RMβCD characteristically O-H band linked with water.[18] A broadening of this band in the KN and FD systems could be explained by changes in the CD capacity of hydration and it is additional evidence of a possible inclusion complex formation.

Optical [OM] and Scanning Electron [SEM] Microscopy

Morphological changes can be employed as a tool for evidence of interaction between molecules and complex formation.[36,37] Selected microphotographs by OM and SEM of the binary systems are presented in Figure 10.8.

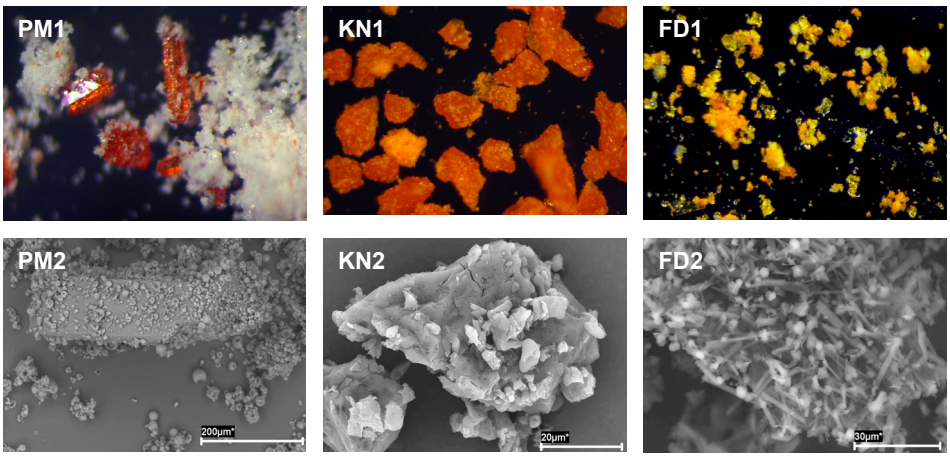

Figure 10.8. Photographs by OM (1) and SEM (2) of equimolar βLAP-RMβCD physical mixture [PM]; kneading [KN] and freeze-dried [FD] systems using a 94.5x magnification.

Orange crystals of βLAP surrounded by amorphous RMβCD particles are detectable in the PM system [PM1]. There was not apparent interaction between both components in PM. On the contrary, significant

modifications in colour and shape were observed after kneading or freeze-drying. The KN system presented granular agglomerates of a strong orange color. It was not possible to distinguish between the two components (Figure 10.8, KN1). SEM (Figure 10.8, KN2) shows compact bulky particles as corresponds to a crystalline material (see XRPD pattern Figure 10.4).

The FD system (Figure 10.8, FD1) showed a heterogeneous system with yellow particles dotted with orange crystals. SEM (Figure 10.8, FD2) presents a mixture of small amorphous particles and acicular crystals. Results confirm the XRPD and DSC data.

Dissolution Studies

Dissolution profiles of β-lapachone and equimolar binary systems βLAP-RMβCD as well as its dissolution efficiencies at 20 min are presented in Figure 10.9.

The increment in dissolution from inclusion complexes for different drugs have been explained on the basis of a higher energetic amorphous state/reduction of crystallinity, a lower interfacial tension between water-insoluble drug, and the dissolution medium induced by the CD and a greater water solubility of the complex.[37]

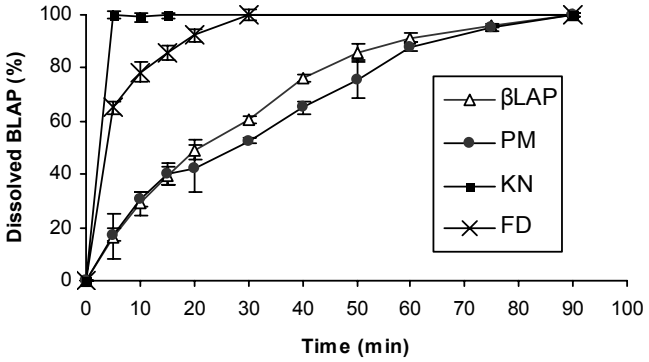

Sample	DE_{20}(SD)
βLAP	27.11(1.56)
PM	27.22(0.43)
KN	88.21(0.76)
FD	67.15(2.29)

Figure 10.9. Dissolution profiles of βLAP; equimolar βLAP-RMβCD physical mixture [PM], kneading [KN] and freeze-dried [FD] systems in *sink conditions*, together with the corresponding mean values of the 20-min dissolution efficiency [DE_{20}].

It is interesting to note that the physical mixture of RMβCD with βLAP does not contribute significantly to an improvement of drug dissolution rate indicating that the increment in local solubilization action of the CD does not explain the dissolution profile of the system.

FD and, especially KN, systems showed profiles with nearly 100 % drug dissolved at 5 minutes. The comparison of drug release profiles was made by the calculation of dissolution efficiency parameter at 20 minutes. The ANOVA of the DE_{20} for the different systems showed significant differences among formulations ($\alpha < 0.05$) and the least significant differences test presented three subsets. The dissolution rate was higher in the following order:

$$\underline{\beta LAP \quad PM} < \underline{FD} < \underline{KN}$$

The formation of readily soluble complexes by freeze-drying or kneading could be deduced in accordance with previous physicochemical characterization. A reduction in the degree of crystallinity is often

associated with an increase in solubility.[27] However, in this case, the degree of crystallinity does not seem to be the only reason involved in the solubility change and probably the generation of new crystal phases (confirmed by XRPD) by the formulation process leading to distinctive microstructural properties is responsible for the different dissolution properties of the KN system. Small differences in drug solubility rate between KN and FD systems should be related to the variability in the particle structure (Figure 10.8), which determines its wettability and deaggregation properties. Moreover, the crystallinity of KN system should improve manufacturability of the product.

10.5. CONCLUSION

In conclusion, βCD derivatives studied, SBβCD and especially RMβCD, present high efficiency for βLAP solubilization. The results suggest that RMβCD possibly forms inclusion complexes by both freeze-drying and kneading techniques with a dramatic improvement in drug dissolution rate against the drug or the βCD/drug physical mixture.

However, the kneading method gives a highly crystalline material that together with the adequate drug dissolution profile make it the best procedure in obtaining inclusion complexes of RMβCD/βLAP convenient for different applications of βLAP.

10.6. ACKNOWLEDGEMENTS

This work was supported by Xunta de Galicia (PGIDIT04BTF203011PR) and the Programme Alβan, the European Union Programme of High level Scholarships for Latin America, scholarship nº E04D043994BR.

The authors thank LAFEPE, Brazil, and Professor Dr Pedro Jose Rolim Neto, Federal University of Pernambuco, Brazil, for their kind gift of the βLAP. The authors are grateful also to Janssen Pharmaceutica, Roquette Freres and CyDex for their generous donation of cyclodextrins.

10.7. REFERENCES

1. Burnett AR, Thomson RH. Naturally occurring quinones. XII. Extractives from Tabebuia chrysantha and other Bignoniaceae. *J Chem Soc C*. 1968; 850-853.

2. Hooker SC, Jr, Shepard HW, Jr, Walsh JG, Jr, Connitt GH. Constitution of lapachol and its derivatives. *J Am Chem Soc.* 1936;58:1190-1197.

3. Guiraud P, Steiman R, Campos-Takaki G, Seigle-Murandi F, Simeon de Buochberg M. Comparison of antibacterial and antifungal activities of lapachol and β-lapachone. *Planta Med*. 1994;60:373-374.

4. Li CJ, Zhang LJ, Dezube BJ, Crumpacker CS, Pardee AB. Three inhibitors of type 1 human immunodeficiency virus long terminal repeat-directed gene expression and virus replication. *Proc Natl Acad Sci USA*. 1993;90:1839-1842.

5. Pereira EM, Machado T de B, Leal IC, et al. Tabebuia avellanedae naphthoquinones: Activity against methicillin-resistant staphylococcal strains, cytotoxic activity and in vivo dermal irritability analysis. *Ann Clin Microbiol Antimicrob*. 2006;5:5.

6. Muller K, Sellmer A, Wiegrebe W. Potential antipsoriatic agents: Lapacho compounds as potent inhibitors of HaCaT cell growth. *J Nat Prod.* 1999;62:1134-1136.

7. Tudan C, Jackson JK, Higo TT, Burt HM. The effect of inhibiting topoisomerase I and II on the anti-apoptotic response associated with pro-inflammatory crystals of calcium pyrophosphate dihydrate in human neutrophils. *Inflamm Res.* 2003;52:8-17.

8. Pinto CN, Dantas AP, De Moura KCG, et al. Chemical reactivity studies with naphthoquinones from tabebuia with anti-trypanosoma efficacy. *Arzneimittelforschung*. 2000;50:1120-1128.

9. Planchon SM, Wuerzberger S, Frydman B, et al. Beta-lapachone-mediated apoptosis in human promyelocytic leukemia (HL-60) and human prostate cancer cells: A p53-independent response. *Cancer Res.* 1995;55:3706-3711.

10. Li Y, Sun X, LaMont JT, Pardee AB, Li CJ. Selective killing of cancer cells by β-lapachone: Direct checkpoint activation as a strategy against cancer. *Proc Natl Acad Sci USA.* 2003;100:2674-2678.

11. Ough M, Lewis A, Bey EA, et al. Efficacy of beta-lapachone in pancreatic cancer treatment: Exploiting the novel, therapeutic target NQO1. *Cancer Biol Ther.* 2005;4:95-102.

12. Suzuki M, Amano M, Choi J, et al. Synergistic effects of radiation and beta-lapachone in DU-145 human prostate cancer cells in vitro. *Radiat Res.* 2006;165:525-531.

13. Jiang Z, Reddy DG, inventors. Pharmaceutical compositions containing β-lapachone or derivatives or analogs. PCT Designated States: Designated States W: AE, AG, AL, AM, AT, AU, AZ, BA, BB, BG, BR, BY, BZ, CA, CH, CN, CO, CR, CU, CZ, DE, DK, DM, DZ, EC, EE, ES, FI, GB, GD, GE, GH, GM, HR, HU, ID, IL, IN, IS, JP, KE, KG, KP, KR, KZ, LC, LK, LR, LS, LT. US patent 7074824. February 13, 2003.

14. Rajewski RA, Stella VJ. Pharmaceutical applications of cyclodextrins. 2. In vivo drug delivery. *J Pharm Sci*. 1996;85:1142-1169.

15. Loftsson T, Brewster ME. Pharmaceutical applications of cyclodextrins. 1. Drug solubilization and stabilization. *J Pharm Sci.* 1996;85:1017-1025.

16. Nasongkla N, Wiedmann AF, Bruening A, et al. Enhancement of solubility and bioavailability of beta-lapachone using cyclodextrin inclusion complexes. *Pharm Res*. 2003;20:1626-1633.

17. Wang F, Blanco E, Ai H, Boothman DA, Gao J. Modulating beta-lapachone release from polymer millirods through cyclodextrin complexation. *J Pharm Sci.* 2006;95:2309-2319.

18. Cao F, Guo J, Ping Q. The physicochemical characteristics of freeze-dried scutellarin-cyclodextrin tetracomponent complexes. *Drug Dev Ind Pharm.* 2005;31:747-756.

19. Davis ME, Brewster ME. Cyclodextrin-based pharmaceutics: Past, present and future. *Nat Rev Drug Discov.* 2004;3:1023-1035.

20. Soares da Cunha Filho MS, Alves FC, Alves GMC, Monteiro DB, Morais de Medeiros FP, Rolim Neto PJ. Beta-lapachone: Development and validation of analytical method for the new therapeutic antineoplastic alternative. *Rev Bras Farm*. 2005;86:39-43.

21. Higuchi T, Connors KA. Phase solubility techniques. *Adv Anal Chem*. 1965;4:117-212.

22. Hedges AR. Industrial applications of cyclodextrins. *Chem Rev.* 1998;98:2035-2044.

23. Balzar D, Audebrand N, Daymond MR, et al. Size-strain line-broadening analysis of the ceria round-robin sample. *Appl Cryst*. 2004;37:911-924.

24. Warren BE, Averbach BL. The effect of cold work in metals on powder pattern intensities. *J Appl Phys.* 1949;20:1066-1069.

25. Roisnel T, Rodriguez-Carvajal J. WinPLOTR: A Windows tool for powder diffraction patterns analysis Materials Science. Proceedings of European Powder Diffraction Conference; May 20-23, 2000; Barcelona, Spain. Stafa-Zurich, Switzerland: Trans Tech Publications; 2000:118-123.

26. Cline JP, Deslattes RD, Staudenmann JL. Certificate SRM 660a. Gaithersburg, MD: NIST; 2000.

27. Veiga MD, Diaz PJ, Ahsan F. Interactions of griseofulvin with cyclodextrins in solid binary systems. *J Pharm Sci*. 1998;87:891-900.

28. US Department of Health and Human Services. Guidance for Industry: Dissolution Testing of Immediate Release Solid Oral Dosage Forms, August 1997. Available at: http://www.fda.gov/cder/guidance/1713bp1.pdf. Accessed January 23, 2007.

29. Khan KA, Rhodes CT. Effect of compaction pressure on the dissolution efficiency of some direct compression systems. *Pharm Acta Helv*. 1972;47:594-607.

30. Fernández-Palacín F, López Sánchez MA, Muñoz Márquez MA, Rodríguez-Chía M, Sánchez-Navas A, Valero-Franco C. Estadística Asistida por Ordenador. Statgraphics Plus 4.1. Cádiz: Universidad de Cádiz; 2000.

31. Mura P, Furlanetto S, Cirri M, Maestrelli F, Corti G, Pinzauti S. Interaction of naproxen with ionic cyclodextrins in aqueous solution and in the solid state. *J Pharm Biomed Anal.* 2005;37:987-994.

32. Jacquet R, Elfakir C, Lafosse M. Characterization of a new methylated beta-cyclodextrin with a low degree of substitution by electrospray ionization mass spectrometry and liquid chromatography/mass spectrometry. *Rapid Commun Mass Spectrom.* 2005;19:3097-3102.

33. Cunha-Filho MS, Landin M, Martinez-Pacheco R, Dacunha-Marinho B. Beta-lapachone. *Acta Crystallogr C*. 2006;62:o473-o475.

34. Frooming K, Szejtli J. Cyclodextrin in Pharmacy. London, UK: Kluwer Academic Publishers; 1994.

35. Cabral Marques HM, Hadgraft J, Kellaway IW. Studies of cyclodextrin inclusion complexes. I. The salbutamol-cyclodextrin complex as studied by phase solubility and DSC. *Int J Pharm*. 1990;63:259-266.

36. Cirri M, Rangoni C, Maestrelli F, Corti G, Mura P. Development of fast-dissolving tablets of flurbiprofen-cyclodextrin complexes. *Drug Dev Ind Pharm*. 2005;31:697-707.

37. Fernandes CM, Teresa Vieira M, Veiga FJB. Physicochemical characterization and in vitro dissolution behavior of nicardipine-cyclodextrins inclusion compounds. *Eur J Pharm Sci*. 2002;15:79-88.

Campus Universitario Norte, USC

Capítulo 11

Intratumoral thermoreversible gels of the novel anticancer drug β-lapachone

Autores: Marcílio S. S. Cunha-Filho[1], Maria de la Fuente[1], Felipe Alvarez Manceñido[1], Carmen Alvarez-Lorenzo[1], Ramón Martínez-Pacheco[1] and Mariana Landín[1]

[1]Departamento de Farmacia y Tecnología Farmacéutica, Facultad de Farmacia, Universidad de Santiago de Compostela, Santiago de Compostela, Spain

Manuscript in preparation

11.1. ABSTRACT

The aim of this work was to evaluate the potential of two Pluronic® varieties, F127 and P123, to be used as thermoreversible vehicles in the formulation of intratumoral dosage forms of β-lapachone (βLAP). The rheological properties of the systems elaborated with different polymer concentrations, their drug solubilization capacity and their *in vitro* release profiles were evaluated in the absence and the presence of ethanol and a randomly methylated-β-cyclodextrin (RMβCD).

Pluronic P123 systems have a higher capacity of βLAP incorporation, especially when ethanol (20 %) is present in the formulation. However, the low gel strength of those systems does not guarantee their permanence at the administration site for a long period of time. In the range of concentrations 18-23 %, the Pluronic F127 presents good perspectives for intratumoral formulations development. Those systems have a high capacity of βLAP solubilization, adequate gel temperature range (20-30 ºC) and gel strength at 37 ºC enough to guarantee the permanence of the formulation in the administration site for a period of time. The βLAP release rate is highly modulable by the concentration of the polymer and the addition of cosolvents, especially the cyclodextrin. The use of ethanol in combination with Pluronic F127 should be avoided as this cosolvent affects negatively their mechanical properties at 37 ºC. Autoclaving can be used as the sterilization method for βLAP-Pluronic systems as it does not affect their physical-chemical properties.

Keywords: β-lapachone; intratumoral; Pluronic; thermoreversible gels; cosolvents; autoclaving.

11.2. INTRODUCTION

Conventional systemic cancer chemotherapy has limited effectiveness in the treatment of solid tumors; the surgical removal being the preferred therapy although recurrence is still frequent (Hunter et al., 1997). The use of local controlled release formulations of anticancer drugs is attracting much attention due to the unique physiology of solid tumours, which comprises a highly disordered vasculature and zones of rapidly proliferation cells where a formulation can be retained (Jackson et al., 2004).

β-lapachone (βLAP) is an antineoplasic drug that acts by a novel mechanism of directly activation checkpoint regulators inducing apoptosis, particularly useful for neoplasms of slow cell cycle like prostate, pancreatic, colon and some ovarian and breast cancer (Pardee et al., 2002; Li et al., 2003; Pink et al., 2000). Despite its great potential, several factors hinder its use, mainly its low aqueous solubility (Nasonkgla et al., 2003, Cunha-Filho et al., 2007) and its non-specific distribution that can lead to a low tumour concentration and/or a systemic toxicity (Ough et al., 2005). An alternative approach for βLAP administration could be an injectable formulation containing appropriate polymers able to undergo a transition to an implant into the tumour tissues (Jackson et al., 2000; Amiji et al., 2002; Jackson et al., 2004).

Pluronics are safe amphiphilic triblock copolymers of ethylene oxide (EO) and propylene oxide (PO) blocks (EOx-POy-EOx) that form polymeric micelles with a relatively hydrophobic core in which poorly soluble drugs can be hosted. The incorporation of the drug into the

micelles can delay drug release and improve its chemical stability (Kabanov et al., 2002; Croy and Kwon, 2006). Therefore, Pluronic micelles could be particularly suitable for the development of formulations of the photosensitive βLAP (Cunha-Filho et al., 2008).

Pluronic micellar solutions undergo a sol to gel transition when heating above a certain temperature (American Pharmaceutical Association, 2006; Kabanov et al., 2002; Pisal et al., 2004). If the concentration is adequately chosen, the micellar entanglements at body temperature provide a depot system with a high viscosity and elasticity and a sustained drug release at the site of application (Amiji et al., 2002; Dumortier et al., 2006a). Furthermore, pluronics can alter the mechanisms responsible for multidrug-resistance in cancer cells (Alakhov et al., 1996; Alakhov et al., 1999).

The aim of the study was to evaluate the potential of two Pluronic varieties, F127 and P123, to be used in the formulation of thermoreversible vehicles of βLAP. For an efficient intratumoral delivery of βLAP, the following essential criteria should be taken into account: i) it should be able to solubilize an adequate ammount of βLAP; ii) it should be syringeable in the tumor; iii) it should form a gel of sufficient consistency to guarantee the formation of a depot system; and iv) the depot should sustain drug release. To carry out the work, aqueous dispersions of the Pluronics at different concentrations were prepared and the effect of additives, such as RMβCD and ethanol, on βLAP solubility and gel properties was evaluated. Additionally, the effect of sterilization by autoclaving on the rheological behaviour and physical stability of the systems was also studied.

11.3. EXPERIMENTAL

Materials

β-lapachone (βLAP; batch L503; 3,4-dihydro-2,2-dimethyl-2H-naphthol-[1,2-b]pyran-5,6-dione; $C_{15}H_{14}O_3$; MW 242.3) was supplied by Laboratorio Farmacêutico do Estado de Pernambuco, LAFEPE (Recife, Brazil) with purity estimated by DSC and HPLC in 99.9 %. Randomly methylated-β-cyclodextrin (RMβCD; degree of molar substitution 0.57) was kindly donated by Roquette (Barcelona, Spain). Pluronic® F127 was purchased from Sigma-Aldrich (St. Louis, USA) and Pluronic® P123 was supplied by BASF (Ludwigshafen, Germany). All other chemicals were of analytical grade. Purified water (Millipore, MilliQ® Plus, Billerica USA) was used.

Preparation of Pluronic dispersions

Pluronic® F127 or P123 were added to water under stirring and kept at 4 ºC until obtaining a clear transparent solution (Kabanov et al., 2002). The concentrations were 18 %, 23 % and 28 % (w/w) for Pluronic F127 and 28 % (w/w) for Pluronic P123. Ethanolic solutions of βLAP at a concentration of 20 $mg \cdot mL^{-1}$ were poured into stock Pluronic solutions under stirring and a final drug concentration of 0.2 $mg \cdot mL^{-1}$ was obtained.

RMβCD was previously dissolved in a small volume of water and added to stock Pluronic dispersions, up to a final concentration of 5 % (w/v). To some systems, ethanol was added up to a 20 % (v/v).

Analytical Methods

βLAP was determined spectrophotometrically at 257 nm (Agilent 8453, Santa Clara, USA). Calibration curve in water/ethanol (1:1 v/v) was made using standard solutions in the range of 2 to 10 $\mu g \cdot mL^{-1}$. No effect of additives on the spectrum of βLAP solution was observed.

Rheological evaluation

The incidence of temperature from 5 ºC to 40 ºC on the loss or viscous (G´´) and storage or elastic (G´) modulus of the dispersions was evaluated in a Rheolyst AR-1000N rheometer (TA Instruments, Newcastle, UK) equipped with an AR2500 data analyzer, a Peltier plate and a cone with a diameter of 40 mm and 1.58 degree. The gap was fitted to 50 µm. Measurements were performed at 0.5 $rad \cdot s^{-1}$ with an oscillatory stress of 0.1 Pa and a ramp of 2 $^{o}C \cdot min^{-1}$. The temperature at which the elastic modulus cross-overs the viscous modulus was considered the gel temperature (Dumortier et al., 2006b).

Creep-recovery assays were performed at 37 ^{o}C. During the creep phase a fixed shear stress of 10 Pa for Pluronic F127 systems and 0.3 Pa for P123 systems was applied for 5min. The samples were equilibrated at 37 ^{o}C during 2h before assay. *Gel strength* was calculated by the reverse of the maximum value of compliance of the retardation phase of creep-recovery profiles. The experiments were carried in triplicate.

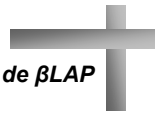

βLAP solubilization

βLAP solubility was evaluated by adding an amount in excess of drug into 3 mL of Pluronic solutions placed in glass ampoules. The suspensions were sonicated during 15min and mechanically shaken (Gallenkamp, Loughborough UK) at 200 rpm for 7 days at 4 ºC. Then, the systems were filtered through 0.45 µm nylon filters (Millipore Corp, Billerica, USA), and diluted with water/ethanol solution (1:1 v/v) to determine spectrophotometrically βLAP concentration. The experiments were carried out in quadruplicate. The *Enhancement Factor* (EF) was calculated by dividing the βLAP solubility value in the system by the βLAP solubility in pure water (0.03 $mg \cdot mL^{-1}$; Cunha-Filho et al., 2007).

In vitro release assays

βLAP diffusion rate from Pluronic systems was studied, in quadruplicate, using horizontal side-by-side diffusion cells (Crown glass Corp., Somerville, NJ), separated by a dialysis membrane of a molecular weight cut-off at 7000 Daltons (Visking corp., London, UK) and a diffusional area of 0.64 cm^2. Pluronic systems (2 mL) containing βLAP at a concentration of 0.2 $mg \cdot mL^{-1}$ were placed in the donor chamber at 37ºC. The receptor medium, phosphate buffer pH 6.8 (Newell et al., 1993), was continuously stirred with magnetic bar. During 20h samples were collected regularly and replaced with fresh buffer in order to keep *sink conditions*. The βLAP in the solutions was determined as previously described.

Autoclaving

Pluronic systems were placed in glass ampoules and autoclaved for 20 minutes at 121 ^{o}C (Raypa model AES-1219, Terrasa, Spain). Samples were then stored at 4 ^{o}C until characterization. Gel temperature and rheological behaviour after autoclaving were studied as described above. Samples were observed under optical microscopy (Olympus SZ60 connected to a video camera Olympus DP12, Tokyo, Japan) and the βLAP remaining in solution was determined spectrophotometrically

Statistical analysis

The statistical analysis of rheological measurements were performed by the one-way analysis of variance (ANOVA) followed by least significant difference test using Statgraphics® plus version (α = 0.05).

11.4. RESULTS AND DISCUSSION

Rheological properties

Gel temperature

Gel temperature is a critical parameter in the development of an intratumoral injection able to form a depot. Aqueous solutions of Pluronics at specific concentrations form micelles due to hydrophobic interactions among the PPO blocks. If the temperature raises, the micelles reorient and form cubit networks, which increase the consistency of the system (gel state), as a result of a progressive dehydration of PPO and PEO

blocks. Both the micellization and the gelation are reversible phenomena and can be affected by the presence of drugs or additives in the formulation (Dumortier et al., 2006b).

The concentration range of Pluronics to produce adequate systems for intratumoral administration were selected on the basis of preliminary studies. Concentrations between 18-28 % for Pluronic F127 and 28 % for Pluronic P123 satisfy those requirements. Below 18 % Pluronic F127 does not form gels at 37 ºC, but above 28 %, gels are formed even below 10 ºC making their handling difficult. The concentration range for obtaining Pluronic P123 systems that undergo the sol-gel transition at body temperature is narrower. Concentrations lower than 28 % form gels above 37 ºC and at a higher concentration the system becomes a gel even at 4 ^{o}C. The gel temperature of the systems studied are shown in Table 11.1. Results of Pluronic F127 systems are in agreement with data in the literature (Dumortier et al., 2006a). In the concentration range studied, a close lineal correlation between polymer concentration and the gel temperature was observed:

Gel temperature (ºC) = 50.67-1.39·[*Pluronic P127* (%)]; r^2=0.9986

The addition of drugs and/or cosolvents must be selected carefully as they can extensively modify the gel temperature of the Pluronic systems (Dumortier et al., 2006b) with important repercussions on their utility for intratumoral administration.

For the Pluronic systems studied, the incorporation of βLAP does not cause significant modifications (α<0.05) in the gel temperature. By contrast, the addition of ethanol dramatically decreases the gel temperature of 23 % Pluronic F127 and 28 % Pluronic P123 (Table 11.1). Additionally, the incorporation of ethanol makes that 18 % Pluronic F127 system remains as a low viscosity solution at 37 ^{o}C; whilst 28 % Pluronic

F128 gel does not soft even below at 4°C. Thus, in these cases the addition of ethanol could turn the systems into inappropriate formulations for intratumoral injection purposes.

The incorporation of RMβCD at 5 % increases the gel temperature of all systems studied especially for the Pluronic P123 dispersions, which is in agreement with results previously reported (Kim et al., 2002).

Table 11.1. Gel temperature of Pluronics F127 and P123 systems. In parenthesis the standard deviations.

		without drug or additives	**+ βLAP**	**+ βLAP + ethanol**	**+ βLAP + RMβCD**
F127	**18%**	25.5 °C (0.0)	24.1 °C (0.6)	6 °C (2.0)	29.1 °C (0.7)
	23%	19.0 °C (0.0)	18.9 °C (0.6)	11.2 °C (0.7)	23.7 °C (0.6)
	28%	11.6 °C (0.6)	12.8 °C (0.6)	-	15.7 °C (0.8)
P123	**28%**	18.9 °C (0.5)	18.8 °C (0.7)	9.6 °C (0.8)	25.0 °C (0.8)

Viscoelastic behaviour

In order to form a depot when injected the polymer systems must maintain enough consistency for a period of time. The viscolastic behaviour and the consistency should influence the drug release. Viscoelastic behaviour was evaluated from the creep-recovery experiments (Figure 11.1). Based on creep-recovery profiles, Pluronic systems studied can be classified into four groups of different rheological behaviours. Group A (with the highest viscosity) which includes the aqueous solutions of Pluronic F127 at 28 % and 23 % formulated without additives, plus βLAP and plus βLAP and RMβCD; group B which includes the aqueous solution of Pluronic F127 at 18 % formulated without additives, plus βLAP and plus βLAP and RMβCD; group C which includes the aqueous solution of F127 at 23 % formulated with the drug and

ethanol; and group D (with the lowest viscosity) which includes the aqueous solution of Pluronic P123 at 28 % in all the conditions studied.

The creep-recovery profiles exhibited an important elastic component for groups A and B (Figure 11.1) with a total recovery around 50 %, which means that these systems form a structured network able to store energy. On the other hand, groups C and D presented a minor elastic recovery (5 %) and a predominant viscous behaviour.

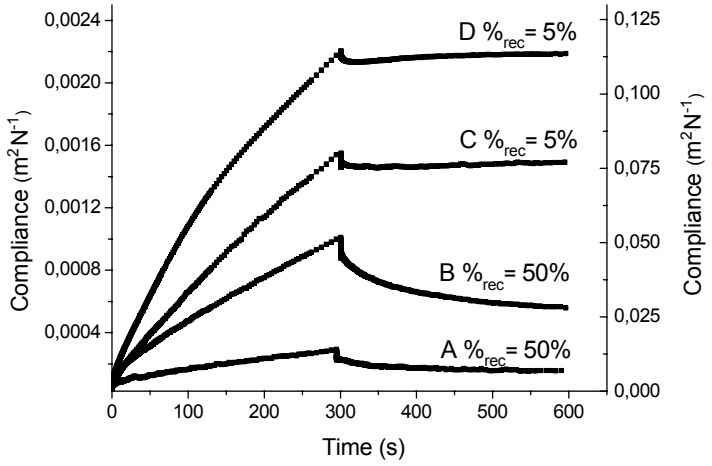

Figure 11.1. Creep-recovery profiles (37 °C) with indications of recovery percentages for the four characteristic rheological behaviour groups, namely, A (left axis): Pluronic F127 at 28 % and 23 % (without additive; drug; drug + RMβCD); B (left axis): Pluronic F127 at 18 % (without additive; drug; drug + RMβCD); C (left axis): F127 at 23 % (drug + ethanol); and D (right axis): Pluronic P123 at 28 % (without additive; drug; drug + ethanol; drug + RMβCD).

Pluronic system consistency was evaluated through the parameter "gel strength" at 37 ºC calculated by the reverse of compliance of the retardation phase of creep-recovery profiles (Table 11.2). As it can be seen, the incorporation of ethanol lead to a strong reduction on gel strength and also a lost of elasticity for Pluronic F127 system. The viscoelastic effect of ethanol on Pluronic P123 was negligible. Similarly,

cyclodextrin did not alter significantly the viscoelastic profiles at 37 ºC (Table 11.2).

Table 11.2. Gel strength ($N \cdot m^{-2}$) of the systems at 37 ºC. Standard deviations in parenthesis.

		without drug or additives	+ βLAP	+ βLAP + ethanol	+ βLAP + RMβCD
F127	18%	1554 (542)	1740 (124)	-	1382 (462)
	23%	5740 (1250)	5698 (2821)	692 (156)	4827 (1763)
	28%	6524 (2300)	5174 (583)	-	5892 (850)
P123	28%	10.8 (12.3)	8.8 (3.3)	10.0 (3.9)	8.5 (0.6)

βLAP solubilization capacity of the Pluronic systems

The solubility of βLAP in the Pluronic systems and the corresponding Enhancement Factor (EF) are shown in Table 11.3. The βLAP solubilization capacity of the Pluronic F127 increases until the concentration 23 % but drops at 28 %. Results are not in agreement with general literature that indicates that above their *critical micelar concetration* the solubility increases linearly with the concentration of the surfactant (Rangel-Yagui et al., 2005). A possible explanation for this phenomenon is the effect of the high viscosity of the system even at 4 ºC that could affect the time to achieve the equilibrium.

The incorporation of βLAP into the Pluronic micelles resulted in increased drug solubility. In agreement with their HLB (Kabanov et. al., 2002), Pluronic P123 (HLB 8) dissolves a higher amount of βLAP than Pluronic F127 (HLB 22), although βLAP solubility still remains below $1 mg \cdot mL^{-1}$. For poorly soluble drugs, the single approach of micellization could be not enough to improve the aqueous solubility to the desirable extent (Rao et al., 2006) being necessary its combination with other

solubilization approaches. Both RMβCD (5 % w/v) and ethanol (20 % v/v) (Table 11.3) enhanced βLAP solubilization to a great extent. RMβCD increased the solubility in almost 50-fold in both Pluronic F127 and P123, reaching drug concentrations close to 1.5 $mg \cdot mL^{-1}$. Ethanol contributes to βLAP solubilization especially, in P123 Pluronic achieving a concentration of 2.4 $mg \cdot mL^{-1}$.

Table 11.3. Data of solubilization of βLAP in F127 and in P123 Pluronic systems at 4°C with and without additives. Standard deviation in parenthesis

Samples		βLAP		βLAP + ethanol		βLAP + RMβCD	
		S^a $mg \cdot mL^{-1}$	EF^b	S^a $mg \cdot mL^{-1}$	EF^b	S^a $mg \cdot mL^{-1}$	EF^b
F127	18%	0.248 (0.032)	8.3	0.660 (0.051)	22.0	1.037 (0.141)	34.6
	23%	0.444 (0.108)	14.8	1.183 (0.102)	34.4	1.487 (0.117)	49.6
	28%	0.208 (0.028)	7.0	-	-	0.767 (0.141)	25.6
P123	28%	0.875 (0.209)	29.2	2.372 (0.385)	79.1	1.478 (0.383)	49.3

[a]Solubilized βLAP; [b]Enhancement Factor

In vitro release assays

The Pluronic systems evaluated behaved as liquids of low viscosity at room temperature, which may be injected through a small-gauge needle forming a viscoelastic depot when reached the body temperature. A controlled release implant could be formed at the site of application. Under these conditions, the volume of fluid around the site of administration is usually small being the dissolution of the polymer and the disintegration of the depot extremely slow. Thus, drug release from an intratumoral implant is mainly controlled by diffusion (Jackson et al. 2000; Amiji et al., 2002).

Pluronic systems containing 0.2 $mg \cdot mL^{-1}$ drug concentration with adequate syringeability and gel temperature for intratumoral purposes were tested as regards their drug release characteristics using diffusion cells. The selected membrane– 7,000 Da cut-off – enabled the movement of the drug towards the receptor compartment; the polymer being retained in the donor compartment.

As it has been previously described for other drugs as sodium diclofenac and quinine release from Pluronic systems (Park et al., 2003; Fawaz et al., 2004), the βLAP release profiles fit mainly zero order kinetics. Formulation including Pluronic F127 23 % plus ethanol is the one having the lowest correlation coefficient (r= 0.967) but the model was maintained in order to compare formulations.

Figure 11.2 shows the drug release profiles from Pluronic F127 systems, with and without RMβCD. In both cases, a negative correlation was observed between the βLAP release rate (Table 11.4) and Pluronic F127 concentration, which can be explained by the systems gel strength (Table 11.2). High concentrations of polymer lead to more entangled structures of poloxamer molecules limiting drug diffusion (Park et al. 2003) until a certain limit where no more effects on viscosity can be noted. This justifies the similar profiles for Pluronic F127 systems at 23 and 28 % with or without RMβCD.

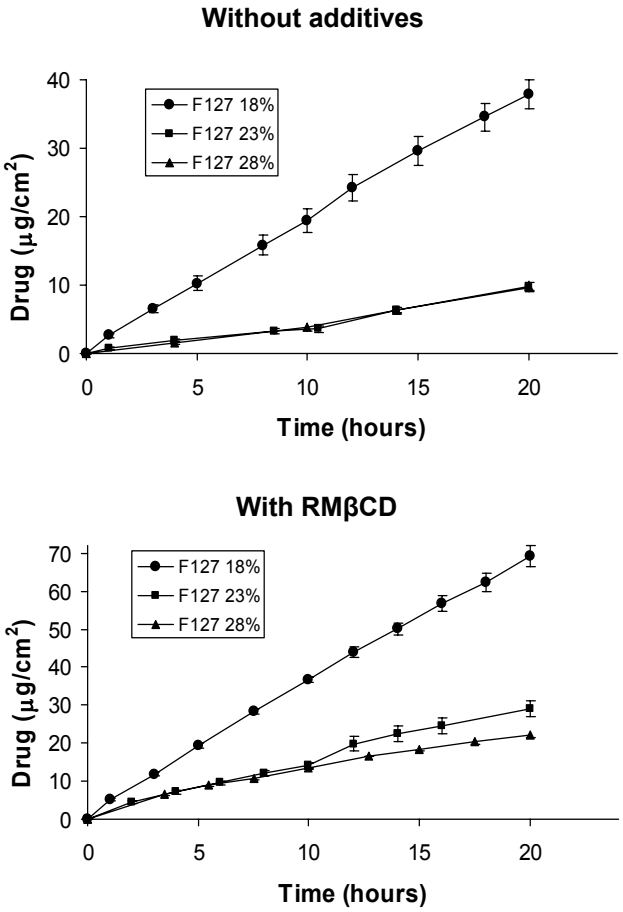

Figure 11.2. βLAP release profile from Pluronic F127 systems formulated with and without RMβCD.

Although RMβCD did not alter the gel strength profiles of the Pluronic systems (Table 11.2), it greatly accelerated drug release (Figure 11.3). This effect can be explained by the increase in βLAP water solubility as a consequence of complexation with RMβCD, the disruption of the micelles by the cyclodextrin (Horsky and Pitha, 1996) and/or the displacement of the drug from micelle core by a competitive mechanism (Bilensoy et al., 2007).

The incorporation of ethanol into the Pluronic F127 systems gives an increase in βLAP release rate (Figure 11.3) that could be explained by the reduction in the gel strength of the system (Table 11.2). On the Pluronic P123 systems, ethanol does not show an effect on drug release as a consequence of having similar rheological behavior.

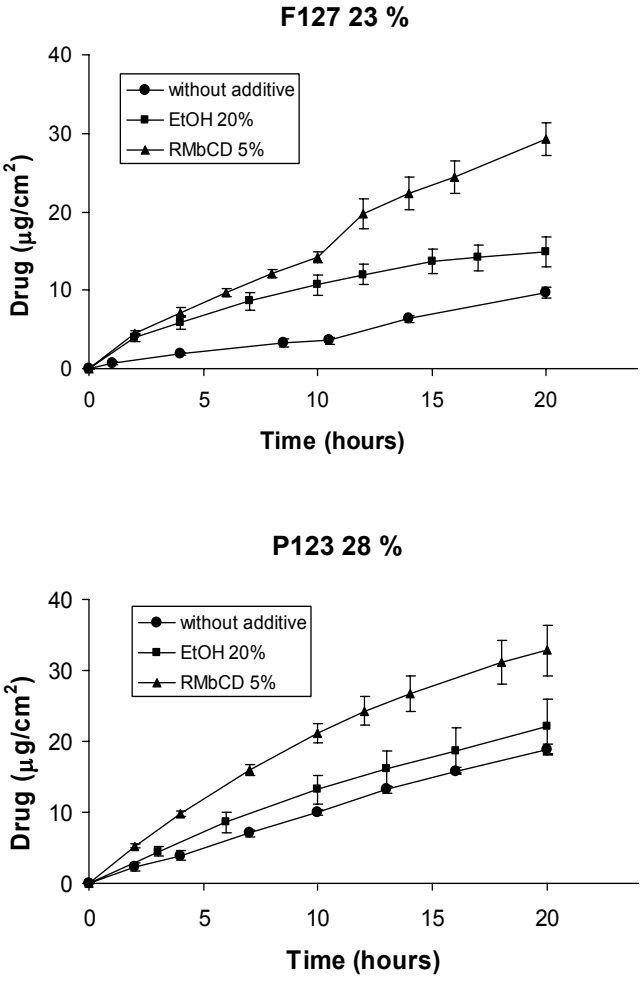

Figure 11.3. βLAP release profile from Pluronic F127 23 % and P123 28 % systems formulated with and without additives

Table 11.4. Data from fitting βLAP release profiles to zero order kinetics and total amount of drug released at the end of the assay (D_{20}).

	Additives	r[a]	slope ($\mu g/h \cdot cm^2$)	D_{20} ($\mu g/cm^2$)
F127 18%	Without	0.999	1.21	37.9
	RMβCD	0.999	2.19	69.2
F127 23 %	Without	0.985	0.30	9.7
	EtOH	0.967	0.46	14.9
	RMβCD	0.996	0.94	29.2
F127 28 %	Without	0.993	0.31	9.9
	RMβCD	0.987	0.68	22.1
P123 28%	Without	0.999	0.61	18.8
	EtOH	0.994	0.70	22.1
	RMβCD	0.986	1.04	32.8

[a] correlation coefficient

Variations in the release rate of βLAP from Pluronic systems in the presence of ethanol could be totally explained by the reduction in the gel strength of the formulations whereas the effect of the addition of the RMβCD should be related to the increment in drug solubility and/or the molecular mechanism of complexation.

Autoclaving

No statistical significant differences were denoted in the gel temperature or gel strength of the samples before and after autoclaving (Tables 11.5 and 11.6) which is understand as physical stability of the pluronic systems as pointed out by different authors for Pluronic systems (Cavalli et al., 1997; Dumortier et al., 2006a). No crystalline growth was observed by optical microscopy and no evidences of drug decomposition

were found at the UV-visible spectra. Autoclaving could be recommended as a sterilization method for those intratumoral formulations.

Table 11.5. Gel temperature of Pluronic systems before and after autoclaving. Standard deviations in parenthesis

		without drug or additives	+ βLAP	+ βLAP + ethanol	+ βLAP + RMβCD
F127 23%	**before autoclaving**	19.0 °C (0.0)	18.9 °C (0.6)	11.2 °C (0.7)	23.7 °C (0.6)
	after autoclaving	18,8 °C (0.8)	19.3 °C (0.0)	10.7 °C (0.4)	22.9 °C (1.4)
P123 28%	**before autoclaving**	18.9 °C (0.5)	18.8 °C (0.7)	9.6 °C (0.8)	25.0 °C (0.8)
	after autoclaving	17.8 °C (0.8)	17.3 °C (1.8)	10.1 °C (0.1)	23.4 °C (1.4)

Table 11.6. Gel strength ($N \cdot m^{-2}$) of Pluronic systems at 37 ºC before and after autoclaving. Standard deviations in parenthesis

		without drug or additives	+ βLAP	+ βLAP + ethanol	+ βLAP + RMβCD
F127 23%	**before autoclaving**	5740 (1250)	5698 (2821)	692 (156)	4827 (1763)
	after autoclaving	6596 (2213)	4695 (1487)	590 (72)	4473 (1409)
P123 28%	**before autoclaving**	10.8 (12.3)	8.8 (3.3)	10.0 (3.9)	8.5 (0.6)
	after autoclaving	9.7 (0.7)	13.5 (6.9)	7.9 (1.9)	9.4 (2.4)

11.6. CONCLUSIONS

Pluronic P123 systems have a higher capacity of βLAP incorporation, especially when ethanol (20 %) is present in the formulation. However, the low gel strength of those systems does not guarantee the permanence of the system for a long period of time.

In the range of concentrations 18-23 % the Pluronic F127 presents better perspectives for intratumoral formulations development. It has a high capacity of βLAP solubilization, adequate gel temperature range (20-30 ºC) and the gel strength at 37 ºC is enough to guarantee the permanence of the formulation in the administration site for a period of time. The βLAP release rate is highly modulable by the concentration of the polymer and the addition of cosolvents, especially the cyclodextrins. The use of ethanol in combination with Pluronic F127 should be avoided as this cosolvent affects negatively their mechanical properties at 37 ºC.

Autoclaving does not affect the physical-chemical properties of the Pluronic systems and could be recommended as the sterilization method for the intratumoral formulations

This preliminary study shows that βLAP formulations in thermo-reversible gels of Pluronics show suitable properties for an intratumoral drug delivery. Future pre-clinical assays must be performed to confirm its utility as intratumoral therapy.

11.7. ACKNOWLEDGEMENTS

Authors thank LAFEPE, Brazil, and Professor Dr Pedro Jose Rolim Neto, Federal University of Pernambuco, Brazil, for their kind gift of the βLAP. This work was supported by Xunta de Galicia (PGIDIT04BTF203011PR) and the Programme Alβan, the European Union Programme of High Level Scholarships for Latin America, scholarship nº E04D043994BR.

11.8. REFERENCES

Alakhov VY, Moskaleva EY, Batracova EV, Kabanov AV. Hypersensibilization of multidrug resistant human ovarian carcinoma cells by Pluronic P85 block copolymer. Bioconjug. Chem. 1996;7:209-216.

Alakhov VY, Klinski E, Li G, Pietrzynski, Venne A, Batracova EV, Bronitch T, Kabanov AV. Block copolymer based formulation of doxorubicin. From cell screen to clinical trials. Colloids Surf. B. Biointerfaces 1999;16:113-134.

American Pharmaceutical Association. Handbook of Pharmaceutical Excipients. Fourth ed., Pharmaceutical Press, London, 2006.

Amiji MM, Lai P, Shenoy DB, Rao M. Intratumoral administration of paclitaxel in an in situ gelling poloxamer 407 formulation. Pharm. Dev. Tech. 2002;7:195-202.

Bilensoy E, Cirpanli Y, Sen M, Dogan A, Calis S. Thermosensitive mucoadhesive gel formulations loaded with 5-Fu:cyclodextrin complex for HPV-induced cervical cancer. J. Incl. Phenom. Macrocycl. Chem. 2007;57:363-370.

Cavalli R, Caputo O, Carlotti ME, Trotta M, Scarnecchia C, Gasco MR. Sterilization and freeze-drying of drug-free and drug-loaded solid lipid nanoparticles. Int. J. Pharm. 1997;148:47-54.

Choi H, Lee M, Kim M, Kim C. Effect of additives on the physicochemical properties of liquid suppository bases. Int. J. Pharm. 1999;190:13-19.

Croy SR, Kwon GS. Polymeric micelles for drug delivery. Current Pharmaceutical Design. 2006; 12: 4669-4684.

Cunha-Filho M, Dacunha-Marinho B, Torres-Labandeira JJ, Martínez-Pacheco R, Landín M. Characterization of β-Lapachone and Methylated β-Cyclodextrin Solid-state Systems. AAPS PharmSciTech 2007;8:Article 60.

Cunha-Filho M, Martínez-Pacheco R, Landín M. Stability and degradation kinetics of the investigational antitumoral drug β-lapachone in solid state. J. Pharm. Biom Anal. 2008. Submitted.

Dumortier G, Kateb NE, Sahli M, Kedjar S, Boulliat A, Chaumeil JC. Development of a thermogelling ophthalmic formulation of cysteine. Drug Dev. Ind. Pharm. 2006a;32:63-72.

Dumortier G, Grossiord JL, Agnely F, Chaumeil JC. A Review of Poloxamer 407 Pharmaceutical and Pharmacological Characteristics. Pharm. Res. 2006b;23:2709-2728.

Fawaz F, Koffi A, Guyot M, Millet P. Comparative in vitro-in vivo of two quinine rectal gel formulations. Int. J. Pharm. 2004;280:151-162.

Horsky J, Pitha J. Hydroxypropyl cyclodextrn: potential synergism with carcinogens. J. Pharm. Sci. 1996;85:96-100.

Hunter WL, Burt HM, Machan L. Local delivery of chemotherapy: a supplement to existing cancer treatments. A case for surgical pastes and coated stents. Adv. Drug Deliv. Rev. 1997;26:199-207.

Jackson JK, Gleave ME, Yago V, Beraldi E, William L, Hunter WL, Burt HM. The suppression of human prostate tumor growth in mice by the intratumoral injection of a slow-release polymeric paste formulation of paclitaxel. Cancer Res. 2000;60:4146-4151.

Jackson JK, Zhang X, Llewellen S, Hunter WL, Burt HM. The characterization of novel polymeric paste formulations for intratumoral delivery. Int. J. Pharm. 2004;270:185-198.

Kabanov AV, Batrakova EV, Alakhov VY. Pluronic block copolymers as novel polymer therapeutics for drug and gene delivery. J. Controlled Release 2002;82:189-212.

Kim E, Gao Z, Park J, Li H, Han K. rhEGF/HP-β-CD complex in poloxamer gel for ophthalmic delivery. Int. J. Pharm. 2002;233:159-167.

Li Y, Sun X, LaMont JT, Pardee AB, Li CJ. Selective killing of cancer cells by β-lapachone: Direct checkpoint activation as a strategy against cancer. Proc. Natl. Acad. Sci. U.S.A. 2003;100:2674-2678.

Nasongkla N, Wiedmann AF, Bruening A, Beman M, Ray D, Bornmann WG, et al. Enhancement of solubility and bioavailability of beta-lapachone using cyclodextrin inclusion complexes. Pharm. Res. 2003;20(10):1626-1633.

Newell K, Franchi A, Pouysségur J, Tannock I. Studies with glycolysis-deficient cells suggest that production of lactic acid is not the only cause of tumor acidity. Proc. Natl. Acad. Sci. U. S. A. 1993;90(3):1127–1131.

Ough M, Lewis A, Bey EA, Gao J, Ritchie JM, Bornmann W, et al. Efficacy of beta-lapachone in pancreatic cancer treatment: exploiting the novel, therapeutic target NQO1. Cancer Biol. Ther. 2005;4(1):95-102.

Pardee AB, Li YZ, Li CJ. Cancer therapy with β-lapachone. Curr. Cancer Drug Targets 2002;2(3):227-242.

Park Y, Yong CS, Kim H, Rhee J, Oh Y, Kim C, Choi H. Effect of sodium chloride on the release, absorption and safety of diclofenac sodium delivered by poloxamer gel. Int. J. Pharm. 2003;263:105-111.

Pink JJ, Planchon SM, Tagliarino C, Varnes ME, Siegel D, Boothman DA. NAD(P)H: quinone oxidoreductase activity is the principal determinant of β-lapachone cytotoxicity. J. Biol. Chem. 2000;275:5416-5424.

Pisal SS, Paradkar AR, Mahadik KR, Kadam SS. Pluronics gels for nasal delivery of Vitamin B12. Part I: Preformulation study. Int. J. Pham. 2004;270:37-45.

Rangel-Yagui CO, Pessoa-Jr A, Costa Tavares L. Micellar solubilization of drugs. J. Pharm. Pharmacut. Sci. 2005;8(2):147-163.

Rao V, Nerurkar M, Pinnamaneni S, Rinaldi F, Raghavan K. Co-solubilization of poorly soluble drugs by micellization and complexation. Int. J. Pharm. 2006;319:98-106.

Fin da viaxe

Capítulo 12

Conclusiones

Los resultados obtenidos en los estudios de preformulación y de desarrollo de aproximaciones tecnológicas útiles para la administración oral e intratumoral de βLAP, han permitido extraer las siguientes conclusiones:

I. La caracterización físico-química llevada a cabo con βLAP origina una amplia base de datos que servirá para delimitar los parámetros de calidad de este fármaco. Además, la fase cristalina ortorrómbica mantenida en distintas condiciones de cristalización, pone de manifiesto la robustez y la estabilidad de la estructura cristalina original de βLAP.

II. La estabilidad de βLAP está fuertemente afectada por las condiciones de almacenamiento. En estado sólido, la luz y la interacción de ésta con la humedad relativa ambiental provocan la aparición de cambios físicos evidentes, como el oscurecimiento cristalino y los cambios en su cristalinidad, acelerando, de forma importante, su descomposición química que sigue una cinética pseudo-orden cero. En disolución acuosa, la βLAP presenta dos rutas de descomposición: en oscuridad un proceso hidrolítico que da lugar a hidroxilapachol, como principal producto de descomposición y, bajo iluminación, un proceso fotolítico, con generación de mezclas complejas de productos de degradación. La formación de complejos de inclusión con la RMβCD protege el fármaco frente al proceso hidrolítico, en tanto que acelera el proceso fotolítico. Además, la hidrólisis de βLAP está sujeta a una catálisis alcalina, con un intervalo de pH de máxima estabilidad comprendido entre 2 y 4.

III. La βLAP es compatible con una amplia variedad de excipientes farmacéuticos de uso frecuente en formas de dosificación sólidas,

incluyendo diferentes ciclodextrinas. Sin embargo, debe evitarse la utilización del lubrificante estearato de magnesio y del diluyente fosfato dicálcico dihidratado, debido a su interacción con βLAP con repercusiones sobre la estabilidad física y química de las mezclas.

IV. El diseño de partículas de βLAP empleando técnicas de precipitación en superficie hidrofílica (PHS) y microprecipitación por cambio de fase (PC) proporcionaron mejoras importantes en la velocidad de disolución de βLAP, que pueden justificarse por la acentuada reducción en el tamaño de partícula del fármaco y por la hidrofilización de la superficie de los microcristales, que favorece su humectación. Los preparados PHS permiten incorporar hasta un 50 % de fármaco, además de utilizar como matriz hidrofílica la celulosa microcristalina, excipiente muy adecuado para compresión directa. Los microprecipitados PC producen mejoras aún mas acentuadas en la velocidad de disolución de βLAP y permiten la incorporación de hasta un 90 % de fármaco a las formulaciones.

V. Distintos derivados de β-ciclodextrina, en especial RMβCD, muestran una elevada capacidad de complejación de βLAP. Los sistemas sólidos conteniendo βLAP- RMβCD en proporción equimolar, preparados por malaxado y liofilizado, cuentan con claras evidencias de formación de complejos de inclusión, incrementando de forma espectacular la velocidad de disolución de βLAP.

VI. Las dispersiones de pluronics F127 y P123 presentan adecuadas características de termogelificación para administración intratumoral de βLAP. La presencia de etanol disminuye la temperatura de gelificación de

los sistemas, pero únicamente el pluronic F127 experimenta cambios en su consistencia, que conducen a una aceleración en el proceso de cesión del fármaco. La incorporación a estos sistemas de ciclodextrina RMβCD incrementa la temperatura de gelificación de los preparados, acelera la cesión de fármaco, sin afectar la consistencia de los geles. Los geles mantienen sus propiedades físico-químicas tras ser sometidos a un proceso de esterilización en autoclave. Además, los geles termorreversibles a base de pluronic F127 o P123 resultan adecuados para una liberación intratumoral sostenida de βLAP modulada por la adición de cosolubilizantes como etanol y RMβCD.